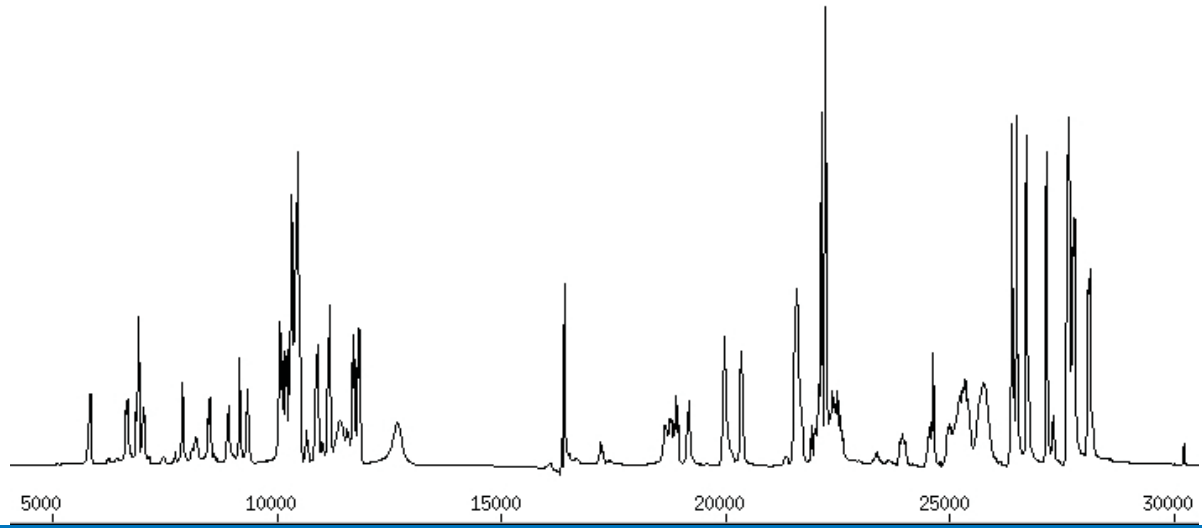

Theory, Dynamics and Applications of

Magnetic Resonance Imaging–I

Edited by Omotayo Bamidele Awojoyogbe

SciencePG
Science Publishing Group

Science Publishing Group

Theory, Dynamics and Applications of Magnetic Resonance Imaging-I

Editor:

Omotayo Bamidele Awojoyogbe

Authors:

Abhishek Gupta, Timothy Stait-Gardner

Bahman Ghadirian, William S. Price

Michael Oluwaseun Dada

SciencePG
Science Publishing Group

Science Publishing Group
548 Fashion Avenue
New York, NY 10018
http://www.sciencepublishinggroup.com

Published by Science Publishing Group 2014

First Edition

ISBN: 978-1-940366-10-4

To order additional copies of this book, please contact:
Science Publishing Group
service@sciencepublishinggroup.com
http://www.sciencepublishinggroup.com

Printed and bound in India

Editor's Introduction

There can be few better examples of the complex and unanticipated interactions of basic research and technological innovation than the development of magnetic resonance imaging (NMR/MRI) techniques for multidisciplinary research. The method has the rather unusual and attractive features that it is totally non-destructive and non-invasive and for these reasons it has interesting applications in almost all fields of research.

Nuclear magnetic resonance imaging (NMRI) is an important modality of medical imaging. NMRI uses magnetic fields to manipulate magnetization in a way that makes it a conveniently measurable signal which encodes spatial location and density information. Physically, this is a complicated process which relies on effects at both the quantum and macroscopic levels. Mathematically, with correctly designed sequence of magnetic field applications, the recorded signal can be extensively explored for maximum applications.

The image is essentially the distribution of water molecules in a tissue slice of the patient. Since tissue densities have varying water contents and NMR has very high contrast, it is possible to obtain detailed images of internal soft tissue. The advantage of this method is that it is very good at contrasting soft tissue since it primarily measures water content of tissues with no ionizing radiation. The disadvantages are that it is expensive, it has long scan times and poor imaging of bone tissues, and it is too slow to image dynamic processes at high resolution.

Nuclear magnetic resonance is a physical phenomenon which is based on the magnetic property of an atom's nucleus. All nuclei that contain odd numbers of nucleons and some that contain even numbers of nucleons have an intrinsic magnetic moment. Hydrogen nuclei, fluorine, carbon-13 and oxygen-17 all have distinctive magnetic properties that make them suitable for NMR studies.

First introduced in the 1940's by Felix Bloch and Edward Purcell to measure the magnetic moment of nuclei in liquids and solids, NMR is based on protons in a nucleus having an intrinsic spin angular momentum, thus a magnetic moment. When a constant magnetic field is applied, a nucleus will resonate like a mechanical oscillator when driven in to an excited energy state by an electromagnetic (EM) wave (in the radio frequency range for NMR) at the correct frequency, which is determined by the strength of the magnetic field and the magnetic moment of the nucleus. Traditionally, NMR was done by sweeping the magnetic field strength while applying a continuous EM wave and measuring where the signal from the nuclei emitted peaked (continuous wave NMR, or CW NMR). However, modern NMR is usually done by applying a pulse of rf wave (pulsed NMR), which contains a broad spectrum of frequency components, and measuring the radio signal, termed the free induction decay (FID) as the signal decays like a damped oscillator, emitted from the nuclei after the pulse. Using a Fourier transform of the FID signal, the resonance frequency of the nuclei can be determined. Moreover, pulsed NMR can provide information concerning the physical properties of the nuclei measured. One of the very important properties of NMR/MRI is the relaxation times, or the time required for the nuclei in the sample to return to their ground state after being saturated by a strong EM pulse of the sample. These parameters

make MRI unique and vastile with many applications in the fields of science, medicine, engineering and agriculture.

Nuclear magnetic resonance is inherently a three-dimensional phenomenon. The spatial resolution of a three-dimensional set of data is usually equal in all three directions. At the core of the NMR, a magnetic resonance imaging (MRI) makes use of the fields dependency on the precession frequency by superimposing a magnetic field gradient onto the static polarizing field $H_o = H_z$ to spatially encode information into the rf (radio frequency) signal. With this three-dimensional data in hand, surfaces can be detected mathematically. A computer translates these signals into highly detailed cross sectional images. The images are essentially maps of the locations of hydrogen in the body.

The sensitivity of nuclear magnetic resonance to molecular structure has made it a valuable research tool in organic chemistry, enabling chemists to determine hydrogen locations in crystals, something that cannot be done using X-ray diffraction. Nuclear magnetic resonance has also been used to study electron densities, chemical bonding, the compositions of mixtures, and to make purity determinations.

The basic requirements for NMR spectroscopy are that the magnetic field be homogenous over the volume of the sample, that there be a radio frequency field rotating in a plane perpendicular to the static field, and that there be a means of detecting the interaction of the frequency field with the sample.

Techniques that have been developed for the observation of NMR signals fall into two categories: pulsed and continuous wave. In the case of the pulsed methods, an applied rotating (or alternating) magnetic field

with a frequency at or near the Larmor frequency (that is, frequency of precession) of the nucleus to be studied is directed at right angle to the static field. If the rotating field is applied at exact resonance, the nuclei precess about that field as though there was no static field. Continuous wave methods are either high resolution or broad line. Broad line widths are produced by most oriented molecules exhibiting strong magnetic dipolar interactions, so broad line spectroscopy does not permit measurements of chemical shifts and spin-spin coupling. High resolution on the other hand, has been used to identify molecules, to measure the electronic effects, to determine structure, to study reaction intermediates, and to follow the motion of molecules or groups of atoms within molecules. For high resolution studies, the magnetic field must be uniform to 1 part in 108 for a 100MHz instrument, if a resolution of 7MHz is to be obtained. In the case of broad line studies, 5 parts in 106 may be adequate.

Nuclear magnetic resonance has been used to study the physics and chemistry of solids, including metals, semiconductors, magnetic solids and organic materials. Physical phenomena that can be studied by NMR include conduction-electron paramagnetism; spin waves and magnetic fluctuations in ordered magnetic materials; metal molecular transitions; charge density wave phenomena; spin-freezing in spin glasses and frequency shift and spin-lattice relaxation effects. At low temperatures, NMR has been used to make temperature measurements and to study the super fluid phases of ^{3}He.

In the fields of organic chemistry and materials science, NMR has been used to study polymers, amorphous systems and complex molecular solids. In many of these systems, the NMR line widths of the

nuclei are dominated by dipolar fields arising from neighbouring magnetic moments. These systems exhibit complex NMR spectra due to shifts in nuclear magnetic resonance frequencies.

In the case of complex molecules in liquid environments, the molecules undergo a tumbling motion, producing very sharp NMR spectra. The technique used to study these systems is known as Fourier transforms NMR Spectroscopy.

Specifically, nuclear magnetic response is extremely useful for analyzing samples non-destructively. Radio waves and static magnetic fields easily penetrate many types of matter and anything that is not inherently ferromagnetic. For example, various expensive biological samples, such as nucleic acids, including RNA (Ribonucleic Acid) and DNA (Deoxyribonucleic Acid), or proteins, can be studied using nuclear magnetic resonance for weeks or months before using destructive biochemical experiments. This also makes nuclear magnetic resonance a good source for analyzing dangerous samples.

Nuclear magnetic resonance has been used in data acquisition in petroleum industry for petroleum and natural gas exploration and recovery. A borehole is drilled into rock and sedimentary strata into which nuclear magnetic resonance logging equipment is lowered. Nuclear magnetic resonance analysis of these boreholes is used to measure rock porosity, estimate permeability from pore size distribution and identify pore fluids (water, oil and gas).

NMR is also a tool used not only in well logging, but also in petrophysics. Additional applications of surface NMR (SNMR or magnetic resonance sounding - MRS) have shown the power of the

method for hydrogeophysical purposes. The power of the NMR method relies on the fact, that it is the only geophysical method which delivers direct information of the water content in samples or the subsurface. Moreover, it allows the determination of important structural parameters like porosity, surface/volume ratio or hydraulic conductivity.

Recently there is an increasing demand for reliable information of the water content and structural parameter like water retention capabilities of soils. For applications on the meter and decimeter scale – like soil physics, precision farming (agrogeophysics) or dam quality and stability investigations – NMR could therefore be a valuable instrument in the fields of agriculture and geophysics.

Nuclear magnetic resonance has also entered the arena of real-time process control and process optimization in oil refineries and petrochemical plants. Two different types of NMR analysis are utilized to provide real time analysis of feeds and products in order to control and optimize unit operations. Time-domain NMR (TD-NMR) spectrometers operating at low field (2-20MHz for ^{1}H) yield free induction decay (FID) data that can be used to determine absolute hydrogen content values, rheological information, and component composition. These spectrometers are used in mining, polymer production, cosmetics and food manufacturing as well as coal analysis.

Volume I, of this book series presents the *Bloch phenomenological equation*, which provides a model for the interactions between applied magnetic fields and the nuclear spins in the objects under consideration. It analyzes macroscopic averaged models that describe the interaction of aggregates of spins, with applied magnetic fields. This is an integrated science text in the direction of promoting a long-term future filled with

important developments in quantitative, theory-based biology towards addressing current disadvantages of MRI. The goal and intention is to see exactly diseased conditions at quantum (molecular) level, in order to have thorough understanding of their specific causes (or how they are caused), trace and monitor their progression and get the best treatment for them. This book is another effort to break down the traditional boundaries between mathematics, physics, chemistry, and biology, and does so in a compelling fashion.

The audience for whom the book is intended is mathematical scientists, biomedical physicists, biomedical engineers, geophysicists and computer scientists. The book can be useful to people that do research in the field of NMR/MRI. It will be more useful to the beginners or scientists that want to see the connection between medical biophysics and mathematics. The book is relevant to current research trends and may advance a beginner's ability to do research in medical MRI physics. The book is of great usefulness for all those persons who want to develop a carrier in MRI.

The Editor wishes to thank Professor M. A. Akanji, the Vice Chancellor, Federal University of Technology, Minna, Nigeria, for his love for academic excellence, Professor Solarin, the Director General, National Mathematical Centre, Abuja, Nigeria, for promoting academic excellence among young scientists and Professor Dilip K. De, my former supervisor and esteemed colleague, who first suggested to me that analytical solutions of the *Bloch phenomenological equation* might be worth a crack. The useful suggestions, advice and thoughtful comments of Professor Ioannis Gkigkitzi, Department of Mathematics, East Carolina University, USA and Professor Manuel Malaver, Universidad Marítima

del Caribe, Departamento de Ciencias Básicas, Catia la Mar, Venezuela are highly appreciated. Finally, the editor appreciates the support from International Centre for Theoretical Physics, Trieste, Italy and the timely suggestions and advice of Professor Akin Ojo, Department of Physics, University of Ibadan, Nigeria and Engineer Olufemi Folorunsho Moses.

By

The Editor

Omotayo Bamidele Awojoyogbe

Contents

Chapter 1

Fundamental Concept for the Theory, Dynamics and Applications of MRI

1

Fundamental Concept for the Theory, Dynamics and Applications of MRI

Abhishek Gupta, Timothy Stait-Gardner, Bahman Ghadirian and William S. Price[1]

Nanoscale Organisation and Dynamics Group, School of Science and Health, University of Western Sydney, Australia

1.1 Introduction

Since its inception in 1973,[1] magnetic resonance imaging (MRI) has been a powerful diagnostic tool which is now routinely used in clinical medicine. Contrary to other non-invasive imaging techniques such as X-ray computed tomography and positron emission tomography, MRI does not use harmful ionizing radiation. Also, MRI offers much better soft-tissue contrast. MRI possesses many contrast generating mechanisms which are sensitive to various tissue parameters and ultimately provide information-rich images.

[1] Author for correspondence. Email: w.price@uws.edu.au

'MRI' is a branch of nuclear magnetic resonance (NMR), but the word 'nuclear' is generally omitted to avoid confusion with ionizing radiation.[2, 3] In simple terms, MRI is the use of one or more magnetic gradients to provide a well-defined spatial dependence to NMR observables. As will be considered further below, the recorded NMR signals are then reconstructed to form a spatial image.[4]

Some fundamental NMR concepts are discussed in the next section followed by a brief description of the theory, contrast and applications of MRI. Although an attempt has been made to make this chapter self-complete, due to the vast subject matter the coverage is nevertheless superficial. Therefore, the reader is suggested to refer to other texts[4-11] for further information.

1.2 Preliminary Concepts

1.2.1 Nuclear Spin and Magnetic Moment

All atomic nuclei have four important properties: mass, electric charge, magnetism and spin. Mass and electric charge are responsible for the physical and chemical properties of matter whereas the latter two properties form the basis of NMR (and hence MRI). Atomic nuclei can act as small bar magnets when placed in an external magnetic field. Spin is an intrinsic quantum mechanical property which is difficult to visualize, but simplistically can be described as atomic nucleus spinning about its own axis. This is associated with an inherent angular momentum, called the spin angular momentum, I, which gives rise to a magnetic moment μ, related to I by:

$$\boldsymbol{\mu} = \gamma \mathbf{I} \tag{1.1}$$

where the proportionality constant, γ, is the gyromagnetic ratio (rad s^{-1} T^{-1}). Equation (1.1) indicates that only the spins[2] with $I \neq 0$ possess a magnetic moment and are thus 'NMR active'. Most elements have at least one NMR active isotope. Commonly used isotopes in NMR studies include ^{13}C, ^{15}N, ^{17}O, and ^{19}F, however MRI is mainly performed with ^{1}H because of its high natural abundance (i.e., 99.9%), high NMR sensitivity (high gyromagnetic ratio) and high concentration in molecules in the body (i.e., water, fat and other organic molecules).

Larmor Precession and Net Magnetization

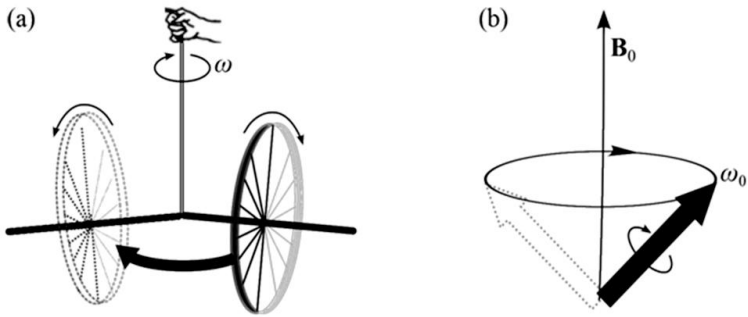

Figure 1.1 *(a) A bicycle wheel spinning about its own axis will start precessing if hung by one end of its axle. (b) Similarly, when placed in an external magnetic field (B_0), a nuclear spin starts precessing about the direction of B_0 with the Larmor precessional frequency, ω_0.*

MRI involves the application of a strong static magnetic field, B_0, to the spins. To understand how spins behave in the presence of B_0, it is useful to discuss the following analogy. Imagine a bicycle wheel hung by one end of its axle as shown in Figure 1.1 (a). If the wheel is not spinning, it will simply fall down under the effect of gravity. But if the wheel is spinning, it will instead start revolving around the fixed end while rotating about its axle. This simultaneous

[2] In NMR jargon, atomic nuclei are often denoted as 'nuclear spins' or 'spins'.

rotating revolving motion is called precession. This is precisely how (the magnetic property of) a nuclear spin interacts with the external magnetic field. Instead of flipping towards the magnetic field, it starts precessing about it (Figure 1.1 (b)). The angular frequency of precession, ω_0, is referred to as Larmor frequency (i.e., the resonance frequency) and its magnitude is dependent on the external magnetic field strength as:

$$\omega_0 = \gamma B_0. \tag{1.2}$$

A small digression: the magnetic field experienced by a nucleus is not necessarily exactly that of the externally applied magnetic field. The electron shells surrounding a nucleus 'shield' the nucleus from the magnetic field and thus the Larmor frequency is slightly changed by the local chemical environment ('the chemical shift'). Thus, for example, the –OH proton of methanol will resonate at a slightly different frequency than the $–CH_3$ protons. Typically though these are extremely small perturbations to the resonance frequency with the values normally being within a few parts per million of ω_0.[12, 13]

Of course, as is the case with the spinning bicycle wheel, the nuclear spin does try to align its magnetic moment with the external magnetic field to minimise the energy of magnetic interaction between them as given by:

$$E = -\boldsymbol{\mu} \cdot \mathbf{B}_0. \tag{1.3}$$

However, in the case of protons, it turns out that the average thermal energy associated with the absolute temperature, kT (where k is the Boltzmann's constant), is much higher than E. For example, using Equations (1.1) and (1.3), the difference in the energy of magnetic interaction of a proton between the two spin states (aligned and anti aligned with external magnetic field) can be calculated to be 4.23×10^{-26} J at 1.5 T magnetic field strength (same as that of

most clinical MRIs). Whereas, the thermal energy associated with the proton at physiological temperatures (37 ℃ or 310.15 K) is 4.28×10^{-21} J, about 10^5 times larger than *E*. This implies that even in the presence of the magnetic field, the spins are mostly randomly oriented with only a small preference towards the direction of the applied field. But since there are an extraordinary number of nuclei even in the smallest sample (e.g., a mg of tissue), this statistically tiny alignment can conduce to a net macroscopic magnetisation, M_0 (Figure 1.2), referred to as the thermal equilibrium value of the net magnetisation.

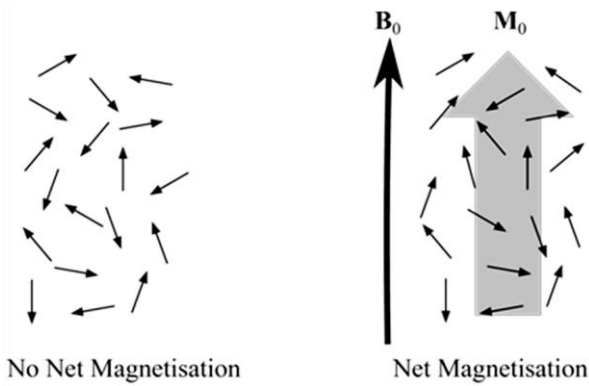

Figure 1.2 *A schematic representation of nuclear spins before (left) and after (right) the application of an external magnetic field, B_0. In the absence of B_0, the magnetic moments of nuclear spins are randomly oriented resulting in no net magnetisation. Whereas, in the presence of B_0, there is a slight preference of magnetic moments to align with B_0 resulting in a small net magnetisation, M_0.*

1.2.2 Radiofrequency Pulse and Signal Detection

To extract information from the sample, it is necessary to be able to detect the net magnetisation. Only the component of the net magnetisation that is oriented perpendicular to B_0 (i.e., transverse magnetisation) is detectable. Thus, an NMR (or MRI) experiment begins by nutating M_0 away from B_0 using a perpendicular magnetic field, B_1, oscillating at the Larmor frequency for a short time. Since the Larmor frequencies at most practical magnetic field strengths lie within the

radio-frequency (rf) range (3 kHz – 300 GHz), this short burst of an oscillating perpendicular magnetic field is termed a radio-frequency pulse (rf pulse). Note that MRI can also be performed in the earth's magnetic field which results in the Larmor frequencies of approximately 2 kHz for protons, lying in the ultra-low frequency or audio frequency range (300 Hz – 3 kHz).[14] However, since clinical MRI and cryogenically cooled research grade MRIs all have Larmor frequencies in the radio-frequency range, the term 'rf pulse' is generally accepted as standard. The resonance between the rf pulse and the Larmor frequency of the nuclei (i.e. $\omega_{rf} = \omega_0$) ensures that the net magnetisation receives a continuous push (actually a nutation) towards the transverse plane. The angle by which the net magnetisation is rotated (rotation angle) depends on the strength and duration of the rf pulse. It is common in NMR to name the rf pulse based on the rotation angle. For example, an rf pulse which rotates the magnetisation by 180 °is called a π pulse or a 180 °pulse.

Since there are two precessions involved (one about B_0 and one about B_1) during the application of an rf pulse, it is much simpler to visualize this effect in a reference frame rotating at the frequency of the rf pulse[3], otherwise known as the rotating frame of reference (RFR). In the RFR, at thermal equilibrium, the spins precessing about B_0 will appear stationary and B_0 can be ignored as its effect has already been accounted for in the rotation of the reference frame. Also, the rf pulse will appear static and the spins will appear as if only precessing about B_1 at a frequency $\omega_{rf} = \gamma B_1$ (Figure 1.3). In this chapter, RFR is represented by italiced axes (x, y, z) and laboratory frame by non-italiced axes (x, y, z).

[3] In many texts, RFR is arbitrarily chosen to be rotating at the Larmor frequency instead of the rf pulse frequency. Although in the present case it would not make a difference since they are both equal, in the quantum mechanical description of MRI it is more useful to describe $\omega_{rfr} = \omega_{rf}$ to account for the very small difference between ω_{rf} and ω_0 at the resonance condition.

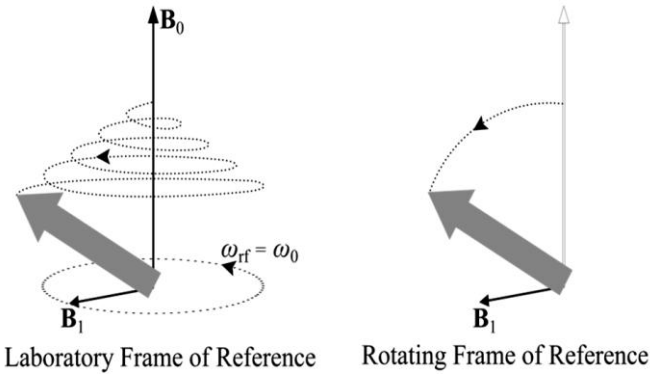

Figure 1.3 *The effect of an rf pulse on the net magnetisation in the laboratory and rotating frame of references. In the laboratory frame of reference, the two simultaneous precessions about the external magnetic field, B_0, and oscillating magnetic field B_1 makes the overall motion of the net magnetisation appear as a spiral. This can be simplified by using a reference frame rotating at the frequency of the rf pulse (or Larmor frequency), called the rotating frame of reference (RFR). In RFR, the effect of B_0 can be ignored and B_1 appears stationary. Thus, the net magnetisation appears to be precessing about B_1 only.*

After the rf pulse is turned off, the net magnetisation, now in the transverse plane, continues its usual precession about B_0. This precessing magnetisation generates a changing magnetic field which induces an oscillating electric current via Faraday induction in a nearby receiver coil. The induced current is then amplified and digitized by an analogue-to-digital converter to give an NMR signal known as the free induction decay (FID). The FID is an exponentially decaying sinusoidal signal in the time domain. As can be seen from Figure 1.4, it is very hard to deduce the Larmor frequencies of nuclei in differing chemical environments (such as situated in or near different functional groups) with different resonance frequencies from the FID. To resolve this, the FID is Fourier transformed to the frequency domain (i.e., an NMR spectrum) in which each exponentially decaying signal is converted to a Lorentzian shaped peak. In an NMR spectrum, the Larmor frequencies can be easily identified by the corresponding peaks (Figure 1.4).[15, 16]

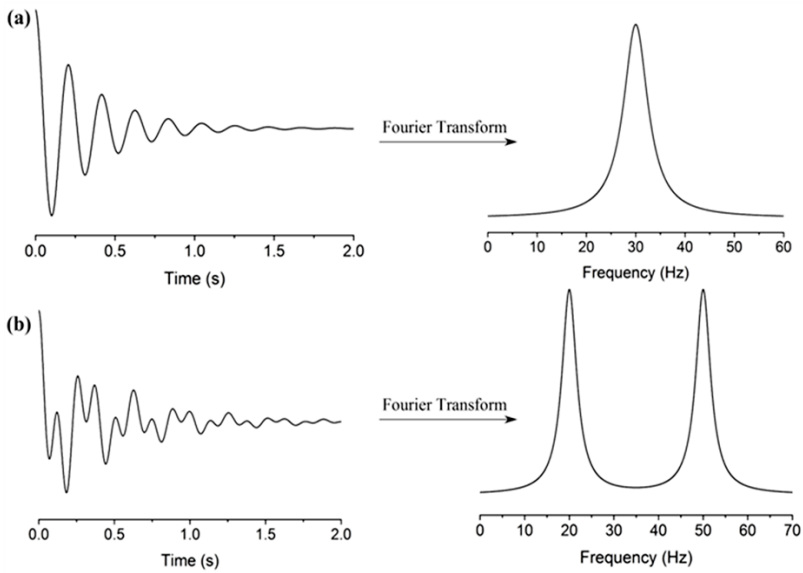

Figure 1.4 *Simulated free induction decays (left) and their NMR spectra (right) obtained by applying the Fourier transforms. The offset Larmor frequencies were set to (a) 30 Hz and (b) 30 and 50 Hz (a situation where either different nuclei are present or the same nuclei are present in two different environments). T_2 was set to 2s in both cases. Whilst it is hard to deduce directly the Larmor frequencies of the nuclei contributing to the FID signal (time domain), the frequencies can be easily identified by the corresponding peaks in the NMR spectrum (frequency domain).*

1.2.3 Relaxation

After the rf pulse, the net magnetisation returns to its equilibrium position by a process known as spin relaxation. This includes the reduction of the transverse magnetisation to zero (transverse relaxation) and the longitudinal magnetisation back to its equilibrium value (longitudinal relaxation).[9, 11] The two processes are outlined in Figure 1.5 and briefly discussed below. Note that for the sake of discussion, B_0 is assumed to be directed along the z-axis, although depending on magnet construction it could be along any direction. Indeed in clinical whole body magnets it is generally taken as being along x.

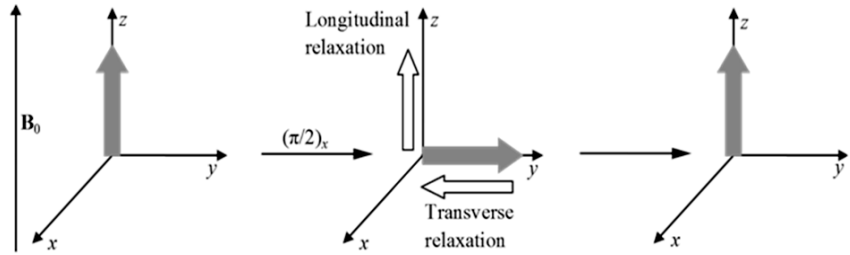

Figure 1.5 *A schematic representation of the relaxation process. The net magnetisation is along the direction of the applied magnetic field, B_0, at equilibrium. The π/2 rf pulse rotates it to the x-y plane. Relaxation drives the transverse magnetisation to zero (transverse relaxation) and the longitudinal magnetisation to its equilibrium value (longitudinal relaxation).*

(1) Longitudinal Relaxation

Longitudinal relaxation is also known as spin-lattice relaxation or somewhat erroneously, T_1 relaxation. At the microscopic scale, it refers to the movement of spin populations back to their Boltzmann distribution values.[9] The return of the *z*-component of the net magnetisation, M_z, to its equilibrium value, M_0, is usually a first-order process given by:

$$\frac{dM_z}{dt} = -\frac{(M_z - M_0)}{T_1} \tag{1.4}$$

where T_1 is the spin-lattice relaxation time constant.[17] After one T_1, M_z returns to 63% of its equilibrium value and by $5T_1$, M_z has returned to almost 100% of its equilibrium value. The T_1 values can be measured experimentally by using the inversion recovery method.[18]

(2) Transverse Relaxation

Transverse relaxation, also known as spin-spin relaxation or, somewhat erroneously, T_2 relaxation corresponds to the loss of transverse magnetisation. This results from the loss of coherence amongst the spins precessing in the

transverse plane. The decay of the *x* and *y* components of magnetisation, M_x and M_y, is also usually a first order process given by:

$$\frac{dM_x}{dt} = -\frac{M_x}{T_2} \text{ or } \frac{dM_y}{dt} = -\frac{M_y}{T_2} \quad (1.5)$$

where T_2 is the spin-spin relaxation time constant.[17] It is important to note that the line-width at half height of the signal (in an NMR spectrum), $\Delta\nu_{1/2,}$ depends on the T_2 of a signal as given by:

$$\Delta\nu_{1/2} = \frac{1}{\pi T_2^*} \quad (1.6)$$

where

$$T_2^* = T_2 + T_{2\,\text{inhomogenous}} \quad (1.7)$$

and $T_{2\ \text{inhomogeneous}}$ is the contribution from the inhomogeneities in the static magnetic field.[19] Therefore, a sample with short T_2 will give a broad peak and *vice-versa*. Although a rough estimate of T_2 can be obtained from the line-width at half height, for accurate measurement it is necessary to suppress the inhomogeneous broadening. This is achieved by using the 'spin-echo' technique. The simplest 'spin-echo' pulse sequence was first proposed by Hahn[20] in 1950 and later modified by Carr and Purcell[21] and Meiboom and Gill[22] to give a widely used pulse sequence named after their initials i.e. the CPMG pulse sequence.

Both T_1 and T_2 contribute to the tissue-contrast in an MRI image by affecting the signal intensity. In MRI, the protons with shorter T_1 conduce to brighter regions whereas the protons with shorter T_2 generate darker regions. This is further discussed in Section 0.

1.3 MRI Theory

1.3.1 Gradients - One Dimensional Imaging

Thus far, it has been discussed how an NMR spectrum can be obtained from a sample placed in a homogenous magnetic field. The next step is to consider how NMR can be used to obtain an image of the sample. Recall that the primary objective of imaging is to obtain information on the nuclear spin density, ρ, at each point in the sample (i.e., ρ(r)). To do so, it is necessary to spatially vary the behaviour of the nuclear spins so that spins at different positions give different signals. This can easily be achieved in NMR by varying the external magnetic field in some direction by applying a spatially well-defined magnetic gradient, G. This spatially varying magnetic field results in otherwise identical spins at different positions having different Larmor frequencies. Thus, in the presence of the magnetic gradient, the Larmor frequency becomes a function of position, r, as given by:

$$\omega(\mathbf{r}) = \gamma \mathbf{B}_0 + \gamma \mathbf{G} \cdot \mathbf{r} \tag{1.8}$$

with the detected signal having the following form:

$$S(t) = \int \rho(\mathbf{r}) \mathrm{e}^{i\gamma \mathbf{G} \cdot \mathbf{r} t} \mathrm{d}\mathbf{r}. \tag{1.9}$$

For example, an hour-glass filled with water placed in a magnetic field gradient will result in an NMR spectrum which is the projection of the distribution of spins onto the gradient direction (Figure 1.6). The amplitude of the signal at each frequency will be proportional to the number of spins in that frequency region, that is ρ (r).[4, 8]

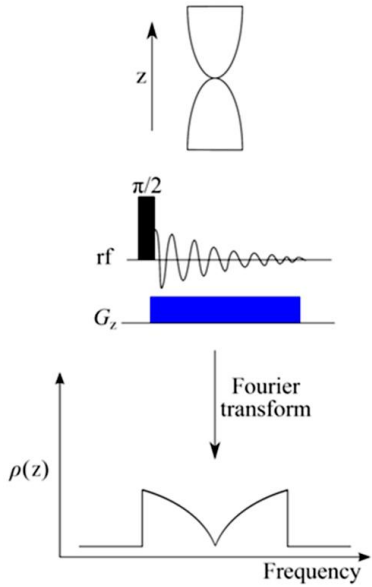

Figure 1.6 *An example of the use of a magnetic gradient to obtain a one dimensional image (i.e., ρ(z)) of an hour-glass filled with water. The external magnetic field and the gradient are applied in the z-direction. Due to the applied gradient, the Larmor frequency becomes a function of the z-position and thus the NMR spectrum represents the distribution of the Larmor frequencies with the signal-amplitude at each frequency proportional to the number of spins in that frequency region. Thus, the image is a 1D projection of ρ(r) along the direction of the gradient, i.e., ρ (z).*

1.3.2 Three Dimensional Imaging - Spatial Encoding

Although the previous example is useful for understanding the effect of applying a magnetic gradient, it is important to consider that for normal (incl. medical) imaging, ρ is almost always a three dimensional (3D) quantity. And by extension of the previous example, the acquisition of a 3D image entails the application of three orthogonal gradients at appropriate junctures in the MRI pulse sequence. How these three gradients are utilized to impart spatial dependence to the nuclear spin density, a process known as spatial encoding, is discussed in the following sections.

1.3.3 Slice Selection

The first gradient is used to select a two dimensional (2D) region of interest from the sample, a process known as slice selection. This is attained by applying a spatially well-defined gradient known as the slice gradient along (say)

the z-axis throughout the sample in conjunction with a frequency selective rf pulse.[2] As depicted in Figure 1.7a, the slice gradient, G_z, varies the precession frequency of the spins linearly along the z-axis while the frequency selective rf pulse affects only those spins within the frequency range of excitation. The result is that only a limited part of the sample (the slice) is excited. Consequently, only the magnetisation contained within the slice is rotated into the transverse plane and contributes to the NMR signal. The slice thickness, Δz, is dependent on the strength of the applied gradient and the bandwidth of the frequencies incorporated into the rf pulse, $\Delta\omega_{rf}$,

$$\Delta z = \frac{\Delta\omega_{rf}}{\gamma G_z}. \tag{1.10}$$

It should be noted that regardless of the physical thickness, the selected slice is considered as a 2D object which can be manipulated to give a 1D or 2D image only. In other words, the selected slice is always considered one voxel (volume element or a '3D pixel') thick and all the information from Δz is averaged to one signal. To get a 3D image, multiple slices can be selected, imaged and stacked on each other. The position of the slice depends on the resonance frequency of the rf pulse with respect to the Larmor frequency,

$$z = \frac{\omega_{rf} - \omega_0}{\gamma G_z}. \tag{1.11}$$

The two commonly used slice selection schemes are shown in Figure 1.7b and c. The magnetisation components within the slice are dephased immediately after the application of the rf pulse which results in the destructive interference of the signals originating from the different positions of the slice.[4] Thus, a negative gradient is applied for a short period of time immediately after the use

of the rf pulse to refocus the magnetisation. Alternatively, depending on the pulse sequence, a π pulse can be used, in which case, the magnetisation refocuses automatically.

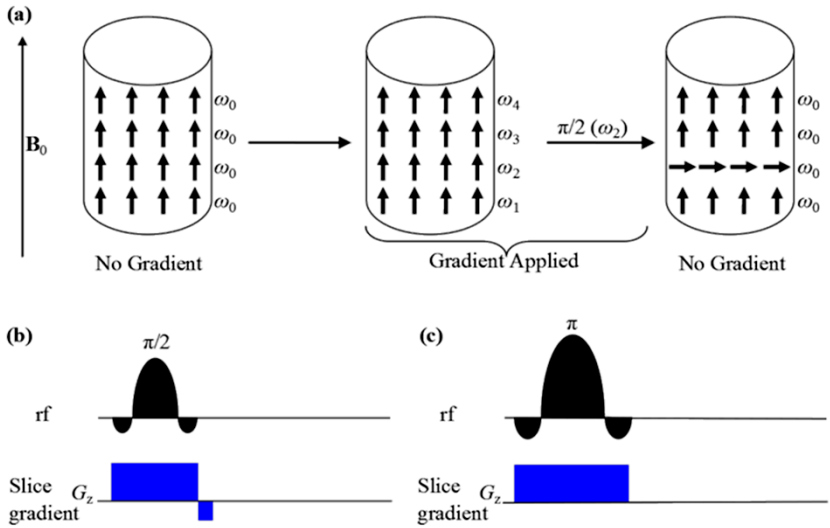

Figure 1.7 *(a) A schematic representation of the slice selection process in MRI. Before the application of a magnetic gradient, all the spins are precessing at the same frequency, ω_0. In the presence of a gradient along the direction of B_0 (i.e. z-axis), the spins at different z-positions start precessing at slightly different frequencies. If a frequency selective rf pulse is applied, only the corresponding spins are rotated into the transverse plane, thus a 'slice' is selected. The two commonly used pulse sequences are shown in (b) and (c). A short negative gradient is applied to refocus the magnetisation that had been dephased after the application of the rf pulse. Alternatively, a π pulse can be used.*

The other two gradients are used to localize the signal within the selected slice so that eventually every voxel gives a different NMR signal. The two common parameters that can be modulated to provide spatial dependence are phase and frequency as discussed in the next section.[23] For simplicity, it has been assumed that the selected slice has nine voxels and every voxel contains only one spin.

1.3.4 Phase Encoding

After the slice has been selected, all the spins within the slice are in the transverse plane. If a gradient is applied along (say) the y-axis for a fixed time *t* before acquiring the signal, the phase, φ, will become a function of position *y* as given by:

$$\phi(\mathrm{y}) = \gamma \int_0^t (B_0 + G_\varphi \mathrm{y}) dt \tag{1.12}$$

where G_φ is the phase gradient. This is because in the presence of the phase gradient, the nuclear spins along the y-axis will start precessing at slightly different frequencies and thus will have different phases at any instant. So when the gradient is stopped, although the spins retain their original precession frequency, the phase differences amongst them still remain the same. This process is known as phase encoding and is depicted in Figure 1.8a. Note that the amplitude of the signal recorded after phase encoding is inversely proportional to the strength of the applied phase gradient. The reason for this is that a stronger phase gradient results in a larger phase difference between the neighbouring spins and although this helps to resolve them better, the total signal from the spins is dephased resulting in lower amplitude.[24]

Rapid switching of the gradients generates eddy currents in the nearby conducting materials, creating a secondary source of gradients.[25, 26] This results in a distorted FID and hence the resulting image contains artifacts. A common solution for this is to use an echo sequence to allow the field distortions to dissipate before signal acquisition begins. The two common types of echo sequences are: ‘spin-echo’ sequences and ‘gradient-echo’ sequences. In the ‘gradient-echo’ sequence, only the gradient induced phase dispersions are refocussed in contrast to the ‘spin-echo’ sequence, in which phase dispersions due to the magnetic inhomogeneities and chemical shifts are refocused as well.[8,

[27, 28] The phase encoding in the 'spin-echo' and 'gradient-echo' pulse sequences are shown in Figure 1.8b and c.

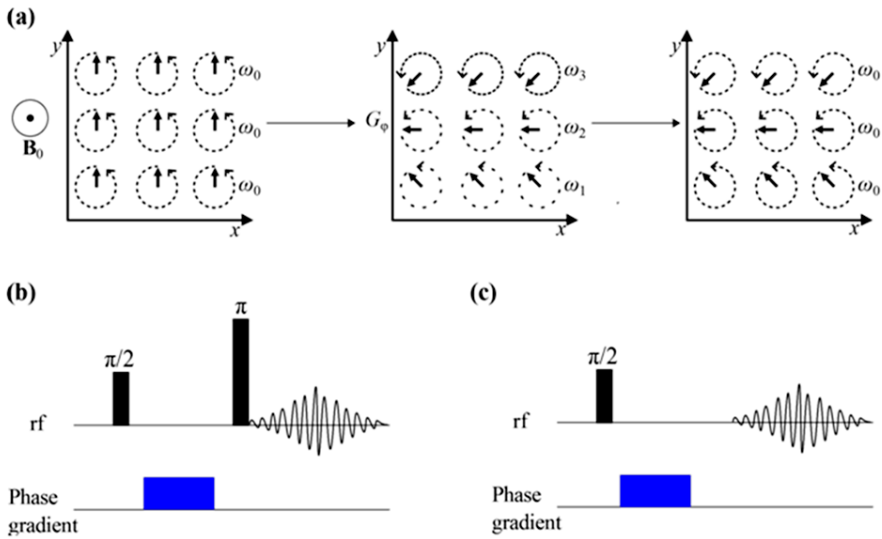

Figure 1.8 *(a) An illustration of the phase encoding process in MRI. On the application of the phase gradient to the selected slice along the y-axis, the spins start precessing at different frequencies and, therefore, have different phases at any instant. After the gradient is stopped, although the spins all regain their original precession frequency (i.e., ω_0), the phase differences amongst them are retained as a function of position. (b) and (c) Phase encoding in the 'spin-echo' and 'gradient-echo' pulse sequences, respectively. The phase gradient can be applied either before or after the π pulse.*

1.3.5 Frequency Encoding

Once the slice is selected and phase encoded, only one more direction needs to be resolved to get different signals from every voxel. The final gradient is applied along the x-axis while the signal is being recorded. This has the same effect as was explained in the one dimensional imaging example above i.e. the Larmor frequencies of the voxels along the x-axis become spatially dependent and Equation (1.8) can be written as:

$$\omega(\mathrm{x}) = \gamma(B_0 + G_\mathrm{f}\mathrm{x}) \tag{1.13}$$

where G_f is the frequency gradient, commonly known as the 'read' gradient.[29] This process is known as frequency encoding and is depicted in Figure 1.9a. It is clear that at the end of phase and frequency encoding, all the voxels in the selected slice are different from each other either in their phase or frequency and will, therefore, give different signals.

Putting it all together, complete basic 'spin-echo' and 'gradient-echo' 3D MRI pulse sequences are illustrated in Figure 1.10 and Figure 1.11. T_E (echo time) is the time between the application of the initial rf pulse and the acquisition of the signal and T_R (repetition time) is the time between two successive applications of a pulse sequence. Thus, T_E closely correlates with the loss of signal due to spin-spin relaxation and T_R correlates with how much longitudinal magnetisation can reform before the next pulse sequence starts. Consequently, the magnitude of the acquired signal depends strongly on both T_E and T_R. It should be noted that although in the above discussion, the slice, phase and frequency gradients have been assumed to be along the z-, y- and x-axes, respectively, in an MRI experiment, they can be applied along any three orthogonal directions.

It should be noted that whilst one frequency gradient is sufficient to resolve the voxels along the x-axis, the entire process from slice selection to signal detection needs to be repeated multiple times with different phase gradients (ranging from relative maximum negative to relative maximum positive) to completely resolve the voxels along the y-axis. The reason behind this is will become apparent in the following sections.

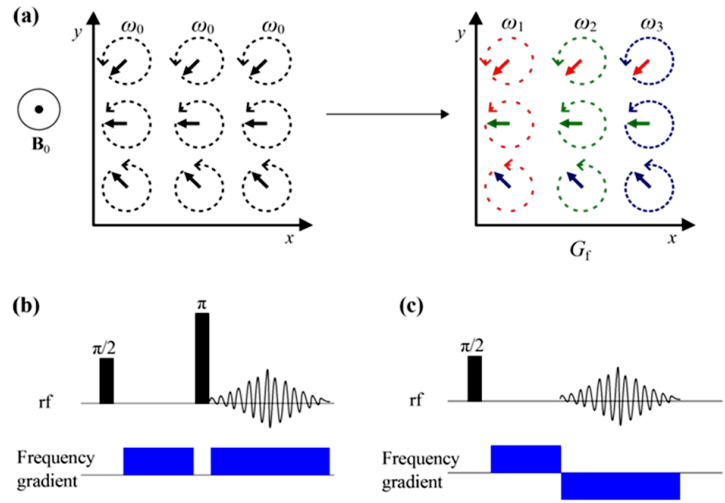

Figure 1.9 *(a) A pictorial representation of the frequency encoding process in MRI. After phase encoding along the y-axis, the signal is recorded in the presence of the frequency gradient along the x-axis. (b) 'spin-echo' scheme in which the sign of the magnetic gradient is effectively negated by the π pulse. In this scheme, phase dispersion due to magnetic inhomogeneities and chemical shifts and gradient-induced dispersions are refocused. (c) 'gradient-echo' scheme in which the magnetic gradients are antiphase. In this scheme, only gradient-induced dispersions are refocused.*

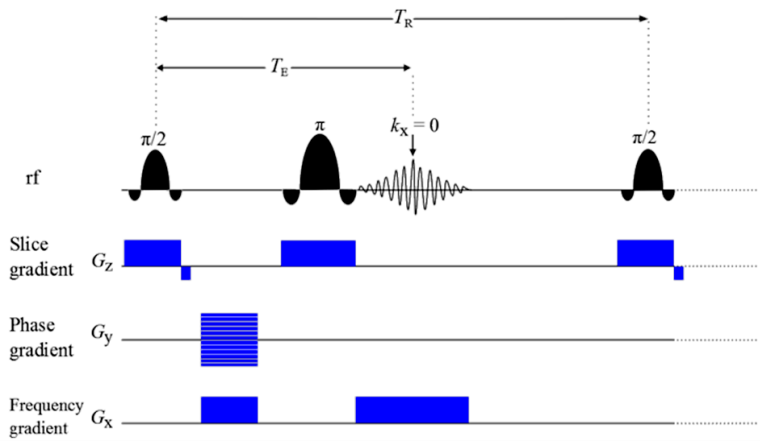

Figure 1.10 *A basic 'spin-echo' MRI pulse sequence. T_R is the repetition time and T_E is the time between the application of the initial rf pulse and the acquisition of the signal, also known as echo time. The phase gradient is drawn with equally spaced horizontal lines to indicate that its magnitude is incremented regularly when the sequence is repeated multiple times.*

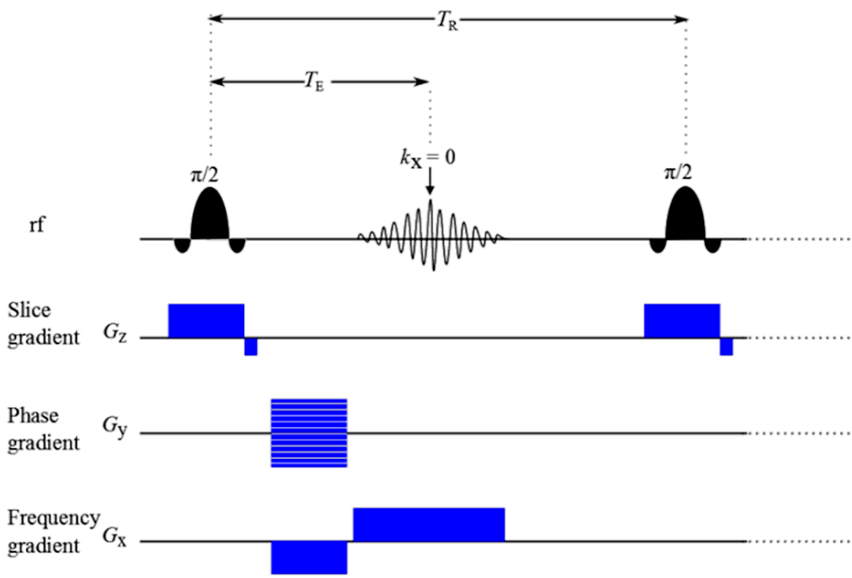

Figure 1.11 *A basic 'gradient-echo' MRI pulse sequence.*

1.3.6 Raw Data Matrix, K - Space and Q - Space

Since a number of scans are needed to obtain enough information on one slice that a detailed 2D MRI image can be reconstructed from it, an efficient way of storing the raw data is essential. An obvious choice is to digitize the recorded echo signal by sampling the amplitudes as a function of time. This digital form of an echo is stored as a row of complex numbers. The same process is repeated for the echoes obtained with different phase gradients and these rows of complex numbers are stacked on top of each other to give a (complex) raw data matrix with the bottommost row representing the maximum negative phase gradient and the topmost row maximum positive (Figure 1.12). It is usual to display the real and imaginary parts of the complex raw data matrix as separate matrices and convert the numbers to greyscale values.

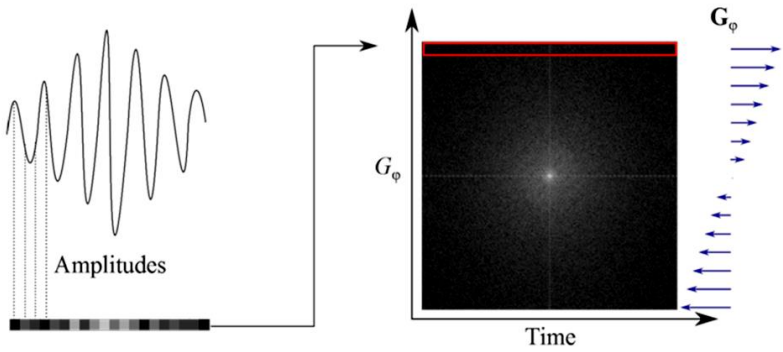

Figure 1.12 *An illustration of how the raw data is stored in MRI. The echoes are digitized by sampling their amplitudes as a function of time to give rows of complex numbers. The real (or imaginary) parts of the complex numbers can be displayed as greyscale values and stacked on top of each other to give a raw data matrix with the bottommost row representing the maximum negative phase gradient and the topmost row maximum positive.*

The raw data matrix has the dimensions of $N_\varphi \times N_f$ where N_φ is the number of phase gradients used and N_f is the number of data points recorded in the frequency encoding direction. The maximum signal is present in the centre of the raw data matrix because it corresponds to where the phase gradient was the weakest. The central region is mainly responsible for the image contrast. The outer regions of the raw data matrix have signals with low amplitudes due to strong phase gradients. These regions contain very little information about the image contrast and mainly contribute to the edge definition of the image.[2]

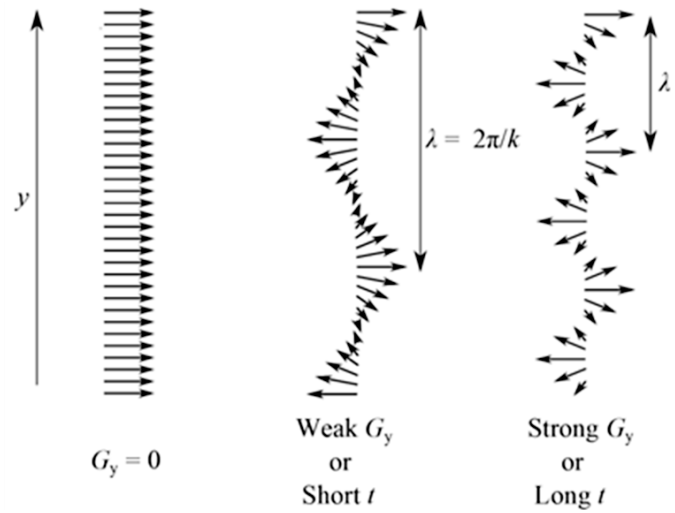

Figure 1.13 *The effect of the gradient strength and/or duration on the wave number, k. The external magnetic field is assumed to be applied along the z-axis and the spins are shown after the application of a π/2 pulse (i.e. the spins are in the transverse plane). When there is no gradient, all the spins are rotating at the same frequency and therefore, in the rotating frame of reference rotating at ω_0, the spins appear stationary with no phase difference. In the presence of a gradient, G_y, the spins start precessing with slightly different frequencies and hence a phase difference is induced, winding them into a helix of pitch $\lambda = 2\pi/k$. As the gradient strength and/or duration, t, increases, the pitch of a helix becomes smaller resulting in a shorter wavelength and correspondingly a higher k value.*

In MRI, the raw data matrix is often described in terms of wave numbers. A wave number, *k*, is the number of wavelengths per 2π units of distance i.e. $k = 2\pi/\lambda$ (rad m^{-1}), where λ is the wavelength. Analogous to frequency which is the number of oscillation per unit time, *k* is also called the spatial frequency. The spatial frequency is proportional to the gradient strength and the duration of the gradient. This is because a higher gradient strength gives a greater frequency differential and a longer duration gradient gives a greater phase differential which results in shorter wavelengths and correspondingly larger *k*-values (Figure 1.13).

Thus, the *k*-values along the phase and frequency encoding axes can be written as:

$$\begin{aligned} k_{\mathrm{y}} &= \gamma G_{\varphi} t \text{ and} \\ k_{\mathrm{x}} &= \gamma G_{\mathrm{f}} t, \end{aligned} \tag{1.14}$$

respectively. Also, after making the adjustments to Equation (1.9), the acquired signal (echo) can be written as a function of *k*,

$$\begin{aligned} S(k_{\mathrm{y}}) &= \int \rho(\mathrm{y}) \mathrm{e}^{i2\pi k_{\mathrm{y}} \mathrm{y}} d\mathrm{y}, \\ S(k_{\mathrm{x}}) &= \int \rho(\mathrm{x}) \mathrm{e}^{i2\pi k_{\mathrm{x}} \mathrm{x}} d\mathrm{x}. \end{aligned} \tag{1.15}$$

Combining these equations, the total signal from the selected slice can be written as:

$$S(k_{\mathrm{x}}, k_{\mathrm{y}}) = \int\int \rho(\mathrm{x},\mathrm{y}) \mathrm{e}^{i2\pi(k_{\mathrm{x}} x + k_{\mathrm{y}} y)} d\mathrm{x} d\mathrm{y}. \tag{1.16}$$

Consequently, the raw data matrix can be edited to replace 'time' with 'k_{x}' along the x-axis and 'G_{φ}' with 'k_{y}' along the y-axis. In other words, each point along the frequency encoding axis now corresponds to the k_{x} value and along the phase encoding axis to the k_{y} value (Figure 1.14). This description of the raw data matrix is known as the k-space formalism; and the raw data matrix itself is in k-space. The k-space formalism is a convenient method for describing the different ways of acquiring data, as explained in Section 0.

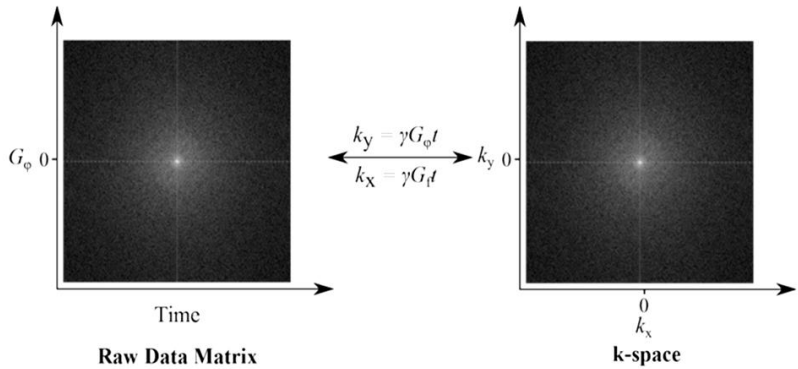

Figure 1.14 *Two descriptions of the raw data storage. Although both the matrices contain the same data, it is convenient to describe the signal as a function of the spatial frequency, k, as it makes it easier to describe different methods of acquiring data using various MRI pulse sequences.*

Similar to k-space which is conjugate to r-space (i.e., the laboratory frame), it is possible to define q-space which is conjugate to displacement $r_0 - r_1$. Obtaining q-space data allows construction of the nuclear spin self-correlation function, $P_s(r_1 - r_0, \Delta)$, which gives the conditional probability that a spin has been displaced by $r_0 - r_1$ during time Δ.[30] Nuclear spin displacement over a given period Δ may be tracked by using a pair of magnetic gradient pulses sandwiching a 180 ° rf pulse with the leading edges of the gradient pulses separated by Δ. q is defined as:

$$\mathbf{q} = \frac{\gamma \mathbf{g} \delta}{2\pi}, \tag{1.17}$$

where δ is the duration of the gradient pulses and g is a constant gradient giving a linear variation in the *z*-component of the magnetisation.

Evidently q has dimensions of inverse distance or m^{-1} in SI units and is analogous to k. q-space is useful for measuring both coherent motion (flow) and incoherent motion (diffusion) by measurement of the phase shift and attenuation

of the magnetisation helices using the pulse gradient spin-echo pulse sequence, respectively.[31] The first gradient winds the magnetisation into a helix; the rf pulse changes the chirality of the helix so that the next gradient pulse will unwind the helix. The helix persists for a duration Δ during which it is affected by flow and diffusion. Diffusion causes the magnetisation helix to attenuate as nuclear spins from one part of the helix diffuse into other parts causing the phases to cancel. If there is flow along the axis of the helix the whole helix will move and there will be an effective phase shift. After unwinding the helix with the second gradient pulse, the attenuation and phase shift persist although the magnetisation is now back in spatial coherence. Information on diffusion and flow can now be acquired simply by acquiring and analyzing the FID (for a variety of gradient strengths). A detailed calculation of the effects of diffusion and flow reveal that the signal will be affected according to:

$$S(\mathbf{g}) = S(0)\exp\left(-\gamma^2\delta^2\mathbf{g}\cdot\mathbf{D}\cdot\mathbf{g}(\Delta-\delta/3) - i\gamma\delta\mathbf{g}\cdot\mathbf{v}\Delta\right), \qquad (1.18)$$

where D is the diffusion tensor and v is the flow velocity. The first term in the exponent of Equation (1.18) gives the attenuation of the signal resulting from diffusion. Note that the greater the diffusion coefficient the greater the attenuation. Attenuation is also greater for larger diffusion time Δ and more powerful gradient pulses. By holding δ and Δ constant and measuring the attenuation for different g the diffusion tensor (or diffusion coefficient for isotropic diffusion) can be constructed. The second term in Equation (1.18) gives the phase shift of the signal which is a function of the velocity of the fluid parallel to the applied gradients. Measurements of phase shift for a variety of gradient strengths provide information on laminar fluid flow characteristics.

1.3.7 Image Reconstruction

In this section, reconstruction of an MRI image and the different ways of acquiring raw data are discussed using the k-space formalism.

Recalling that an MRI image is essentially the nuclear spin density in 'real space' (i.e. $\rho(x, y)$) and realizing from Equation (1.16) that the signal in k-space is in fact an inverse Fourier transform of the nuclear spin density in 'real space', it is evident that an MRI image of the selected slice can be reconstructed by the 2D Fourier transform of the signal in k-space (Figure 1.15) as given by:

$$\rho(\mathrm{x},\mathrm{y}) = \int\int S(k_\mathrm{x}, k_\mathrm{y})\mathrm{e}^{-i2\pi(k_\mathrm{x}x+k_\mathrm{y}y)}dk_\mathrm{x}dk_\mathrm{y}. \tag{1.19}$$

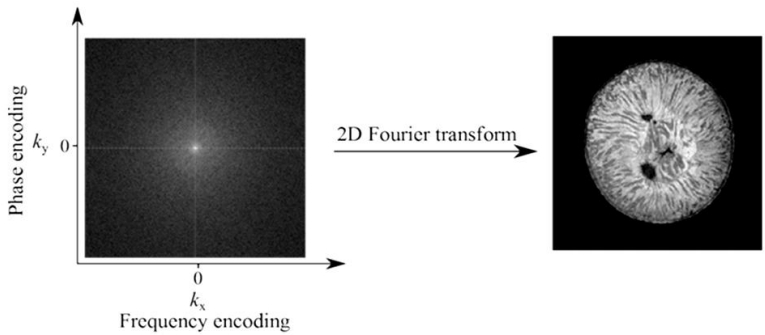

Figure 1.15 *An MRI image can be reconstructed by applying a 2D Fourier transform to the k-space data. Note only the magnitude of the k-space data is shown here (as k-space data from MRI is inherently complex).*

Note that even though k-space stores all the data that is required to construct an image, it is usually hard to predict what the final image will look like after the 2D Fourier transform of the k-space data. This is exemplified in Figure 1.16 by simulating some basic shapes and their k-space images.

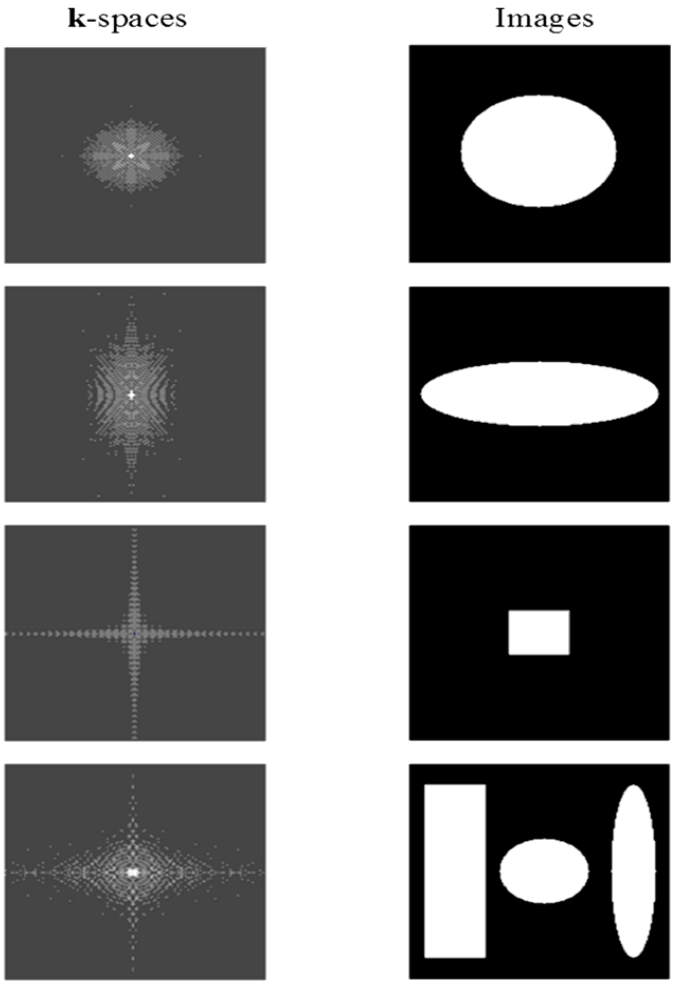

Figure 1.16 *A few simulated k-spaces and their corresponding images. For basic symmetrical shapes (circle, ellipse and square), it is possible to predict what the final image will look like from its k-space. But even for slightly complicated shapes (bottom most), the k-space becomes non indicative of the final image.*

It is important to acquire a detailed k-space data set to obtain a good quality image. In fact, the resolution of the image depends on the number of points in k-space. For example, a 128×256 k-space data set will result in an image with 128 pixels along the phase encoding axis and 256 pixels along the frequency encoding axis. So, the higher the number of points in k-space the better the image resolution. However, this requires a lot of time which is of prime importance in MRI. So, various pulse sequences have been designed to more

efficiently acquire sufficient k-space data. These sequences use different combinations of the phase and frequency gradients to map data in k-space in a quicker yet efficient manner. The geometry in which the k-space data is acquired is called a 'raster'. Two common examples are the Cartesian raster sampling and polar raster sampling.[4, 32]

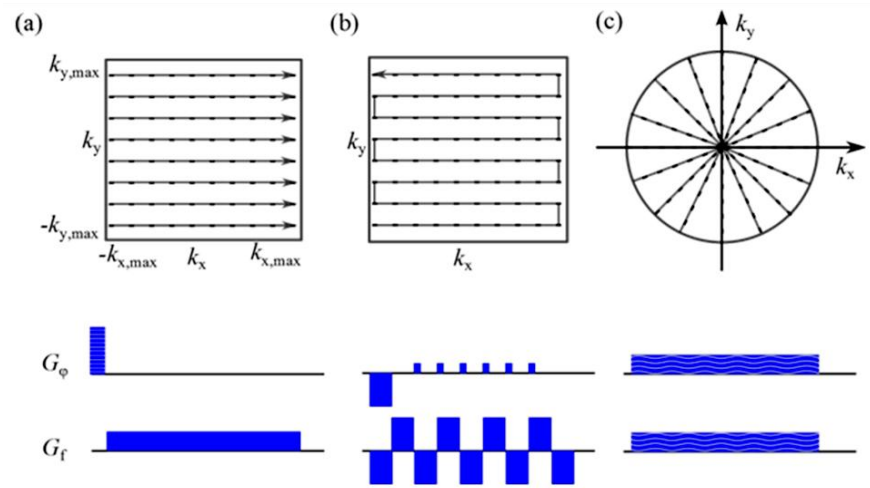

Figure 1.17 *Examples of different ways of acquiring k-space data in a geometry plane known as a 'raster'. Cartesian rasters can be obtained by 2D Fourier transform imaging pulse sequences such as a spin- or gradient-echo (a) and echo planar imaging pulse sequence (b). Projection reconstruction imaging pulse sequences, such as filtered back projection reconstruction pulse sequence (c), acquire k-space in polar rasters.*

The imaging process in which the selected slice is sampled in a Cartesian raster is called Fourier imaging. For example, the spin-echo and gradient-echo pulse sequences (Figure 1.10 and Figure 1.11) acquire the raw data in the Cartesian raster in a linear fashion as shown in Figure 1.17a. The stepping of the phase gradient from the most negative to most positive value in fixed intervals traverses k-space from $-k_{y,max}$ to $k_{y,max}$ and for each phase gradient, the applied frequency gradient samples the points from $-k_{x,max}$ to $k_{x,max}$. Another

example of the k-space traversal in the Cartesian raster is shown in Figure 1.17b by using an echo planar imaging pulse sequence.[33]

If k-space is traversed in a polar raster, the imaging process is called projection reconstruction imaging.[34] For example, the filtered back projection reconstruction pulse sequence and its polar raster are shown in Figure 1.17c. In this pulse sequence, the phase and frequency gradients are applied simultaneously following the sine and cosine relationships respectively, which is equivalent to applying a net gradient, $G = \sqrt{G_\varphi^2 + G_f^2}$ rotating around the polar angle, $\tan\theta = G_\varphi/G_f$.[4, 35]

1.4 MRI Contrast

Contrast between different tissue types is of utmost importance for every imaging modality. In MRI, this contrast results from spatial variations in the spin density of the observed nucleus and the physical and chemical environment of the nucleus.[32] These sources of contrast can be broadly classified into two categories: endogenous and exogenous. These are briefly discussed below.

1.4.1 Endogenous Sources

Important endogenous sources of contrast in MRI include spin density, relaxation times of the observed nuclei, magnetic susceptibility, diffusion and flow. Spin density contrast provides contrast on the basis of the number of spins (e.g. water protons) present in a voxel which differs across the tissue types. Since M_Z of each voxel is composed of the individual spins within that voxel, this variation in spin density affects the signal intensity in an MRI image. For example, in ^{1}H MRI, blood will appear brighter than muscles which in turn will appear much brighter than bones. Also, the molecular dynamics within the

tissue can affect T_1 and T_2 of the water protons. Therefore, the water protons present in different tissue types will have different relaxation times which again affect the net magnetisation and thus the signal intensity. By carefully engineering the imaging pulse sequence, it is also possible to obtain dynamic contrast in MRI due to diffusion and flow. An example of such pulse sequences is diffusion tensor imaging which can be used to probe the transport properties within a tissue e.g. diffusion of water in brain tissue (note that in such imaging techniques, the q-space formalism is used as well as the k-space formalism as explained in the section above).[36] In MRI, it is possible to set the experimental parameters like the repetition and echo time to enhance or diminish the contrast based on one contrast factor. For example, in T_1-weighted imaging, T_2 effects can be minimised by setting the echo time such that $T_E << T_2$ (more details on this can be found in the literature[37]). However, regardless of the parameters selected, the resulting image will always depend on other contrast factors to some extent.

The chemical environment of the observed nuclei can also induce contrast in MRI by affecting observables like chemical shift, spin-spin coupling constants and inter nuclear dipolar interactions. As an example, chemical shift imaging can be used to explore an extra dimension in the imaging experiment by probing the frequency spread due to different chemical shifts in a sample with two different chemical species (e.g. water and fat in biological systems).[38, 39] Due to this extra dimension, in its ultimate form, chemical shift imaging is sometimes referred to as 'four dimensional imaging' (three from the spatial axes and one from the chemical shift).[40] There are many other forms of contrast in MRI such as magnetic susceptibility,[41] temperature[42] and blood oxygenation level dependence (BOLD),[43, 44] details on which can be found elsewhere.

1.4.2 Exogenous Sources - Contrast Agents

The naturally occurring contrast between tissues is often insufficient to distinguish between diseased and healthy tissue especially in cases such as cancer. This gives rise to the need of contrast enhancement which is achieved by the use of chemicals known as contrast enhancement agents or contrast agents (CAs). In MRI, CAs modulate the relaxation times of water protons inside tissue to provide enhanced image contrast. The efficiency of a CA is measured in terms of its relaxivity (r_1 or r_2), which is defined as the change in the relaxation rate of water protons upon the addition of a CA, normalised to its concentration:

$$r_i = \frac{\Delta 1/T_i}{[\mathrm{CA}]}; \quad i = 1, 2. \tag{1.20}$$

All CAs increase both r_1 and r_2 to varying degrees, depending on whether they are categorised as positive (r_2/r_1 = 1–2) or negative (r_2/r_1 as high as 10 or more) CAs.[45] Negative or T_2 CAs are mostly constructed from superparamagnetic iron oxide (SPIO) and induce negative contrast by decreasing the signal intensity of the affected water protons.[46, 47] Positive or T_1 CAs are mainly comprised of paramagnetic metal ions such as Gd (III) chelated to multi-dentate ligands. These CAs induce positive contrast by increasing the signal intensity of the affected water protons and are, therefore, preferred over the negative CAs by MRI practitioners.[48, 49] There have also been some studies on ^{19}F-based CAs, which can be detected directly by ^{19}F MRI.[50, 51]

1.5 Applications

MRI has numerous applications in a vast variety of areas. However, unsurprisingly biological studies were and still remain the major application of

MRI. Due to its non-invasive and safe nature, MRI has been used to explore systems that were previously inaccessible. Also with the advancement of technology, clinical MRI scanners are constantly moving to higher fields to provide better image resolution, thus enabling clinicians to detect minor abnormalities which could not have been seen before. Some of the many clinical applications of MRI include the anatomical and physiological studies of embryo,[52] heart,[53, 54] kidney[55] and brain.[56, 57] With the use of CAs, MRI has also proven very efficient in detecting tumours.[58] Moreover, MRI has been used in plant studies to examine various aspects such as water flow characteristics in the phloem and xylem,[59, 60] freezing behaviour in plants[61] and plant histochemistry.[62]

MRI is also a distinctive tool to study the distribution of species and phase transitions in chemical systems. Some examples include the spatial localization of hydrogen in the H-Pd system,[63] observation of chromatographic bands of gadolinium chelates[64] and 3D imaging of $^{1}H_2$, $^{2}H_2$ and their isotopic mixtures.[65] Apart from these, there are many more applications ranging from food science,[66] polymers[67] to petrochemicals[68] which are outside the scope of this chapter.

References

[1] P. C. Lauterbur, *Nature*, 1973, 242, 190-191.

[2] M. A. Brown and R. C. Semelka, *MRI: basic principles and applications*, Wiley-Blackwell, New Jersey, 2010.

[3] M. E. Haacke, R. W. Brown, M. R. Thompson and R. Venkatesan, *Magnetic resonance imaging: physical principles and sequence design*, Wiley-Liss, New York, 1999.

[4] W. S. Price, in *Annu. Rep. NMR Spectrosc.*, ed. G. A. Webb, Academic Press, 1998, pp. 139-216.

[5] P. T. Callaghan, *Translational dynamics and magnetic resonance*, Oxford, Oxford, 2011.

[6] P. Storey, in *Magnetic resonance imaging: methods and biological applications*, ed. P. V. Prasad, Humana Press, New Jersey, 2006.

[7] P. T. Callaghan, *Principles of nuclear magnetic resonance microscopy*, Clarendon Press, Oxford, 1991.

[8] S. L. Talagala and I. J. Lowe, *Concepts Magn. Res.*, 1991, 3, 145-159.

[9] M. H. Levitt, *Spin dynamics: basics of nuclear magnetic resonance*, Wiley, New York, 2008.

[10] C. Westbrook, C. K. Roth and J. Talbot, *MRI in practice*, Blackwell, Oxford, 2005.

[11] J. Keeler, *Understanding NMR spectroscopy*, Wiley, Chichester, 2010.

[12] J. W. Akitt and B. E. Mann, *NMR and chemistry: an introduction to modern NMR spectroscopy*, Stanley Thornes, New York, 2000.

[13] F. A. Bovey, P. A. Mirau and H. Gutowsky, *Nuclear magnetic resonance spectroscopy*, Academic Press, 1988.

[14] M. E. Halse, A. Coy, R. Dykstra, C. Eccles, M. Hunter, R. Ward and P. T. Callaghan, *J. Magn. Reson.*, 2006, 182, 75-83.

[15] J. C. Hoch and A. S. Stern, *NMR data processing*, Wiley, New York, 1996.

[16] R. R. Ernst and W. A. Anderson, *Rev. Sci. Instrum.*, 1966, 37, 93-102.

[17] J. H. Nelson, *Nuclear magnetic resonance spectroscopy*, Prentice Hall, New Jersey, 2003.

[18] R. L. Vold, J. S. Waugh, M. P. Klein and D. E. Phelps, *J. Chem. Phys.*, 1968, 48, 3831.

[19] J. Kowalewski and L. Mäler, *Nuclear spin relaxation in liquids: theory, experiments, and applications*, Taylor & Francis, New York, 2006.

[20] E. L. Hahn, *Phys. Rev.*, 1950, 80, 580.

[21] H. Y. Carr and E. M. Purcell, *Phys. Rev.*, 1954, 94, 630.

[22] S. Meiboom and D. Gill, *Rev. Sci. Instrum.*, 1958, 29, 688-691.

[23] S. A. Huettel, A. W. Song and G. McCarthy, *Functional magnetic resonance imaging*, Sinauer, Massachusetts, 2004.

[24] D. G. Mitchell and M. S. Cohen, *MRI principles*, Saunders, Pennsylvania, 2004.

[25] S. Robertson, D. G. Hughes, Q. Liu and P. S. Allen, *Magn. Reson. Med.*, 1992, 25, 158-166.

[26] M. Burl and I. R. Young, in *Encyclopedia of Nuclear Magnetic Resonance*, eds. D. M. Grant and R. K. Harris, Wiley, New York, 1996, pp. 1841-1846.

[27] J. Hennig, *Concepts Magn. Res.*, 1991, 3, 179-192.

[28] J. Hennig, *Concepts Magn. Res.*, 1991, 3, 125-143.

[29] R. Mulkern, *Concepts Magn. Res.*, 1992, 4, 307-325.

[30] P. T. Callaghan, C. D. Eccles and Y. Xia, *J. Phys. E: Sci. Intrum.*, 1988, 21, 820.

[31] W. S. Price, *Concepts Magn. Res.*, 1997, 9, 299-336.

[32] Y. Xia, *Concepts Magn. Res.*, 1995, 8, 205-225.

[33] M. K. Stehling, R. Turner and P. Mansfield, *Science*, 1991, 254, 43-50.

[34] G. H. Glover and J. M. Pauly, in *Encyclopedia of Nuclear Magnetic Resonance*, eds. D. M. Grant and R. K. Harris, Wiley, New York, 1996, pp. 3772-3778.

[35] G. H. Glover and J. M. Pauly, *Magn. Reson. Med.*, 1992, 28, 275-289.

[36] P. J. Basser, J. Mattiello and D. LeBihan, *Biophys. J.*, 1994, 66, 259-267.

[37] M. L. Lipton, in *Totally accessible MRI*, Springer, New York, 2008, pp. 38-46.

[38] L. Brateman, *Am. J. Roentgenol.*, 1986, 146, 971-980.

[39] P. E. Sijens, M. J. Van Den Bent, P. J. C. M. Nowak, P. van Dijk and M. Oudkerk, *Magn. Reson. Med.*, 1997, 37, 222-225.

[40] A. Maudsley, S. Hilal, W. Perman and H. Simon, *J. Magn. Reson.*, 1983, 51, 147-152.

[41] J. L. Boxerman, L. M. Hamberg, B. R. Rosen and R. M. Weisskoff, *Magn. Reson. Med.*, 1995, 34, 555-566.

[42] D. L. Parker, V. Smith, P. Sheldon, L. E. Crooks and L. Fussell, *Med. Phys.*, 1983, 10, 321.

[43] S. Ogawa, T. M. Lee, A. R. Kay and D. W. Tank, *Proc. Natl. Acad. Sci. U. S. A.*, 1990, 87, 9868-9872.

[44] K. R. Thulborn, J. C. Waterton, P. M. Matthews and G. K. Radda, *Biochim. Biophys. Acta*, 1982, 714, 265-270.

[45] P. Caravan, J. J. Ellison, T. J. McMurry and R. B. Lauffer, *Chem. Rev.*, 1999, 99, 2293-2352.

[46] J. W. M. Bulte and D. L. Kraitchman, *NMR Biomed.*, 2004, 17, 484-499.

[47] Y. X. Wang, S. Hussain and G. Krestin, *Eur. Radiol.*, 2001, 11, 2319-2331.

[48] R. B. Lauffer, *Chem. Rev.*, 1987, 87, 901-927.

[49] A. Accardo, D. Tesauro, L. Aloj, C. Pedone and G. Morelli, *Coord. Chem. Rev.*, 2009, 253, 2193-2213.

[50] H. Peng, I. Blakey, B. Dargaville, F. Rasoul, S. Rose and A. K. Whittaker, *Biomacromolecules*, 2009, 10, 374-381.

[51] R. Díaz-López, N. Tsapis and E. Fattal, *Pharm. Res.*, 2010, 27, 1-16.

[52] D. Prayer, ed., *Fetal MRI*, Springer, New York, 2011.

[53] C. Higgins, *Am. J. Roentgenol.*, 1988, 151, 239-248.

[54] C. B. Higgins and A. d. Roos, eds., *MRI and CT of the cardiovascular system*, Lippincott Williams and Wilkins, Pennsylvania, 2006.

[55] P. V. Prasad, in *Magnetic resonance imaging: methods and biological applications*, ed. P. V. Prasad, Humana Press, New Jersey, 2006.

[56] L. Cecconi, A. Pompili, F. Caroli and E. Squillaci, in *MRI atlas of central nervous system tumors*, Springer, 1992, pp. 33-83.

[57] H. M. Duvernoy and B. Parratte, *The human brain: surface, three-dimensional sectional anatomy with MRI, and blood supply*, Springer Vienna, 1999.

[58] T. Barrett, H. Kobayashi, M. Brechbiel and P. L. Choyke, *Eur. J. Radiol.*, 2006, 60, 353-366.

[59] N. M. Holbrook, E. T. Ahrens, M. J. Burns and M. A. Zwieniecki, *Plant Physiol.*, 2001, 126, 27-31.

[60] C. W. Windt, F. J. Vergeldt, P. A. De Jager and H. Van As, *Plant Cell Environ.*, 2006, 29, 1715-1729.

[61] H. Ide, W. S. Price, Y. Arata and M. Ishikawa, *Tree Physiol.*, 1998, 18, 451-458.

[62] V. Sarafis, H. Rumpel, J. Pope and W. Kuhn, *Protoplasma*, 1990, 159, 70-73.

[63] E. W. McFarland and D. Lee, *J. Magn. Reson. A*, 1993, 102, 231-234.

[64] U. Tallarek, E. Baumeister, K. Albert, E. Bayer and G. Guiochon, *J. Chromatogr. A*, 1995, 696, 1-18.

[65] J. M. Moore, P. Blumler, M. H. Sherwood, C. G. Wade, G. W. Collins and E. R. Mapoles, *J. Magn. Reson. A*, 1994, 110, 248-251.

[66] B. Hills, *Magnetic resonance imaging in food science*, Wiley New York, 1998.

[67] M. Maryanski, R. Schulz, G. Ibbott, J. Gatenby, J. Xie, D. Horton and J. Gore, *Phys. Med. Biol.*, 1994, 39, 1437.

[68] W. P. Rothwell and H. Vinegar, *Appl. Opt.*, 1985, 24, 3969-3972.

Chapter 2

Fundamental Mathematical Formulation for the Theory, Dynamics and Applications of Magnetic Resonance Imaging

2

Fundamental Mathematical Formulation for the Theory, Dynamics and Applications of Magnetic Resonance Imaging

Michael Oluwaseun Dada and Omotayo Bamidele Awojoyogbe

Department of Physics, Federal University of Technology, Minna, Niger State, Nigeria

awojoyogbe@yahoo.com, abamidele@futminna.edu.ng

Abstract

All Magnetic Resonance Imaging (MRI) techniques are based on the Bloch NMR flow equations. Over the years, researchers have explored the Bloch NMR equations to significantly improve healthcare for accurate diagnosis, prognosis and treatment of deceases. However, MRI scan is still one of the most expensive anywhere. Method to achieve the best image quality with the lowest cost is still a big challenge. In this chapter, the generalized time dependent non homogenous second order differential equation derived from the Bloch NMR flow equations is modeled into basic and well known equations such as Bessel

equation, Diffusion equation, Wave equation, Schrödinger's equation, Legendre's equation, Euler's equation and Boubaker polynomials. Solutions to these equations are abundantly available in standard text books and several research studies on Mathematics, Physics, Chemistry and Engineering. Unexpected NMR/MRI methodological developments may be possible based on the analytical solutions of these equations and may further enhance the power of NMR. There will be spectacular applications in a variety of fields, ranging from cognitive neuroscience, biomedical engineering, imaging-science, molecular imaging to medicine, and providing unprecedented insights into chemical, biological and geophysical processes. This may initiate unforeseen technological and biomedical possibilities based on a much improved understanding of nature.

Keywords

Bloch NMR Flow Equation, Bessel Equation, Diffusion Equation, Wave Equation, Schrödinger's Equation, Legendre's Equation, Euler's Equation and Boubaker Polynomials.

2.1 Introduction

Advances in computers, mathematics, and science, is giving way to nonsurgical tools in the diagnosis of certain diseases. Besides X-ray imaging, now over 100 years old, the technologies include computed tomography (CT scans), positron-emission tomography (PET scans), ultrasound imaging, or sonography and magnetic resonance imaging (MRI).

Magnetic Resonance Imaging [1-34] uses a powerful magnetic field along with radio waves (not X-rays) and a computer to produce highly detailed "slice-by-slice" pictures of virtually all internal structures of the body. The results

enable physicians to examine parts of the body in minute detail and identify disease in ways that are not possible with other techniques. For example, MRI is one of the few imaging tools that can see through bone, making it an excellent tool for examining the brain and other soft tissue.

Patients must remain still during the imaging process. And because the scan takes place as the patient slides through a rather small tunnel in the machine, some people experience claustrophobia. In recent times, though, open MRI scanners have been developed for patients who are anxious or obese. Naturally, no metal objects such as pens, watches, jewelry, hairpins, and metal zippers as well as credit cards and other magnetically sensitive items are allowed into the examination room.

If a contrast fluid is used, there is a slight risk of allergic reaction, but the risk is less than that associated with the iodine-based substances commonly used with X-rays and CT scans. Otherwise, MRI poses no known risk to the patient. However, because of the effect of the strong magnetic field, patients with certain surgical implants or metal fragments from injuries may be unable to have an MRI. So if an MRI is recommended, be sure to tell your doctor and your MRI technologist if you have any of these things. MRI does not use potentially harmful radiation, and it is particularly good at detecting tissue abnormalities, especially those that may be obscured by bone.

At present, the main thrust of research seems to be to improve technology that is already available. For example, researchers are developing MRI scanners that operate with a much weaker magnetic field than that of present devices, thus considerably reducing costs. A new technology under development is called molecular imaging (MI). Designed to detect changes within the body at the molecular level, MI promises very early detection and treatment of disease. MRI technology has reduced the need for many painful, risky, and even

unneeded exploratory operations. And when imaging leads to early diagnosis and treatment of disease, the outcome may be much better. The equipment, however, is expensive—some machines costing well over a million dollars.

Despite over 50 years of the use of MRI for various investigations, the choice of technique parameters still relies to a great extent on experience. Research efforts to optimize the choice of parameter settings which yield sufficient image quality at the lowest possible cost are still rare. True optimization requires 1) estimation of the image quality needed to make a correct diagnosis and 2) methods to investigate all possible means of achieving this image quality in order to be able to decide which of them gives the lowest cost. Since the Bloch NMR equations are fundamental to all NMR/MRI computations, simulations and experiments, it can be fruitful, rewarding and beneficial with exciting results if these problems could be approached purely mathematically by solving the fundamental Bloch NMR equations analytically using all known mathematical techniques available both classical and quantum formulations. As such it presents significant challenge for the mathematical scientists, physicists, engineers and computer scientists to apply any of the fundamental and well known equations derived from the Bloch NMR flow equation as presented in this chapter to reveal most of the current unknowns but can enhance present understandings in the field of NMR/MRI.

Many of human diseases such as cancer, diabetes, arteriosclerosis and stroke, Alzheimer's disease, AIDS, etc, have all been known to be diseased conditions which take place at quantum (molecular) level. If we can see exactly what goes on at that level, we may have thorough understanding of their specific causes (or how they are caused), trace and monitor their progression and get the best cure for them. It is hoped that due to the ability of magnetic resonance to probe right to the fundamental level, we may be able to image human cellular

functions and such imaging modalities would definitely help in the understanding of the human diseased conditions. Information gathered from the images can then be added to the present medical database to make it more comprehensive and thus permit the physician to make a more specific diagnosis, prognosis and possibly the appropriate therapy. The basic challenge in this direction is finding the right mathematical frameworks which appropriately describe the processes involved.

2.2 The Bloch NMR Equations

Magnetic resonance is a physical phenomenon whereby nuclei containing an odd number of particles, when in the presence of a magnetic field, absorb radio frequency waves at specific (resonance) frequencies. The magnitude of the radio frequency (RF) waves provides information about the molecules containing the nuclei. The nuclei have an intrinsic spin property, which generates a local magnetic field. The nuclei are also precessing around their axes with a velocity that is proportional to the strength of the external field (the Larmor equation). The nuclei are therefore often called spins. Magnetic resonance imaging (MRI) is a non-invasive technique used to obtain tomographic images of any desired plane of the body and by means of magnetic resonance velocity mapping; it is possible to quantify blood flow. In MRI, the spins or magnetic moments are exposed to a strong external magnetic field which will force the spins to line up in alignment with the field. In this state, the spins are at the lowest energy state and posses longitudinal magnetic properties. The magnetization at this point is the equilibrium magnetization M_0. Applying a radio frequency (RF) signal in a direction perpendicular to the spins at their resonance (Larmor) frequency causes the spin to absorb energy and hence tips the net magnetization vector of all the spins toward the transverse plane. This

creates a net transverse magnetization vector. This vector will also precess about the external field and begin to relax towards alignment with the external field again (the lowest energy states). That is, the net magnetization moves back to align with the external field and hence we say that motion has occurred. This motion of the net magnetization is guided by a set of equations known as the Bloch equations which are the equations of motion for the net magnetization vector M of a sample of spins placed in a main magnetic field B_0 (where the components of M are M_x, M_y and M_z).

The behaviour of the transverse magnetization vector can be detected by the receiving unit in the scanner, the rf coil, and produce an rf signal. This rf signal is a fine wave at the Larmor frequency. The rate at which the net longitudinal magnetization vector builds up again to the equilibrium values is constant and is expressed by the T_1 relaxation time. The rate at which the transverse magnetization vector decreases is also constant and expressed by the T_2 relaxation time. T_1 and T_2 are the major parameters influencing the amplitude of the magnetic resonance signal. They depend on the molecular environment of the tissue and allow the distinction of different types of tissues.

The magnetic vector μ of a spinning, charged particle lies along the axis of rotation. The surrounding magnetic field symbolized by the vector H, exerts a torque that tends to bring μ and H into alignment. However, this torque also interacts with the angular momentum vector; the effect of this interaction is to cause the spin axis to describe a cone about the direction of the magnetic field. This phenomenon is called the Larmor precession, named after Sir Joseph Larmor, the Irish Physicist, who was the first to calculate the rate at which energy is radiated by an accelerated electron and the first to explain the splitting of spectrum lines by a magnetic field.

When the natural frequency of the precessing nuclear magnets corresponds to the frequency of a weak external radio wave striking the material, energy is absorbed from the radio wave. This selective absorption, called resonance, may be produced either by tuning the natural frequency of the nuclear magnets to that of a weak radio wave of fixed frequency or by tuning the frequency of the weak radio wave to that of nuclear magnets determined by the strong constant external magnetic field. This motion of the magnetization vector of uncoupled spins is easily expressed in terms of the Bloch NMR equations.

Almost all MRI concepts, dynamics and experiments are governed by the Bloch NMR equations. These equations relate the macroscopic model of magnetization to the applied radiofrequency, gradient and static magnetic fields. The dynamics of the changes in bodies containing NMR - sensitive nuclei, its physical changes (for example, freely diffusing or bound within a cavity) are carefully captured by the Bloch equation: a phenomenological equation describing the physics of magnetic moments – such as the moment of the water proton as a precessional gyroscopic motion in the presence of exponential damping (T_1 and T_2), perturbing magnetic fields (the fixed B_o, and the time - varying radiofrequency B_1).

The Bloch NMR equations are a set of coupled differential equations describing the behaviour of the macroscopic magnetization vector under any conditions. A form of the equations [35-41] is given as:

$$\frac{dM_x}{dt} = -\frac{M_x}{T_2} \tag{2.1}$$

$$\frac{dM_y}{dt} = \gamma M_z B_1(x) - \frac{M_y}{T_2} \tag{2.2}$$

$$\frac{dM_z}{dt} = -\gamma M_z B_1(x) + \frac{M_o - M_z}{T_1} \tag{2.3}$$

The parameters are defined in the macroscopic frame of reference M_x, M_y (Transverse magnetization) and M_z (longitudinal magnetization) are magnetizations along x, y and z directions, M_o is the equilibrium magnetization (along the z direction), $B_1(x)$ is the Radiofrequency (RF) magnetic field which can be constant, depending on x and/or t. T_1 is the longitudinal or spin-lattice relaxation time, T_2 is the transverse or spin-spin relaxation time and γ is the gyro magnetic ratio of fluid spins.

The total magnetic field is given as:

$$\vec{B} = \vec{B}_o + \vec{B}_1(x) \tag{2.4}$$

where B_o is the static magnetic field. All these parameters, as may be related to MRI will be discussed in full detail in section.

Since the MRI spin are always in motion, they must be treated with reference to their dynamics. The features of this dynamics are very much pronounced in fluids especially in biological systems.

From the kinematic theory of moving fluids, given a property M of the fluid, then the rate at which this property changes with respect to a point moving along with the fluid will be the total derivative:

$$\frac{dM}{dt} = \frac{\partial M}{\partial t} + \frac{\partial M}{\partial x}\frac{dx}{dt} + \frac{\partial M}{\partial y}\frac{dy}{dt} + \frac{\partial M}{\partial z}\frac{dz}{dt} \tag{2.5}$$

where $\frac{dx}{dt}$, $\frac{dy}{dt}$, $\frac{dz}{dt}$, are the components of the fluid velocity $\vec{v}$. The change in the parameter, *dM*, occurring during the time *dt*, at the position of a moving fluid particle which moves from *x, y, z* to *x+dx, y+dy, z+dz* during this time, will be:

$$dM = M(x+dx, y+dy, z+dz, t+dt) - M(x, y, z, t)$$

$$dM = \frac{\partial M}{\partial t}dt + \frac{\partial M}{\partial x}dx + \frac{\partial M}{\partial y}dy + \frac{\partial M}{\partial z}dz$$

equation (2.5) is obtained if $dt \to 0$. We can also write this equation in the form:

$$\frac{dM}{dt} = \frac{\partial M}{\partial t} + \frac{\partial M}{\partial x}v_x + \frac{\partial M}{\partial y}v_y + \frac{\partial M}{\partial z}v_z \tag{2.6}$$

and

$$\frac{dM}{dt} = \frac{\partial M}{\partial t} + \vec{v} \cdot \nabla M \tag{2.7}$$

where the second expression is shorthand for the first, in accordance with the conventions for using the symbol ∇. The total derivative $\frac{\mathrm{dM}}{\mathrm{dt}}$ is also a function of *x, y, z,* and *t*. A similar relation holds between partial and total derivative of any quantity, and we may write, symbolically,

$$\frac{d}{dt} = \frac{\partial}{\partial t} + v \cdot \nabla$$

where *v* is the fluid velocity and $\nabla = \frac{\partial}{\partial x} + \frac{\partial}{\partial y} + \frac{\partial}{\partial z}$.

The Bloch equations become:

$$\frac{dM_x}{dt} = \frac{\partial M_x}{\partial t} + v \cdot \nabla M_x = -\frac{M_x}{T_2} \tag{2.8}$$

$$\frac{dM_y}{dt} = \frac{\partial M_y}{\partial t} + v \cdot \nabla M_y = \gamma M_z B_1(x) - \frac{M_y}{T_2} \tag{2.9}$$

$$\frac{dM_z}{dt} = \frac{\partial M_z}{\partial t} + v \cdot \nabla M_z = -\gamma M_z B_1(x) + \frac{M_o - M_z}{T_1} \tag{2.10}$$

Considering fluid flow along horizontal x – direction, partial derivatives along the y and z directions are ignored. Therefore:

$$v \cdot \nabla M_x = v \frac{\partial M_x}{\partial x}$$

Similarly, $v \cdot \nabla M_y = v \frac{\partial M_y}{\partial x}$ and $v \cdot \nabla M_z = v \frac{\partial M_z}{\partial x}$

Equations (2.8 - 2.10) then become:

$$\frac{dM_x}{dt} = \frac{\partial M_x}{\partial t} + v \frac{\partial M_x}{\partial x} = -\frac{M_x}{T_2} \tag{2.11}$$

$$\frac{dM_y}{dt} = \frac{\partial M_y}{\partial t} + v \frac{\partial M_y}{\partial x} = \gamma M_z B_1(x) - \frac{M_y}{T_2} \tag{2.12}$$

$$\frac{dM_z}{dt} = \frac{\partial M_z}{\partial t} + v \frac{\partial M_z}{\partial x} = -\gamma M_z B_1(x) + \frac{M_o - M_z}{T_1} \tag{2.13}$$

2.3 The General Bloch NMR Flow Equation

The Bloch NMR flow equations can be written as:

$$\frac{\partial M_x}{\partial t} + v \frac{\partial M_x}{\partial x} = -\frac{M_x}{T_2} \tag{2.14}$$

$$\frac{\partial M_y}{\partial t} + v \frac{\partial M_y}{\partial x} = \gamma M_z B_1(x) - \frac{M_y}{T_2} \tag{2.15}$$

$$\frac{\partial M_z}{\partial t} + v\frac{\partial M_z}{\partial x} = -\gamma M_z B_1(x) + \frac{M_o - M_z}{T_1} \tag{2.16}$$

From equation (2.16), we have:

$$v\frac{\partial M_z}{\partial x} + \frac{\partial M_z}{\partial t} + \frac{M_z}{T_1} = -\gamma M_y B_1(x) + \frac{M_o}{T_1}$$

or

$$\left(v\frac{\partial}{\partial x} + \frac{\partial}{\partial t} + \frac{1}{T_1}\right)M_z = -\gamma M_y B_1(x) + \frac{M_o}{T_1}$$

$$M_z = \left(-\gamma M_y B_1(x) + \frac{M_o}{T_1}\right)\frac{1}{\left(v\frac{\partial}{\partial x} + \frac{\partial}{\partial t} + \frac{1}{T_1}\right)} \tag{2.17}$$

Substituting for M_z in equation (2.15) gives:

$$\frac{\partial M_y}{\partial t} + v\frac{\partial M_y}{\partial x} = \gamma\left(-\gamma M_y B_1(x) + \frac{M_o}{T_1}\right)\frac{1}{\left(v\frac{\partial}{\partial x} + \frac{\partial}{\partial t} + \frac{1}{T_1}\right)_z} B_1(x) - \frac{M_y}{T_2}$$

$$v\frac{\partial M_y}{\partial x}\left(v\frac{\partial}{\partial x} + \frac{\partial}{\partial t} + \frac{1}{T_1}\right) + \frac{\partial M_y}{\partial t}\left(v\frac{\partial}{\partial x} + \frac{\partial}{\partial t} + \frac{1}{T_1}\right) + \frac{M_y}{T_2}\left(v\frac{\partial}{\partial x} + \frac{\partial}{\partial t} + \frac{1}{T_1}\right) = \gamma\left(-\gamma M_y B_1(x) + \frac{M_o}{T_1}\right)B_1(x) \tag{2.18a}$$

For general pulsed NMR/MRI experiment $B_1(x)$ in equation (2.18a) will be replaced by $B_1(x,t)$. This is valid even ia a rotating frame. Equation (2.18a) can then be written in a more general form as [38]:

$$v^2\frac{\partial^2 M_y}{\partial x^2}+v\frac{\partial^2 M_y}{\partial x\partial t}+\frac{v}{T_1}\frac{\partial M_y}{\partial x}+v\frac{\partial^2 M_y}{\partial x\partial t}+\frac{\partial^2 M_y}{\partial t^2}+\frac{1}{T_1}\frac{\partial M_y}{\partial t}$$
$$+\frac{v}{T_2}\frac{\partial M_y}{\partial x}+\frac{1}{T_2}\frac{\partial M_y}{\partial t}+\frac{1}{T_1T_2}M_y$$
$$=-\gamma^2 {B_1}^2(x,t)M_y+\frac{\gamma B_1(x,t)M_o}{T_1}$$

$$v^2\frac{\partial M_y}{\partial x^2}+2v\frac{\partial^2 M_y}{\partial x\partial t}+v\left(\frac{1}{T_1}+\frac{1}{T_2}\right)\frac{\partial M_y}{\partial x}$$
$$+\left(\frac{1}{T_1}+\frac{1}{T_2}\right)\frac{\partial M_y}{\partial t}+\frac{\partial^2 M_y}{\partial t^2}+\left(\frac{1}{T_1T_2}+\gamma^2{B_1}^2(x,t)\right)M_y \qquad (2.18b)$$
$$=\frac{\gamma B_1(x,t)M_o}{T_1}$$

Equation (2.18b) is a general second order differential equation which can be applied to any fluid flow problem. At any given time t, we can obtain information about the system, provided that appropriate boundary conditions are applied. From equation (2.18b), we can obtain the diffusion equation, the wave equation, telephone and telegraph equations e.t.c, and solve them in terms of NMR parameters by the application of appropriate initial or boundary conditions. Hence, we could get very important information about the dynamics of the system. It should be noted however that the term $F_0\gamma B_1(x,t)$ is the forcing function $(F_0 = M_0/T_1)$. If the function is zero, we have a freely vibrating system; else, the system is undergoing a forced vibration.

2.4 The Time - Independent Bloch NMR Flow Equation

For a steady flow, all partial derivatives with respect to time can be set to zero (time independent). Hence equations (2.11-2.13) become:

$$v\frac{dM_x}{dx} = -\frac{M_x}{T_2} \tag{2.19}$$

$$v\frac{dM_y}{dx} = \gamma M_z B_1(x) - \frac{M_y}{T_2} \tag{2.20}$$

$$v\frac{dM_z}{dx} = -\gamma M_z B_1(x) + \frac{M_o - M_z}{T_1} \tag{2.21}$$

From equation (2.21) we write:

$$v\frac{dM_z}{dx} = -\gamma M_y B_1(x) + \frac{M_o}{T_1} - \frac{M_z}{T_1} \tag{2.22}$$

collecting the like term in equation (2.22) gives:

$$\left(v\frac{d}{dx} + \frac{1}{T_1}\right)M_z = -\gamma M_y B_1(x) + \frac{M_o}{T_1} \tag{2.23}$$

From equation (2.20, 2.21 and 2.23) we have,

$$v\frac{dM_y}{dx}\left(v\frac{d}{dx} + \frac{1}{T_1}\right) + \frac{M_y}{T_2}\left(v\frac{d}{dx} + \frac{1}{T_1}\right) = -\gamma^2 M_y B_1{}^2(x) + \frac{\gamma B_1(x) M_o}{T_1} \tag{2.24}$$

$$v^2\frac{d^2M_y}{dx^2} + v\left(\frac{1}{T_1} + \frac{1}{T_2}\right)\frac{dM_y}{dx} + \left(\frac{1}{T_1T_2} + \gamma^2 B_1{}^2(x)\right)M_y = \frac{\gamma B_1(x) M_o}{T_1}$$

$$v^2\frac{d^2M_y}{dx^2} + vT_o\frac{dM_y}{dx} + \left(T_g + \gamma^2 B_1{}^2(x)\right)M_y = \frac{M_o}{T_1}\gamma B_1(x) \tag{2.25}$$

Equation (2.25) is a time independent Bloch NMR flow equation [39-46].

2.5 The Time - Dependent Bloch NMR Flow Equation

For a flow that is independent of the space coordinate, *x*, that is, the magnetization does not change appreciably over a large *x* for a very long time, then all partial derivatives with respect to *x* could be set to zero (time dependent) [38]. From equation (2.3) we write:

$$\frac{dM_z}{dt} = -\gamma M_y B_1(t) + \frac{M_o}{T_1} - \frac{M_z}{T_1} \tag{2.26}$$

$$\left(\frac{d}{dt} + \frac{1}{T_1}\right) M_z = -\gamma M_y B_1(t) + \frac{M_o}{T_1} \tag{2.27}$$

Substituting for M_z in equation (2.27) into equation (2.26) gives:

$$\frac{dM_y}{dt}\left(\frac{d}{dt} + \frac{1}{T_1}\right) + \frac{M_y}{T_2}\left(\frac{d}{dt} + \frac{1}{T_1}\right) = -\gamma^2 B_1{}^2(t) M_y + \frac{\gamma B_1(t) M_o}{T_1}$$

$$\frac{d^2M_y}{dt^2} + T_o\frac{dM_y}{dt} + \left(T_g + \gamma^2 B_1{}^2(t)\right) M_y = \frac{M_o}{T_1}\gamma B_1(t)$$

$$\frac{d^2M_y}{dt^2} + \frac{1}{T_1}\frac{dM_y}{dt} + \frac{1}{T_2}\frac{dM_y}{dt} + \frac{1}{T_1T_2} M_y + \gamma^2 B_1{}^2(t) M_y = \frac{\gamma B_1(t) M_o}{T_1} \tag{2.28}$$

Equations (2.18b, 2.25, 2.28) are fundamental equations that can appropriately guide the generation of MRI signal of any kind in any coordinate. This is possible because these equations can easily be transformed to known equations commonly used in Mathematics, Physics and Engineering to solve real life problems. Some of the equations will be derived in the next sections.

2.6 Diffusion MRI Equation

Starting from equation (2.18b), we can assume a solution of the form:

$$M_y(x,t) = Ae^{\mu x+\eta t} \tag{2.29}$$

subject to the following theoretical conditions (the limiting case of non adiabatic small rf limit):

$$\gamma^2 B_1{}^2(x,t) << \frac{1}{T_1 T_2} \tag{2.30}$$

where μ and η are dependent on the NMR parameters and B_1 is independent of x and t.

Taking $\eta^2 = T_g$ and $2\eta = T_o$.

Equation (2.18b) becomes:

$$v^2 \frac{\partial^2 M_y}{\partial x^2} + T_o \frac{\partial M_y}{\partial t} = F_o \gamma B_1(x,t) \tag{2.31}$$

If we write

$$D = -\frac{v^2}{T_o} \tag{2.32}$$

Then equation (2.31) becomes:

$$\frac{\partial M_y}{\partial t} = D\frac{\partial^2 M_y}{\partial x^2} + F_o \gamma B_1(x,t) \tag{2.33}$$

This can be written in generalized co-ordinate as [47-55]:

$$\frac{\partial M_y}{\partial t} = D\nabla^2 M_y + F_o \gamma B_1(x,t) \tag{2.34}$$

If *D* represents the diffusion coefficient, then Equation (2.34) is the equation of diffusion of magnetization as the nuclear spins move. The function

$F_o \gamma B_1(x,t)$ is the forcing function, which shows that the application of the rf B_1 field has an influence on the diffusion of magnetization within a voxel. It is interesting to note that the dimension of Equation (2.33) exactly matches that of diffusion coefficient.

Equation (2.34) is only applicable when *D* in non – directional. That is, we have a constant diffusion coefficient (isotropic medium). In a later section equation (2.34) will be considered for restricted diffusion in various geometries.

This model would work quite well for molecules that move very short distances over a very considerable amount of time.

where

$$F_o = \frac{M_o}{T_1};\ T_g = \frac{1}{T_1 T_2} \text{ and } T_0 = \frac{1}{T_1} + \frac{1}{T_2}$$

γ is the gyromagnetic ratio, *D* is the diffusion coefficient, v is the fluid velocity, T_1 is the spin lattice relaxation time, T_2 is the spin relaxation time, M_o is the equilibrium magnetization, $B_1(x, t)$ is the applied magnetic field and M_y is the transverse magnetization. Solutions to equation (2.1) have been discussed by a number of analytical methods [12, 21], and for the present purpose it is sufficient to design the NMR system in such a way that the transverse magnetization M_y, takes the form of a plane wave,

2.7 Wave MRI Equation

Based on equations (2.29), we can write equation (2.18b) in the form wave equation:

$$v^2 \frac{\partial^2 M_y}{\partial x^2} + \frac{\partial^2 M_y}{\partial t^2} = F_o \gamma B_1(x,t) \tag{2.35}$$

Equation (2.35) only holds when:

$$\eta T_o = -\frac{1}{T_1 T_2}\ ,\ \ 2\eta = -T_o \tag{2.36}$$

In three dimensions equation (2.35) becomes:

$$v^2 \nabla^2 M_y + \frac{\partial^2 M_y}{\partial t^2} = F_o \gamma B_1(r,t) \tag{2.37}$$

In the spherical polar geometries, we can write equation (2.37) as:

$$v^2\left(\frac{\partial^2 M_y}{\partial r^2} + \frac{1}{r}\frac{\partial M_y}{\partial r} + \frac{1}{r^2}\frac{\partial^2 M_y}{\partial \phi^2}\right) + \frac{\partial^2 M_y}{\partial t^2} = F_o \gamma B_1(r,t) \tag{2.38}$$

When the rf B_1 field is at its peak, it is expected that the angle between the initial position and the resulting one is π. If the transverse magnetization is radially symmetric, we can write:

$$v^2\left(\frac{\partial^2 M_y}{\partial r^2} + \frac{1}{r}\frac{\partial M_y}{\partial r}\right) + \frac{\partial^2 M_y}{\partial t^2} = F_o \gamma B_1(r,t) \tag{2.39}$$

2.8 The Bessel Equation

We study the flow properties of the modified time independent Bloch NMR flow equations which describes the dynamics of the hydrogen atom under the influence of rf magnetic field as follows [1-10]:

$$v^2 \frac{d^2 M_y}{dx^2} + T_0 v \frac{dM_y}{dx} + S(x) M_y = \frac{M_0 \gamma B_1(x)}{T_1} \tag{2.40}$$

where $S(x) = \gamma^2 B_1^2(x) + T_g$, $T_g = \frac{1}{T_1 T_2}$, $T_0 = \frac{1}{T_1} + \frac{1}{T_2}$.

In equation (2.25), the spin velocity ν is constant and distance x can be defined as:

$$\nu = xT_o = \frac{x}{\tau} \text{ and } T_o = \frac{1}{\tau} \tag{2.41}$$

where T_o is the T1 an T2 relaxation rates of the spins which may be changing from pixel to pixel within the distance x. If the MRI signal is sampled when the applied radiofrequency energy successfully displaces most of the spin unto the transverse plane ($M_0 \approx 0$), equation (2.40) then becomes:

$$x^2 \frac{d^2 M_y}{dx^2} + T_o^2 x \frac{dM_y}{dx} + \left((k^2 x^2 + \beta^2\right) M_y = 0 \tag{2.42}$$

where

$$\gamma B_1(x) = \gamma G x \tag{2.43a}$$

$$\mathbf{k} = \gamma \mathbf{G} \mathbf{T}_o$$

and

$$\beta^2 = \frac{T_o^2}{T_1 T_2} \tag{2.43b}$$

Equation (2.42) is an equation transformable to Bessel function. When there is no gradient G, all the spins are rotating at the same frequency and therefore, in the rotating frame of reference at rotating at ω_o, the spins appears stationary with no phase difference. In the presence of gradient G, the spins start presecing with slightly difference frequencies winding them into a helix and hence a phase difference is induced. As the gradient strength and/or duration τ, increases, the pith of a helix become becomes smaller resulting in a smaller wavelength and correspondingly a higher k value.

The equation for the total MRI signal from a slice in the x, y, pane is:

$$S(k_x, k_y) = \int \int f(x, y) e^{-i(k_x x + k_y y)} dxdy \tag{2.44a}$$

where

$$k_y = \gamma G_y T_o \tag{2.44b}$$

$$k_x = \gamma G_x T_o \tag{2.44c}$$

Equation (2.44) is the fundamental equation for MRI. It gives detail information on MRI signal within a voxel. f(x, y) is the distribution of the MRI signal over the slice d, at the time just after the excitation. Equations (2.44b, 2.44c) are the k- values along the phase and frequency encoding axes respectively. The Fourier transform of equation (2.44) is:

$$f(x, y) = \int \int S(k_x, k_y) e^{-i(k_x x + k_y y)} dk_x k_y \tag{2.45}$$

2.9 The NMR Schrodinger Wave Equation

NMR is a quantum phenomenon and like all other quantum phenomena is best described by quantum mechanics. It will be enormously valuable if quantum mechanics as a tool for understanding the NMR microscopic nature is developed in parallel with the growth of NMR Physics. It is our goal to develop the Bloch NMR flow equations in terms of quantum mechanical wave functions which can predict analytically and precisely the probability of events or outcome.

In equation (2.25) It is convenient to use as dependent variable the departure of the stream function from its classical form and write:

$$M_y = \psi(x)e^{\lambda x} \tag{2.46}$$

where $\lambda = \frac{-1}{2vT_o}$, ν is the instantaneous velocity of the fluid and ψ(x) is a special function of the transverse magnetization M_y, which depends on the dynamical state of the fluid particle. When M_y is maximum and M_o is minimum (say $M_o = 0$). For a maximum value of M_y (when $M_o = 0$) we can write equation (2.40) as:

$$\frac{d^2\psi}{dx^2} + \frac{\gamma^2 B_1^2}{v^2}\psi = 0 \tag{2.47a}$$

subject to the following conditions:

(i) $$e^{\lambda x} \neq 0 \tag{2.47b}$$

(ii) Resonance condition exists at Larmor frequency

$$f_o = \gamma B - \omega = 0$$

(iii) $\gamma^2 B_1^2(x) >> \left(T_g - T_R\right)$

where $T_g = \frac{1}{T_1 T_2}$, $T_R = \frac{1}{4T_o^2}$ and $\frac{1}{T_o} = \frac{1}{T_1} + \frac{1}{T_2}$.

γ denotes the gyromagnetic ratio of fluid spins; ω/2π is the rf excitation frequency; fo/γ is the off- resonance field in the rotating frame of reference. T1 and T2 are the spin-lattice and spin-spin relaxation times respectively, the reciprocals of T1 and T2 are defined as relaxation rates. rf B1 is treated as constant and of the order of 1G. The exponential function in equation (2.47b) can be defined as follows,

$$e^{\lambda x} = \sum_{n=0}^{\infty} \frac{(\lambda x)^n}{n!} = F(x) \tag{2.48}$$

Equation (2.48) is extremely useful in obtaining approximations to complicated formulas, valid when x is small. In particular, when:

$$x = 4vT_o \tag{2.49}$$

Equation (2.47c) becomes:

$$F(x) = 1$$

Equation (2.27a) becomes the Schrödinger wave equation in 1-D given by [40]:

$$\frac{d^2\psi}{dx^2} + \frac{2\mu}{\hbar^2}(E - E_p(x))\psi = 0 \tag{2.50}$$

where

$$\frac{\gamma^2 B_1^2(x)}{v^2} = \frac{2\mu}{\hbar^2}[E - E_p(x)] \tag{2.51}$$

E and $E_p(x)$ are the total energy and potential energy of the fluid particle respectively. Equation (2.48) can easily be solved if E_p is constant, with a solution of the form $e^{\pm ikx}$. But if E_p varies with x, one may find solution in the form:

$$\psi(x) = e^{iw(x)} \tag{2.52}$$

To simplify this problem,

$$\text{Let } k(x) = \left\{\frac{2\mu}{\hbar^2}(E - v)\right\}^{\frac{1}{2}} \tag{2.53}$$

Substituting equation (2.52) into (2.51) gives equation for the x-dependent phase.

Hence, w(x) satisfies:

$$i\frac{d^2w}{dx^2}-\left(\frac{dw}{dx}\right)^2+[k(x)]^2=0 \tag{2.54}$$

Note that equations (2.54) and (2.51) are equivalent.

For a free particle, $\frac{d^2w}{dx^2}=0$. Hence we can neglect the second derivative term $\frac{d^2w}{dx^2}$ in equation (2.54) and this will lead to our first approximationw_0 in w.

$$\begin{aligned}&\left(\frac{dw_0}{dx}\right)^2=[k(x)]^2\\&w'^2_0=[k(x)]^2\\&w'_0=k(x)\\&w_0=\pm\int^x k(x)dx+C\end{aligned} \tag{2.55}$$

Equation (2.55) is the approximation to the wave function.

Setting up a successive approximation; from equation (2.54), we can write:

$$\left(\frac{dw}{dx}\right)^2=i\frac{d^2w}{dx^2}+[k(x)]^2 \tag{2.56}$$

By substituting the n[th] approximation on the R.H.S, we obtain the (n+1)[th] approximation by quadrature.

$$w_{n+1}=\pm\int^x\sqrt{[k(x)]^2+iw_n''(x)}dx+C_{n+1} \tag{2.57}$$

Thus, for n=0, we obtain:

$$w_1 = \pm\int^{x} \sqrt{\left[k(x)\right]^2 + iw_0''(x)}dx + C_1$$
$$w_1 = \pm\int^{x} \sqrt{\left[k(x)\right]^2 + ik'(x)}dx + C_1 \tag{2.58}$$

It is expected that w_1 be close to w_0, for this approximation to approximate the wave function.

Hence

$$|k'(x)| << |k^2(x)| \tag{2.59}$$

If condition (2.59) holds, one may expand the integrand in equation (58) and obtain:

$$w_1(x) \cong \pm\int\left[k(x) + \frac{i}{2}\frac{k'(x)}{k(x)}\right]dx + C_1$$
$$w_1(x) \cong \pm\int^{x} k(x)dx + \frac{i}{2}\log k(x) + C_1 \tag{2.60}$$

The constant of integration only affects the normalization of $\Psi(x)$. It can be neglected until the desired approximation is made.

Hence the approximation in equation (2.54-2.60), called WKB approximation, leads to the approximate wave function.

$$\psi(x) = \frac{1}{\sqrt{k(x)}} e^{\pm i\int^{x} k(x)dx} \tag{2.61}$$

Taking k(x) as the effective wave number, we can define our wavelength as $\lambda(x) = \frac{2\pi}{k(x)}$.

Therefore condition (2.59) can be re-written as:

$$\lambda(x)\left|\frac{dp}{dx}\right| << |p(x)| \tag{2.62}$$

Consider a turning point and assuming that except in its immediate neighbourhood, WKB approximation is applicable. Changing the dependent and independent variables, we write:

$$u(x) = \sqrt{k(x)}\psi(x) \tag{2.63}$$

And

$$y = \int^{x} k(x)dx \tag{2.64}$$

By manipulating, we obtain:

$$\frac{d^2u}{dy^2} + \left[\frac{1}{4k^2}\left(\frac{dk}{dy}\right)^2 - \frac{1}{2k}\frac{d^2k}{dy^2} + 1\right]u = 0 \tag{2.65}$$

Substituting the particular value of k(x) given by equation (2.63), the integral of equation (2.64) can be evaluated, and choosing the lower limit of the integration as 0, we obtained,

$$y = \frac{\sqrt{2\mu}}{\sqrt{\hbar^2}\sqrt{E}}\left(\sqrt{E}\cdot\sqrt{\frac{4\pi\varepsilon_0 Ex^2 + ze^2x}{4\pi\varepsilon_0}} + \frac{ze^2}{4\pi\varepsilon_0}\ln\left\{\frac{\sqrt{4\pi\varepsilon_0 Ex} + \sqrt{4\pi\varepsilon_0 Ex + ze^2}}{\sqrt{ze^2}}\right\}\right) \tag{2.66}$$

where y is the measure of the distance from the classical turning point. Hence y is small near the turning point assuming the two limits of integration are close to each other. At points very far to the left or right from the turning point, WKB is applicable.

Expressing y in terms of k, and finding its derivative, equation (2.65) becomes:

$$\frac{d^2u}{dy^2}+\left(1+\frac{5}{36y^2}\right)u=0 \tag{2.67}$$

Let us attempt the solution of equation (2.67) in the form:

$$u(y)=y^{\lambda}\int e^{yt}\,f(t)\cdot dt \tag{2.68}$$

Substituting (2.68) into (2.67) gives,

$$\int\left[\lambda(\lambda-1)+2\lambda yt+y^2t^2+y^2+\frac{5}{36}\right]e^{yt}f(t)\cdot dt=0 \tag{2.69}$$

Choosing λ such that the terms which are constant in y vanish, it is required that:

$$\lambda(\lambda-1)+\frac{5}{36}=0 \tag{2.70a}$$

$$\lambda=\frac{1}{6},\frac{5}{36} \tag{2.70b}$$

The remaining expression in equation (2.69) is:

$$\int f(t)\left[2\lambda t+\left(1+t^2\right)\frac{d}{dt}\right]e^{yt}\cdot dt=0 \tag{2.71}$$

Integrating by part,

$$\int f(t)\left[2\lambda t+\left(1+t^2\right)\frac{d}{dt}\right]e^{yt}\cdot dt=0 \tag{2.72}$$

$$\int\left\{2\lambda tf(t)-\frac{d}{dt}\left[\left(1+t^2\right)f(t)\right]\right\}e^{yt}dt+\int\frac{d}{dt}\left[\left(1+t^2\right)f(t)e^{yt}\right]=0 \tag{2.73}$$

To successfully construct a solution of the proposed form in equation (2.68), the integrand in the first integral should be made to vanish and the path of integration is chosen so that the second integral disappears.

We therefore require:

$$2\lambda tf(t)=\frac{d}{dt}\left[\left(1+t^2\right)f(t)\right]$$

$$f(t)=f(0)\left(1+t^2\right)^{\lambda-1}$$

Using equation (2.70), we can write the general form of (2.67) as:

$$\frac{d^2u}{dy^2}+\left(1+\frac{\lambda(\lambda-1)}{y^2}\right)u=0 \tag{2.74}$$

It should be noted that if u_λ is a solution, $u_{1-\lambda}$ is also a solution of equation (2.74).

In deriving the WKB connection formulas,

$$u_\lambda^+(y)=y^\lambda\int_i^{-i\infty}\frac{e^{yt}}{\left(1+t^2\right)^{1-\lambda}}dt \tag{2.75}$$

and

$$u_\lambda^-(y)=y^\lambda\int_{-i}^{-i\infty}\frac{e^{yt}}{\left(1+t^2\right)^{1-\lambda}}dt \tag{2.76}$$

Recall that λis not an integer, this implies that $t = \pm i$ are branch points of the function $(1 + t^2)^{1-\lambda}$.

The asymptotic expansion of u_λ^+ and u_λ^- are needed in the WKB expansion for large imaginary values of y. Hence, we substitute in $u_\lambda^\pm$:

$$t = \pm i - \frac{z}{y} \tag{2.77}$$

and obtain:

$$u_\lambda^\pm(y) = -y^{\lambda-1} e^{\pm iy} \int_0^\infty \left(\frac{z^2}{y^2} \mp 2i \frac{z}{y} \right)^{\lambda-1} e^{-z} dz \tag{2.78}$$

For |y|large enough, a reasonable approximation to the asymptotic expansion of u is obtained by expanding the parenthesis in powers of $\frac{z}{y}$, then integrate term by term,

$$u_\lambda^+(y) \approx \mp 2^{\lambda-1} i \Gamma(\lambda) e^{\pm iy - i\lambda\left(\pi \mp \frac{\pi}{2}\right)} \tag{2.79}$$

Since $\left(\pi \mp \frac{\pi}{2}\right)$ is negative imaginary, the form of this solution is in agreement with the WKB approximation in the region of negative kinetic energy.

When the variable y is negative real, a different integration path is taken; we will choose a different limit of integration.

$$u_\lambda(y) = y^\lambda \int_{-i}^{+i} \frac{e^{yt}}{\left(1 + t^2\right)^{1-\lambda}} dt \tag{2.80}$$

and

$$u_\lambda(y) \approx 2^\lambda i\Gamma(\lambda)e^{i\pi\lambda}\cos\left(y+\lambda\frac{\pi}{2}\right). \tag{2.81}$$

This solution also agrees with the WKB approximation in the region of positive kinetic energy. Unless λ is half-integral, $u_\lambda(y)$ and $u_{1-\lambda}(y)$ are two linearly independent solution.

From equations (2.75), (2.76) and (2.80), we can define:

$$u_\lambda(y) = u_\lambda^-(y) - u_\lambda^+(y) \tag{2.82}$$

and

$$u_{1-\lambda}(y) = u_{1-\lambda}^-(y) - u_{1-\lambda}^+(y) \tag{2.83}$$

Near the turning point $y=0$, the integral in equation (2.80) gives:

$$u_\lambda(y) = i\frac{\Gamma\left(\frac{1}{2}\right)\Gamma(\lambda)}{\Gamma\left(\lambda+\frac{1}{2}\right)}y^\lambda\left[1+0\left(y^2\right)\right] \tag{2.84}$$

This proves that the wave function in equations (2.46, 2.47, 2.50):

$$\psi = \frac{u}{\sqrt{k}} \propto \frac{u}{y^{\frac{1}{6}}} \tag{2.85}$$

Perfectly behave well near the turning point.

2.10 Time - Dependent NMR Schrodinger Equaion

At the molecular level the diffusion coefficient of a fluid particle is defined as:

$$D = -\frac{\hbar}{2im} \tag{2.86}$$

Substituting equation (2.86) into equation (2.33) gives the time-dependent NMR Schrodinger equation:

$$i\hbar \frac{\partial M_y}{\partial t} = -\frac{\hbar^2}{2m}\frac{\partial^2 M_y}{\partial x^2} + \frac{i\hbar F_o}{T_o}\gamma B_1(x,t) \tag{2.87}$$

We can represent the transverse magnetization M_y as the propagation of a plane harmonic wave in the x-direction in the form of equation (2.29) and write:

$$M_y(x,t) = Ae^{i(kx-\omega t)} \tag{2.88}$$

where A is a constant, $\mu = ik$ and $\eta = -i\omega$. Equation (2.88) represents a typical propagating matter wave where k, measures the wave vector and ω, the angular frequency of the wave. Splitting the transverse magnetization into its space and time parts in the form,

$$M_y(x,t) = X(x)T(t) \tag{2.89}$$

we can write

$$X(x) = A_1 e^{ikx} \tag{2.90}$$

$$T(t) = A_2 e^{-i\omega t} \tag{2.91}$$

A wave in the x-t space propagates by joint oscillations represented by equations (2.90-2.91) each of them is capable of exciting the other. By differentiating equation (2.90) twice and making use of:

$$E = \frac{k^2\hbar^2}{2m} + E_p(x) \tag{2.92}$$

we arrive at the Schrodinger's time-independent wave equation, expressed as in equation (2.50):

$$-\frac{\hbar^2}{2m}\frac{d^2X(x)}{dx^2} = [E - E_p(x)]X(x) \tag{2.93}$$

where E and $E_p(x)$ denote the total and potential energies of the particle respectively. Similarly, differentiating equation (2.91) once with respect to t and making use of the relation:

$$E = \hbar\omega$$

we arrive at,

$$-i\hbar\frac{dT(t)}{dt} = ET(t) \tag{2.94}$$

On combining equations (2.93) and (2.94) one arrives at the Schrodinger's time-dependent equation.

$$\hat{H}M_y(x,t) = i\hbar\frac{\partial}{\partial t}M_y(x,t) \tag{2.95}$$

where the $\hat{H}$ operator stand for:

$$\hat{H} = -\frac{\hbar^2}{2m}\frac{\partial^2}{\partial x^2} + E_p(x) \tag{2.96}$$

Equation (2.96) is well-known as the Hamiltonian of the particle. It should be mentioned that equation (2.95) is the true equation representing the motion of microscopic particles through a given space. This is applicable even during a quantum measurement. As long as matter exhibits wave-particle dualism,

equations (2.93) and (2.94) are both valid and their solutions are readily obtainable by solving them. The most general wave function may then be obtained by forming a suitable product of X(x) and T(t).

2.11 NMR Legendre Equation and Boubaker Polynomial

When M_y is maximum and M_o is minimum (say $M_o = 0$), we can write equation (2.25) as:

$$\frac{d^2M_y}{dx^2} + \frac{T_0}{v}\frac{dM_y}{dx} + \frac{S(x)}{v^2}M_y = 0 \tag{2.97}$$

Where $T_0 = \frac{1}{T_1} + \frac{1}{T_2}$, $S(x) = \gamma^2 B_1^2(x) + \frac{1}{T_1 T_2}$.

If we then write that:

$$\frac{T_0}{v} = \frac{1}{l}\cot\frac{x}{l} \tag{2.98}$$

$$\frac{S(x)}{v^2} = \frac{1}{l^2}n(n+1) \tag{2.99}$$

The small rf limiting condition:

$$\frac{1}{T_1 T_2} >> \gamma^2 B_1^2(x)$$

gives

$$\frac{1}{T_1 T_2 v^2} = \frac{n(n+1)}{l^2}$$

$$\frac{l^2}{T_1 T_2 v^2} = n(n+1)$$

where l is a parameter in length or any other unit of distance. It is worthy of note that equation (2.97) is obtainable from the expression:

$$\frac{d^2M_y}{dx^2}+\frac{T_0}{v}\frac{dM_y}{dx}+\frac{S(x)}{v^2}M_y=\frac{M_0}{T_1}\gamma B_1(x) \tag{2.100}$$

Under two conditions

1. When the rf $B_1(x)$ field applied, has a maximum value, so that M_y is maximum; and $M_0 \approx 0$.
2. When the rf $B_1(x)$ field is just removed (so that $\gamma B_1(x) = 0$).

However, condition 1 seems to favour most part of this particular write-up.

Equation (2.97) can then be written as:

$$\begin{aligned}&\frac{d^2M_y}{dx^2}+\frac{1}{l}\cot\frac{x}{l}\frac{dM_y}{dx}+\frac{1}{l^2}n(n+1)M_y=0\\&\frac{d^2M_y}{dx^2}+\frac{1}{l}\frac{\cos\frac{x}{l}}{\sin\frac{x}{l}}\frac{dM_y}{dx}+\frac{1}{l^2}n(n+1)M_y=0\end{aligned} \tag{2.101}$$

Multiplying equation (2.101) all through by $sin\frac{x}{l}$, it follows that:

$$\sin\frac{x}{l}\frac{d^2M_y}{dx^2}+\frac{1}{l}\cos\frac{x}{l}\frac{dM_y}{dx}+\frac{1}{l^2}\sin\frac{x}{l}n(n+1)M_y=0 \tag{2.102}$$

It would be noted that:

$$\sin\frac{x}{l}\frac{d^2M_y}{dx^2}+\frac{1}{l}\cos\frac{x}{l}\frac{dM_y}{dx}\equiv\frac{d}{dx}\left(\sin\frac{x}{l}\frac{dM_y}{dx}\right) \tag{2.103}$$

Hence, equation (2.101) becomes:

$$\frac{d}{dx}\left(\sin\frac{x}{l}\frac{dM_y}{dx}\right)+\frac{1}{l^2}\sin\frac{x}{l}n(n+1)M_y=0 \tag{2.104}$$

If we define:

$$\varsigma=\cos\frac{x}{l} \tag{2.105}$$

and

$$\frac{dM_y}{dx}=\frac{dM_y}{d\varsigma}\cdot\frac{d\varsigma}{dx}=-\frac{1}{l}\sin\frac{x}{l}\frac{dM_y}{d\varsigma}$$

$$\sin\frac{x}{l}\frac{dM_y}{dx}=-\frac{1}{l}\sin^2\frac{x}{l}\frac{dM_y}{d\varsigma}$$

but

$$-\sin^2\frac{x}{l}=\cos^2\frac{x}{l}-1=\varsigma^2-1 \tag{2.106}$$

Therefore, equation (2.106) becomes:

$$\frac{d}{dx}\left\{\frac{\left(\varsigma^2-1\right)}{l}\frac{dM_y}{d\varsigma}\right\}+\frac{1}{l^2}\sin\frac{x}{l}n(n+1)M_y=0$$

Since $\frac{\mathrm{d}}{\mathrm{dx}}=\frac{\mathrm{d}}{\mathrm{d}\varsigma}\cdot\frac{\mathrm{d}\varsigma}{\mathrm{dx}}$, it follows that:

$$\begin{aligned}
&\frac{d}{d\varsigma}\left\{\frac{\left(\varsigma^2-1\right)}{l}\frac{dM_y}{d\varsigma}\right\}\frac{d\varsigma}{dx}+\frac{1}{l^2}\sin\frac{x}{l}n(n+1)M_y=0\\
&\frac{d}{d\varsigma}\left\{\frac{\left(\varsigma^2-1\right)}{l}\frac{dM_y}{d\varsigma}\right\}\left(-\frac{1}{l}\sin\frac{x}{l}\right)+\frac{1}{l^2}\sin\frac{x}{l}n(n+1)M_y=0\\
&\frac{d}{d\varsigma}\left\{\frac{-\left(\varsigma^2-1\right)}{l}\frac{dM_y}{d\varsigma}\right\}\frac{1}{l}\sin\frac{x}{l}+\frac{1}{l^2}\sin\frac{x}{l}n(n+1)M_y=0
\end{aligned} \tag{2.107}$$

Now, since l is a constant, equation (2.107) can be written as:

$$\frac{d}{d\varsigma}\left\{\left(1-\varsigma^2\right)\frac{dM_y}{d\varsigma}\right\}\frac{1}{l^2}\sin\frac{x}{l}+\frac{1}{l^2}\sin\frac{x}{l}n(n+1)M_y=0 \tag{2.108}$$

Dividing all through by $\frac{1}{l^2}\sin\frac{x}{l}$, it follows that:

$$\frac{d}{d\varsigma}\left\{\left(1-\varsigma^2\right)\frac{dM_y}{d\varsigma}\right\}+n(n+1)M_y=0 \tag{2.109}$$

$$\left(1-\varsigma^2\right)\frac{d^2M_y}{d\varsigma^2}-2\varsigma\frac{dM_y}{d\varsigma}+n(n+1)M_y=0 \tag{2.110}$$

This is the Legendre differential equation and has a solution of the form:

$$M_y=C_1P_n(\varsigma)+C_2Q_n(\varsigma) \tag{2.111}$$

where $P_n(\varsigma)$ are the Legendre polynomials of the first kind (which are regular at finite points) while $Q_n(\varsigma)$ are the Legendre Polynomials [56-57] of the second kind (which are singular at ±1). C_1 and C_2 are constants.

It is worthy of note that $P_n(\varsigma)$ and $Q_n(\varsigma)$ are two linearly independent solutions to the equation (2.110). We can write that:

$$M_y=P_n(\varsigma)=M_{yn}$$

$$\left\{P_n(\varsigma)=P_0\left(\cos\frac{x}{l}\right)\right\}$$

$$P_n(\varsigma)=\sum_{p=0}^{m}\frac{(-1)^p(2n-2p)!}{2^n\,p!(n-p)!(n-2p)!}\varsigma^{n-2p} \tag{2.112a}$$

$$M_{yn}(\varsigma)=\sum_{p=0}^{m}\frac{(-1)^p(2n-2p)!}{2^n\,p!(n-p)!(n-2p)!}\varsigma^{n-2p} \tag{2.112b}$$

$$m=\frac{n}{2}\,or\,\frac{(n-1)}{2}$$

whichever m is an integer. We have noted earlier that this expression implies

$$m=\frac{2n+\left((-1)^n-1\right)}{4}$$

Then,

$$M_{yn}(\varsigma)=\sum_{p=0}^{\frac{2n+\left((-1)^n-1\right)}{4}}\frac{(-1)^p(2n-2p)!}{2^n\,p!(n-p)!(n-2p)!}\varsigma^{n-2p}$$

This solution can be written as:

$$\mathrm{M_{yn}}(\varsigma)=\frac{(2\mathrm{n}-1)(2\mathrm{n}-3)...1}{\mathrm{n}!}\left\{\varsigma^{\mathrm{n}}-\frac{\mathrm{n}(\mathrm{n}-1)}{2(2\mathrm{n}-1)}\varsigma^{\mathrm{n}-2}+\frac{\mathrm{n}(\mathrm{n}-1)(\mathrm{n}-2)(\mathrm{n}-3)}{2\cdot4(2\mathrm{n}-1)(2\mathrm{n}-3)}\varsigma^{\mathrm{n}-4}+...\right\} \tag{2.113}$$

However, for the purpose of the Boubaker Polynomial problem [44, 59], we shall write that:

$$\mathrm{M_{yn}}(\varsigma)=\frac{(2\mathrm{n})!}{2^{\mathrm{n}}\,\mathrm{n}!\mathrm{n}!}\left\{\varsigma^{\mathrm{n}}-\frac{\mathrm{n}(\mathrm{n}-1)}{1!\cdot2(2\mathrm{n}-1)}\varsigma^{\mathrm{n}-2}+\frac{\mathrm{n}(\mathrm{n}-1)(\mathrm{n}-1)(\mathrm{n}-2)(\mathrm{n}-3)}{2!\cdot2(2\mathrm{n}-1)(2\mathrm{n}-2)(2\mathrm{n}-3)}\varsigma^{\mathrm{n}-4}+...\right\}$$

(The expression of equation (2.113) is based on some sort of definition which is a choice made in order that $P_n(1)=1$).

$$M_{yn}(\varsigma)=\frac{(2n)!}{2^n n!n!}\left\{\varsigma^n-\frac{n(n-1)}{2(2n-1)\cdot(1!)}\varsigma^{n-2}+\frac{n(n-1)(n-1)(n-2)(n-3)}{2(2n-1)(2n-2)(2n-3)\cdot(2!)}\varsigma^{n-4}+\ldots\right\} \tag{2.114}$$

For

$$\frac{(2n)!}{2^n n!n!}=1 \tag{2.115a}$$

Then, $n=0,1$.

This condition will cause all other co-efficient of ς to be equal to zero, so that:

$$M_{yn}(\varsigma)=\varsigma^n \text{ (for } n=0,1) \tag{2.115b}$$

However in addition to condition (2.115a), if we can establish that:

$$\left.\begin{aligned} n-4&\equiv\frac{n\cdot(n-1)}{2\cdot(2n-1)}\\ n-8&\equiv\frac{n\cdot(n-1)(n-1)(n-2)}{2\cdot(2n-1)(2n-2)(2n-3)}\\ n-12&\equiv\frac{n\cdot(n-1)(n-1)(n-2)(n-3)}{2\cdot(2n-1)(2n-2)(2n-3)(2n-4)(2n-5)}\end{aligned}\right\} \tag{2.116}$$

It follows that:

$$M_{yn}(\varsigma)=1\cdot\varsigma^n-(n-4)\varsigma^{n-2}+\frac{(n-8)(n-3)}{2!}\varsigma^{n-4}-\frac{(n-12)(n-4)(n-5)}{3!}\varsigma^{n-6}+\ldots$$

Since the sum:

$$\frac{(n-8)(n-3)}{2!}\varsigma^{n-4}-\frac{(n-12)(n-4)(n-5)}{3!}\varsigma^{n-6}+\ldots$$

is given by

$$\sum_{p=2}^{4}{}^{\frac{2n+\left((-1)^n-1\right)}{}}\left\{\frac{(n-4p)}{p!}\prod_{j=p+1}^{2p-1}(n-j)\right\}(-1)^p\varsigma^{n-2p}$$

we obtain:

$$\begin{aligned}M_{yn}(\varsigma) &= 1\cdot\varsigma^{n}-(n-4)\varsigma^{n-2} \\ &+\sum_{p=2}^{4}{}^{\frac{2n+\left((-1)^n-1\right)}{}}\left\{\frac{(n-4p)}{p!}\prod_{j=p+1}^{2p-1}(n-j)\right\}(-1)^p\varsigma^{n-2p}\end{aligned} \tag{2.117}$$

If the assumption would hold for the Legendre polynomials of the second kind, the procedure can be extended to the transverse magnetization in the form:

$$M_{yn}(\varsigma)=Q_n(\varsigma) \tag{2.118}$$

2.12 Sturm - Liouville Problem

The Legendre polynomials have the orthogonality property expressed as follows:

$$\int_{-1}^{1}P_m(x)P_n(x)dx=\frac{2}{2n+1}\delta_{mn} \tag{2.119}$$

The reason for this orthogonality property is that Legendre differential equation can be viewed as a Sturm-Liouville problem:

$$\frac{d}{dx}\left\{(1-x^2)\frac{d}{dx}y(x)\right\}=-\lambda y(x) \tag{2.120}$$

where $y(x)\equiv M_y$ and $\lambda\equiv n(n+1)$.

We shall make an assumption of the form:

$$\frac{T_0}{v} = \frac{1}{l}\cot\frac{x}{l} \tag{2.121}$$

(l is a parameter to be determined). Hence, the time-independent equation:

$$\frac{d^2M_y}{dx^2} + \frac{T_0}{v}\frac{dM_y}{dx} + \frac{S(x)}{v^2}M_y = 0$$

becomes

$$\frac{d^2M_y}{dx^2} + \frac{1}{l}\cot\frac{x}{l}\frac{dM_y}{dx} + \frac{S(x)}{v^2}M_y = 0 \tag{2.122}$$

$$\begin{aligned}
&\frac{d^2M_y}{dx^2} + \frac{1}{l}\frac{\cos\frac{x}{l}}{\sin\frac{x}{l}}\frac{dM_y}{dx} + \frac{S(x)}{v^2}M_y = 0 \\
&\sin\frac{x}{l}\frac{d^2M_y}{dx^2} + \frac{1}{l}\cos\frac{x}{l}\frac{dM_y}{dx} + \sin\frac{x}{l}\frac{S(x)}{v^2}M_y = 0 \\
&\frac{d}{dx}\left(\sin\frac{x}{l}\frac{dM_y}{dx}\right) + \sin\frac{x}{l}\frac{S(x)}{v^2}M_y = 0
\end{aligned} \tag{2.123}$$

If $n(n+1) = l^2\sin\frac{x}{l}\frac{S(x)}{v^2}$:

$$\sin\frac{x}{l}\frac{S(x)}{v^2} = \frac{1}{l^2}n(n+1)$$

It follows that:

$$\frac{d}{dx}\left(\sin\frac{x}{l}\frac{dM_y}{dx}\right) + \frac{1}{l^2}n(n+1)M_y = 0$$

$$\frac{d}{dx}\left(\sin\frac{x}{l}\frac{dM_y}{dx}\right) = -\frac{1}{l^2}n(n+1)M_y$$

$$l^2 \frac{d}{dx}\left(\sin\frac{x}{l}\frac{dM_y}{dx}\right) = -n(n+1)M_y$$

Since l^2 is not dependent on x, we have:

$$\frac{d}{dx}\left(l^2 \sin\frac{x}{l}\frac{dM_y}{dx}\right) = -n(n+1)M_y \tag{2.124}$$

This is not exactly the same as equation (2.120), but equation (2.124) can be compared to the form that we stated earlier, that is,

$$\frac{d}{dx}\left\{p(x)\frac{dy}{dx}\right\} + \left[q(x) + \lambda r(x)\right]y = 0$$

Where

$$y(x) \equiv M_y,$$

$$p(x) = l^2 \sin\frac{x}{l}$$

and

$$\left[q(x) + \lambda r(x)\right] = n\cdot(n+1) = l^2 \sin\frac{x}{l}\frac{S(x)}{v^2} = \frac{l^2}{v^2}\sin\frac{x}{l}\left(\gamma^2 B_1^2(x) + T_g\right)$$

However, earlier on, equation (2.109) is given as:

$$\begin{aligned}\frac{d}{d\varsigma}\left\{\left(1-\varsigma^2\right)\frac{dM_y}{d\varsigma}\right\} + n(n+1)M_y &= 0\\ \frac{d}{d\varsigma}\left\{\left(1-\varsigma^2\right)\frac{dM_y}{d\varsigma}\right\} = -n(n+1)M_y &= 0\end{aligned} \tag{2.125}$$

Hence, for ς -dependence, we can establish Sturm-Liouvile problem in the form of equation (2.125).

2.13 The Diffusion - Advection Equation

The diffusion - advection equation is a differential equation describing the process of diffusion and advection. For the investigation of the diffusion process of magnetization in a fluid moving at a uniform velocity which is constant in time, we have to take the process of advection into consideration. The equation which describes such a process is known as the Advection equation. The advection equation is the partial differential equation that governs the motion of a conserved scalar as it is advected by a known velocity field. It is derived using the scalar's conservation law, together with Gauss's theorem, and taking the infinitesimal limit.

The diffusion - advection equation (a differential equation describing the process of diffusion and advection) is obtained by adding the advection operator to the main diffusion equation. In the Cartesian coordinates, the advection operator [58] is:

$$\vec{v} \cdot \nabla = v_x \frac{\partial}{\partial x} + v_y \frac{\partial}{\partial y} + v_z \frac{\partial}{\partial z}$$

where the velocity vector v has components v_χ, v_y and v_z in the x, y and z directions respectively.

Therefore, from Equation (2.18b),

$$\begin{aligned} & v^2 \frac{\partial^2 M_y}{\partial x^2} + 2v \frac{\partial^2 M_y}{\partial x \partial t} + vT_o \frac{\partial M_y}{\partial x} + T_o \frac{\partial M_y}{\partial t} \\ & + \frac{\partial^2 M_y}{\partial t^2} + \left\{ T_g + \gamma^2 B_1{}^2 (x,t) \right\} M_y \\ & = F_o \gamma B_1 (x,t) \end{aligned}$$

we can write:

$$\frac{\partial^2 M_y}{\partial t^2} + 2v\frac{\partial^2 M_y}{\partial x \partial t} + \left\{T_g + \gamma^2 B_1{}^2(x,t)\right\} M_y = 0 \tag{2.126}$$

It then follows that:

$$v^2 \frac{\partial^2 M_y}{\partial x^2} + vT_o \frac{\partial M_y}{\partial x} + T_o \frac{\partial M_y}{\partial t} = F_o \gamma B_1(x,t) \tag{2.127}$$

$$vT_o \frac{\partial M_y}{\partial x} + T_o \frac{\partial M_y}{\partial t} = -v^2 \frac{\partial^2 M_y}{\partial x^2} + F_o \gamma B_1(x,t) \tag{2.128}$$

If we multiply Equation (2.128) all through by $\frac{1}{T_0}$, it follows therefore that:

$$v\frac{\partial M_y}{\partial x} + \frac{\partial M_y}{\partial t} = -\frac{v^2}{T_o}\frac{\partial^2 M_y}{\partial x^2} + \frac{F_o}{T_o}\gamma B_1(x,t) \tag{2.129}$$

where

$$D = -\frac{v^2}{T_o} \tag{2.130}$$

hence,

$$v\frac{\partial M_y}{\partial x} + \frac{\partial M_y}{\partial t} = D\frac{\partial^2 M_y}{\partial x^2} + \frac{F_o}{T_o}\gamma B_1(x,t) \tag{2.131}$$

Provided that D is the diffusion coefficient, and since v is the fluid velocity, equation (2.131) is the diffusion – advection equation for the NMR transverse magnetization. It is very interesting to note that equation (2.131) exactly match the advection equation without any special transformation whatsoever.

2.14 The Euler NMR Equation

Based on equations (2.18b) and (2.29), we can define for constant fluid velocity v, and $\gamma^2 B_1^2$ field:

$$\eta T_o = -T_g; \qquad \nu\mu T_o = \gamma^2 B_1^2 \tag{2.132}$$

or

$$\eta T_o = \gamma^2 B_1^2; \qquad \nu\mu T_o = -T_g \tag{2.133}$$

When the maximum NMR signal is received at maximum rf B_1 field and $M_o = 0$, equation (2.18b) becomes:

$$v^2 \frac{\partial^2 M_y}{\partial x^2} + 2v \frac{\partial^2 M_y}{\partial x \partial t} + \frac{\partial^2 M_y}{\partial t^2} = 0 \tag{2.134}$$

This equation can also be derived for the following rf limits.

For $\gamma^2 B_1^2 \ll T_g$, equation (2.18b) becomes:

$$v^2 \frac{\partial^2 M_y}{\partial x^2} + 2v \frac{\partial^2 M_y}{\partial x \partial t} + \frac{\partial^2 M_y}{\partial t^2} = 0 \tag{2.135}$$

provided that:

$$\eta T_o + v\mu T_o = -T_g \tag{2.136}$$

$$\eta = v\mu \tag{2.137}$$

$$2\eta T_o = -T_g \tag{2.138}$$

Equation (2.135) is called the Euler's equation.

2.15 Analytical Solutions to the Generalized Bloch NMR Flow Equation

It may be very important to solve equation (2.18b) analytically for various applications as highlighted in the editorial introduction.

Equation (2.18b) can be written as:

$$\begin{aligned} &v^2\frac{\partial^2 M_y}{\partial x^2}+2v\frac{\partial^2 M_y}{\partial x\partial t}+\frac{\partial^2 M_y}{\partial t^2}+T_o v\frac{\partial M_y}{\partial x}\\ &+T_o\frac{\partial M_y}{\partial t}\left(\gamma^2 B_1^2(x,t)+T_g\right)M_y\\ &=F_o\gamma B_1(x,t)\end{aligned} \tag{2.139}$$

where

$$T_0=\frac{1}{T_1}+\frac{1}{T_2},\ T_g=\frac{1}{T_1T_2},\ F_0=\frac{M_0}{T_1}$$

Because of the difficulty involved in solving a differential equation which does not have its coefficient to be constant, we shall consider the case where:

$$T_g >> \gamma^2 B_1^2(x,t)$$

Equation (2.139) becomes:

$$\begin{aligned} &v^2\frac{\partial^2 M_y}{\partial x^2}+2v\frac{\partial^2 M_y}{\partial x\partial t}+\frac{\partial^2 M_y}{\partial t^2}+T_0 v\frac{\partial M_y}{\partial x}+T_0\frac{\partial M_y}{\partial t}+T_g M_y\\ &=F_0\gamma B_1(x,t)\end{aligned} \tag{2.140}$$

Assuming a solution of the form:

$$M_y(x,t)=\sum_{n=1}^{\infty}U_n(t)\sin\frac{n\pi x}{\rho}+\sum_{n=1}^{\infty}U_n(t)\cos\frac{n\pi x}{\rho} \tag{2.141}$$

(ρ is a term which has the same dimension as x). It then follows that:

$$\frac{\partial M_y}{\partial x} = \sum_{n=1}^{\infty}\left(\frac{n\pi}{\rho}\right)U_n(t)\cos\frac{n\pi x}{\rho} - \sum_{n=1}^{\infty}\left(\frac{n\pi}{\rho}\right)U_n(t)\sin\frac{n\pi x}{\rho}$$

$$\frac{\partial^2 M_y}{\partial x} = -\sum_{n=1}^{\infty}\left(\frac{n\pi}{\rho}\right)^2 U_n(t)\sin\frac{n\pi x}{\rho} - \sum_{n=1}^{\infty}\left(\frac{n\pi}{\rho}\right)^2 U_n(t)\cos\frac{n\pi x}{\rho}$$

$$\frac{\partial^2 M_y}{\partial x \partial t} = \sum_{n=1}^{\infty}\left(\frac{n\pi}{\rho}\right)\frac{dU_n}{dt}\cos\frac{n\pi x}{\rho} - \sum_{n=1}^{\infty}\left(\frac{n\pi}{\rho}\right)\frac{dU_n}{dt}\sin\frac{n\pi x}{\rho}$$

$$\frac{\partial M_y}{\partial t} = \sum_{n=1}^{\infty}\frac{dU_n}{dt}\sin\frac{n\pi x}{\rho} + \sum_{n=1}^{\infty}\frac{dU_n}{dt}\cos\frac{n\pi x}{\rho}$$

$$\frac{\partial^2 M_y}{\partial t^2} = \sum_{n=1}^{\infty}\frac{d^2U_n}{dt^2}\sin\frac{n\pi x}{\rho} + \sum_{n=1}^{\infty}\frac{d^2U_n}{dt^2}\cos\frac{n\pi x}{\rho}$$

Equation (2.140) then becomes:

$$\begin{aligned}
&-v^2\sum_{n=1}^{\infty}\left(\frac{n\pi}{\rho}\right)^2 U_n\sin\frac{n\pi x}{\rho} - v^2\sum_{n=1}^{\infty}\left(\frac{n\pi}{\rho}\right)^2 U_n \\
&\cos\frac{n\pi x}{\rho} + 2v\sum_{n=1}^{\infty}\left(\frac{n\pi}{\rho}\right)\frac{dU_n}{dt}\cos\frac{n\pi x}{\rho} \\
&-2v\sum_{n=1}^{\infty}\left(\frac{n\pi}{\rho}\right)\frac{dU_n}{dt}\sin\frac{n\pi x}{\rho} + \sum_{n=1}^{\infty}\frac{d^2U_n}{dt^2}\sin\frac{n\pi x}{\rho} + \sum_{n=1}^{\infty}\frac{d^2U_n}{dt^2}\cos\frac{n\pi x}{\rho} \\
&+T_0 v\sum_{n=1}^{\infty}\left(\frac{n\pi}{\rho}\right)U_n\cos\frac{n\pi x}{\rho} - T_0 v\sum_{n=1}^{\infty}\left(\frac{n\pi}{\rho}\right)U_n \\
&\sin\frac{n\pi x}{\rho} + T_0\sum_{n=1}^{\infty}\frac{dU_n}{dt}\sin\frac{n\pi x}{\rho} + T_0\sum_{n=1}^{\infty}\frac{dU_n}{dt}\cos\frac{n\pi x}{\rho} + T_g\sum_{n=1}^{\infty}U_n \\
&\sin\frac{n\pi x}{\rho} + T_g\sum_{n-=1}^{\infty}U_n\cos\frac{n\pi x}{\rho} = F_0\gamma B_1(x,t)
\end{aligned} \tag{2.142}$$

$$\sum_{N=1}^{\infty}\left\{\frac{d^2U_n}{dt^2}\sin\frac{n\pi x}{\rho}+T_0\frac{dU_n}{dt}\sin\frac{n\pi x}{\rho}-2v\left(\frac{n\pi}{\rho}\right)\frac{dU_n}{dt}\sin\frac{n\pi x}{\rho}\right.$$
$$+T_gU_n\sin\frac{n\pi x}{\rho}-T_0v\left(\frac{n\pi}{\rho}\right)U_n\sin\frac{n\pi x}{\rho}-v^2\left(\frac{n\pi}{\rho}\right)^2U_n\sin\frac{n\pi x}{\rho}$$
$$+T_0\frac{dU_n}{dt}\cos\frac{n\pi x}{\rho}+2v\left(\frac{n\pi}{\rho}\right)\frac{dU_n}{dt}\cos\frac{n\pi x}{\rho}+T_gU_n \qquad (2.143)$$
$$\cos\frac{n\lambda x}{\rho}+T_0v\left(\frac{n\lambda}{\rho}\right)U_n\cos\frac{n\pi x}{\rho}-v^2\left(\frac{n\pi}{\rho}\right)^2U_n$$
$$\left.\cos\frac{n\lambda x}{\rho}+T_0v\left(\frac{n\lambda}{\rho}\right)U_n\cos\frac{n\pi x}{\rho}-v^2\left(\frac{n\pi}{\rho}\right)^2U_n\cos\frac{n\pi x}{\rho}\right\}$$

$$\sum_{n=1}^{\infty}\left\{\frac{d^2U_n}{dt^2}+T_0\frac{dU_n}{dt}+2v\left(\frac{n\pi}{\rho}\right)\frac{dU_n}{dt}+T_gU_n-T_0v\left(\frac{n\pi}{\rho}\right)U_n-v^2\left(\frac{n\pi}{\rho}\right)^2U_n\right\}\sin\frac{n\pi x}{\rho}$$
$$+\sum_{n=1}^{\infty}\left\{\frac{d^2U_n}{dt^2}+T_0\frac{dU_n}{dt}+2v\left(\frac{n\pi}{\rho}\right)\frac{dU_n}{dt}+T_gU_n+T_0v\left(\frac{n\pi}{\rho}\right)U_n-v^2\left(\frac{n\pi}{\rho}\right)^2U_n\right\}\cos\frac{n\pi x}{\rho}$$
$$=F_0\gamma B_1(x,t) \qquad (2.144)$$

$$\sum_{n=1}^{\infty}\left\{\frac{d^2U_n}{dt^2}+(T_0-2v\frac{n\pi}{\rho})\frac{dU_n}{dt}+(T_g-T_0v\left(\frac{n\pi}{\rho}\right)-v^2\left(\frac{n\pi}{\rho}\right)^2)U_n\right\}\sin\frac{n\pi x}{\rho}$$
$$\sum_{n=1}^{\infty}\left\{\frac{d^2U_n}{dt^2}+(T_0+2v\frac{n\pi}{\rho})\frac{dU_n}{dt}+(T_g+T_0v\left(\frac{n\pi}{\rho}\right)-v^2\left(\frac{n\pi}{\rho}\right)^2)U_n\right\}\cos\frac{n\pi x}{\rho}$$
$$=F_o\gamma B_1(x,t)$$

Multiplying equation: (2.144) all through by $\cos\frac{p\pi x}{\rho}$, it follows that:

$$\sum_{n=1}^{\alpha}\left\{\frac{d^2U_n}{dt^2}+\left(T_0-2v\frac{n\pi}{\rho}\right)\frac{dU_n}{dt}+\left(T_g-T_0v\left(\frac{n\pi}{\rho}\right)-v^2\left(\frac{n\pi}{\rho}\right)^2U_n\right\}\right.$$
$$\sin\frac{n\pi x}{\rho}\cos\frac{p\pi x}{\rho}+$$
$$\sum_{n=1}^{\infty}\left\{\frac{d^2U_n}{dt^2}+\left(T_0+2\frac{vn\pi}{\rho}\right)\frac{dU_n}{dt}+\left(T_g+T_ov\left(\frac{n\pi}{\rho}\right)-v^2\left(\frac{n\pi}{\rho}\right)^2\right)U_n\right\} \quad (2.145)$$
$$\cos\frac{n\pi x}{\rho}\cos\frac{p\pi x}{\rho}=F_0\gamma B_1(x,t)\cos\frac{p\pi x}{\rho}$$

Integrating both sides from 0 to ρ with respect to x, we have:

$$\int_0^{\rho}\sum_{n=1}^{\alpha}\left\{\frac{d^2U_n}{dt^2}+\left(T_0-2v\frac{n\pi}{\rho}\right)\frac{dU_n}{dt}+\left(T_g-T_0v\left(\frac{n\pi}{\rho}\right)-v^2\left(\frac{n\pi}{\rho}\right)^2U_n\right\}\right.$$
$$\sin\frac{n\pi x}{\rho}\cos\frac{p\pi x}{\rho}dx+$$
$$\int_0^{\rho}\sum_{n=1}^{\infty}\left\{\frac{d^2U_n}{dt^2}+\left(T_0+2\frac{vn\pi}{\rho}\right)\frac{dU_n}{dt}+\left(T_g+T_ov\left(\frac{n\pi}{\rho}\right)-v^2\left(\frac{n\pi}{\rho}\right)^2\right)U_n\right\} \quad (2.146)$$
$$\cos\frac{n\pi x}{\rho}\cos\frac{p\pi x}{\rho}dx$$
$$=\int_0^{\rho}F_0\gamma B_1(x,t)\cos\frac{p\pi x}{\rho}dx$$

However, for the integral on the LHS of equation (2.146) to be valid, p = n, so that:

$$\int_0^{\rho}\sum_{n=1}^{\alpha}\left\{\frac{d^2U_n}{dt^2}+\left(T_0-2v\frac{n\pi}{\rho}\right)\frac{dU_n}{dt}+\left(T_g-T_0v\left(\frac{n\pi}{\rho}\right)-v^2\left(\frac{n\pi}{\rho}\right)^2U_n\right\}\right.$$
$$\sin\frac{n\pi x}{\rho}\cos\frac{n\pi x}{\rho}dx+$$
$$\int_0^{\rho}\sum_{n=1}^{\infty}\left\{\frac{d^2U_n}{dt^2}+\left(T_0+2\frac{vn\pi}{\rho}\right)\frac{dU_n}{dt}+\left(T_g+T_ov\left(\frac{n\pi}{\rho}\right)-v^2\left(\frac{n\pi}{\rho}\right)^2\right)U_n\right\} \quad (2.147)$$
$$\cos^2\frac{n\pi x}{\rho}dx$$
$$=\int_0^{\rho}F_0\gamma B_1(x,t)\cos\frac{n\pi x}{\rho}dx$$

$$\frac{d^2U_n}{dt^2}+\left(T_0-2v\frac{n\pi}{p}\right)\frac{dU_n}{dt}+\left(T_g-T_0v\frac{n\pi}{\rho}-v^2\left(\frac{n\pi}{\rho}\right)^2\right)U_n$$
$$\int_0^{\rho}\sin\frac{n\pi x}{\rho}\cos\frac{n\pi x}{\rho}dx$$
$$+\frac{d^2U_n}{dt^2}+\left(T_0+2v\frac{n\pi}{\rho}\right)\frac{dU_n}{dt}+\left(T_g+T_0v\frac{n\pi}{\rho}-v^2\left(\frac{n\pi}{\rho}\right)^2\right)U_n \quad (2.148)$$
$$\int_o^{\rho}\cos^2\frac{n\pi x}{\rho}dx$$
$$=\int_0^{\rho}F_o\gamma B_1(x,t)\cos\frac{n\pi x}{\rho}dx$$

but

$$\int_0^{\rho}\sin\frac{n\pi x}{\rho}\cos\frac{n\pi x}{\rho}dx$$
$$=\int_0^{\rho}\frac{1}{2}\sin\frac{2n\pi x}{\rho}dx=\frac{1}{2}\frac{\rho}{2n\pi}\left[-\cos2\frac{n\pi x}{\rho}\right]_o^{\rho}$$
$$=\frac{\rho}{4n\pi}\left[-\cos2n\pi+1\right]=0$$

and

$$\int_0^{\rho} \cos^2 \frac{n\pi x}{\rho} dx$$

$$= \int_0^{\rho} \frac{1}{2}\left(1+\cos\frac{2n\pi x}{\rho}\right)dx = \frac{1}{2}\left[x+\frac{\rho}{2n\pi}\sin\frac{2n\pi x}{\rho}\right]_o^{\rho}$$

$$= \frac{1}{2}\left[\rho+\frac{\rho}{2n\pi}\sin 2n\pi - 0\right] = \frac{\rho}{2}$$

Equation (2.148) becomes:

$$\frac{\rho}{2}\frac{d^2U_n}{dt^2}+\frac{\rho}{2}\left(T_0+2v\frac{n\pi}{\rho}\right)\frac{dU_n}{dt}+\frac{\rho}{2}\left[T_g+T_o v\frac{n\pi}{\rho}-v^2\left(\frac{n\pi}{\rho}\right)^2\right]U_n$$

$$= F_0\int_0^{\rho}\gamma B_1(x,t)\cos\frac{n\pi x}{\rho}dx$$

$$\frac{d^2U_n}{dt^2}+\left(T_o+2v\frac{n\pi}{\rho}\right)\frac{dU_n}{dt}+\left(T_o+T_o v\frac{n\pi}{\rho}-v^2\left(\frac{n\pi}{\rho}\right)^2\right)U_n \quad (2.149)$$

$$= \frac{2F_o}{\rho}\int_o^{\rho}\gamma B_1(x,t)\cos\frac{n\pi x}{\rho}dx$$

We can write:

$$\frac{d^2U_n}{dt^2}+2\tau\frac{dU_n}{dt}+\xi^2U_n = \frac{2F_o}{\rho}\int_o^{\rho}\gamma B_1(x,t)\cos\frac{n\pi x}{\rho}dx \quad (2.150)$$

where $2\tau = T_0+2v\frac{n\pi}{\rho}$, $\xi^2 = T_g+T_o v\frac{n\pi}{\rho}-v^2\left(\frac{n\pi}{\rho}\right)^2$.

The homogeneous equation of equation (2.150) is given as:

$$\frac{d^2U_n}{dt^2}+2\tau\frac{dU_n}{dt}+\xi^2U_n = 0 \quad (2.151)$$

Assuming a solution of the form:

$$U_n(t) = Ae^{\beta t}$$

$$\frac{dU_n}{dt} = \beta A e^{\beta t}$$

$$\frac{d^2U_n}{dt^2} = \beta^2 A e^{\beta t}$$

Equation (2.151) becomes:

$$\beta^2 A e^{\beta t} + 2y\left(\beta A e^{\beta t}\right) + \xi^2 A e^{\beta t} = 0$$

$$\beta^2 + 2\tau\beta + \xi^2 = 0$$

It follows that:

$$\beta = -2\tau \pm \left(\frac{4\tau^2 - 4\xi^2}{2}\right)^{1/2}$$

$$\beta = -2\tau \pm 2\left(\frac{\tau^2 - \xi^2}{2}\right)^{1/2}$$

if we let $\tau^2 - \xi^2 = \Delta^2, \beta = -2\tau \pm \frac{2\Delta}{2}$

$$\beta = -\tau + \Delta \text{ or } \beta = -\tau + -\Delta$$

Therefore,

$$\begin{aligned} U_n(t) &= A_1 e^{(-\tau+\Delta)t} + A_2 e^{(-\tau-\Delta)t} \\ &= A_1 e^{-\tau t} e^{\Delta t} + A_2 e^{-\tau t} e^{-\Delta t} \\ &= e^{-\tau t}\left[A_1 e^{\Delta t} + A_2 e^{-\Delta t}\right] \\ U_n(t) &= (a\cosh\Delta_n t + b\sinh\Delta_n t)e^{-\tau t} \end{aligned} \tag{2.152}$$

where $a = A_1 + A_2$, $b = A_1 - A_2$, $e^{\Delta t} = \cosh\Delta t + \sinh\Delta t$, $e^{-\Delta t} = \cosh\Delta t - \sinh\Delta t$.

It is worthy of note that the form of our solution is as a result of the fact that:

$$(2\tau)^2 - 4\xi^2 > 0.$$

Equation (2.152) is the complementary function of equation (2.150).

We shall find the integral solution to the equation (2.150):

$$\frac{d^2U_n}{dt^2} + 2\tau\frac{dU_n}{dt} + \xi^2 U_n = \frac{2F_0}{\rho}\int_0^{\rho} \gamma B_1(x,t)\cos\frac{n\pi x}{\rho}\,dx \tag{2.153}$$

If we take the Radio frequency field to be a sinusoidal wave travelling towards the right (in the positive x-direction), then we can either have:

Case (i)

$$\gamma B_1(x,t) = A\cos(kx - \omega t) = A\cos\left(\frac{2\pi x}{\lambda} - \omega t\right)$$

Case (ii)

$$\gamma B_1(x,t) = A\sin(kx - \omega t) = A\sin\left(\frac{2\pi x}{\lambda} - \omega t\right)$$

(where A is the amplitude of the rf wave).

When the rf field is just removed, we have:

$$\frac{d^2U_n}{dt^2} + 2\tau\frac{dU_n}{dt} + \xi^2 U_n = 0$$

and the solution would essentially be equation (2.152):

$$U_n(t) = \left[a\cosh\Delta_n t + b\sinh\Delta_n t\right]e^{-\pi t}$$

It would be recalled:

$$M_y(x,t) = \sum_{n=1}^{\infty} U_n(t) \sin\frac{n\pi x}{\rho} + \sum_{n=1}^{\infty} U_n(t) \cos\frac{n\pi x}{\rho}$$

Applying the initial condition:

$$M_y(x,t) = 0;$$

$$M_y(x,0) = \sum_{n=1}^{\infty} U_n(0) \sin\frac{n\pi x}{\rho} + \sum_{n=1}^{\infty} U_n(0) \cos\frac{n\pi x}{\rho} = 0$$

$$\text{since } \sin\frac{n\pi x}{\rho} \neq 0 \text{ and } \cos\frac{n\pi x}{\rho} \neq 0$$

$$U_n(0) = 0$$

$$\left[a\cosh 0 + b\sinh 0\right]e^0 = 0$$

$$a\cosh 0 + b\sinh 0 = 0$$

$$a = 0$$

$$(\text{since } \cosh 0 \neq 0)$$

Therefore,

$$U_n(t) = (b\sinh\Delta_n t)e^{-\pi t}$$
$$U_n(t) = be^{-\pi t}\sinh\Delta_n t \tag{2.154}$$

then

$$M_y(x,t) = \sum_{n=1}^{\infty} be^{-\tau t}\sinh\Delta_n t \sin\frac{n\pi x}{\rho} + \sum_{n=1}^{\infty} be^{-\tau t}\sinh\Delta_n t \cos\frac{n\pi x}{\rho} \tag{2.155}$$

(where b is an arbitrary constant).

It is important to note that this method of solution to the problem requires that ρ be a sort of boundary condition parameter such that ρ tells us either:

(a) how far the radio frequency wave can travel in the x-direction, or

(b) how far we can allow the radio frequency wave to travel in the x-direction.

The value of ρ can then be determined by the theory of NMR Physics or in an NMR experiment.

Secondly, this method of solution will work best if $\rho = m\lambda$ (where λ is the wavelength of the radio frequency wave and m is a number whose value must be determined).

We shall evaluate the integral in equation (2.153) in order to determine the particular solution and hence the general solution of $U_n(t)$ when $B_1(x,t) \neq 0$. The integral cannot be solved unless m is known. However, if we assume that m=1, so that we will have a representation of what the actual solution (for which the value of m is fixed) looks like:

Case (i)

$$\gamma B_1(x,t) = A\cos\left(\frac{2\pi x}{\lambda} - \omega t\right)$$

Equation (2.153) becomes:

$$\frac{d^2U_n}{dt^2} + 2\tau\frac{dU_n}{dt} + \xi^2 U_n = \frac{2F_o}{\lambda} A\int_0^{\rho} \cos\left(\frac{2\pi x}{\lambda} - \omega t\right)\cos\frac{n\pi x}{\lambda}\,dx. \qquad (2.156)$$

In the integral,

$$\frac{2AF_0}{\lambda}\int_o^{\lambda} \cos\left(\frac{2\pi x}{\lambda} - \omega t\right)\cos\frac{n\pi x}{\lambda}\,dx \qquad (2.157)$$

we let:

$$I_1 = \int_o^{\lambda} \cos\left(\frac{2\pi x}{\lambda} - \omega t\right)\cos\frac{n\pi x}{\lambda}\,dx$$

$$= \left[\cos\left(\frac{2\pi x}{\lambda} - \omega t\right)\frac{\lambda}{n\pi}\sin\frac{n\pi x}{\lambda}\right]_0^{\lambda} - \int_0^{\lambda}\left[-\frac{2\pi}{\lambda}\sin\left(\frac{2\pi x}{\lambda} - wt\right)\frac{\lambda}{n\pi}\sin\frac{n\pi x}{\lambda}\right]dx$$

$$= \frac{\lambda}{n\pi}\cos(2\pi - \omega t)\sin n\pi - 0 + \frac{2\pi}{\lambda}\frac{\lambda}{n\pi}\int_0^{\lambda}\sin\left(\frac{2\pi x}{\lambda} - \omega t\right)\sin\frac{n\pi x}{\lambda}\,dx$$

but Sin $n\pi = 0$:

$$I_1 = \frac{2}{n}\int_0^{\lambda}\sin\left(\frac{2\pi x}{\lambda} - \omega t\right)\sin\frac{n\pi x}{\lambda}\,dx$$

$$= \frac{2}{n}\left\{\left[\mathrm{Sin}\left(\frac{2\pi x}{\lambda} - \omega t\right).-\frac{\lambda}{n\pi}\cos\frac{n\pi x}{\lambda}\right]_0^{\lambda} - \int_0^{\lambda}\left[\frac{2\pi x}{\lambda}\cos\left(\frac{2\pi x}{\lambda} - \omega t\right).-\frac{\lambda}{n\pi}\cos\frac{n\pi x}{\lambda}\,dx\right]\right\}$$

$$= \frac{2}{n}\left\{\left[-\frac{\lambda}{n\pi}\sin\left(\frac{2\pi x}{\lambda} - \omega t\right)\cos\frac{n\pi x}{\lambda}\right]_0^{\lambda} + \frac{2}{n}\int_0^{\lambda}\left[\cos\left(\frac{2\pi x}{\lambda} - \omega t\right)\cos\frac{n\pi x}{\lambda}\,dx\right]\right\}$$

$$I_1 = \frac{2}{n}\left\{-\frac{\lambda}{n\pi}\sin(2\pi - \omega t) + \frac{\lambda}{n\pi}\sin(-\omega t)\cos 0 + \frac{2}{n}I_1\right\}$$

$$I_1 = \frac{2\lambda}{n^2\pi}\sin(2\pi - \omega t)\cos n\pi + \frac{2\lambda}{n^2\pi}\sin(-\omega t) + \frac{4}{n^2}I_1$$

$$I_1 = -\frac{2\lambda}{n^2\pi}\sin(2\pi - \omega t)\cos n\pi - \frac{2\lambda}{n^2\pi}\sin\omega t + \frac{4}{n^2}I_1$$

but since $\sin(-\omega t) = -\sin\omega t$ and,
$\sin(2\pi - \omega t) = \sin 2\pi\cos\omega t - \cos 2\pi\sin\omega t = -\sin\omega t$,

we have:

$$I_1 = -\frac{2\lambda}{\left(n^2 - 4\right)\pi}\left(-\cos n\pi\sin\omega t + \sin\omega t\right)$$

$$I_1 = \frac{2\lambda}{\left(n^2 - 4\right)\pi}\left(\cos n\pi - 1\right)\sin\omega t$$

The integral (equation (2.17)) becomes:

$$\frac{4AF_0}{\left(n^2-4\right)\pi}\left(\cos n\pi-1\right)\sin\omega t$$

and we write equation (2.156) as:

$$\frac{d^2U_n}{dt^2}+2\tau\frac{dU_n}{dt}+\xi^2Un=\frac{4AF_0}{\left(n^2-4\right)\pi}\left(\cos n\pi-1\right)\sin\omega t \tag{2.158}$$

If we assume a solution,

$$U_n\left(t\right)=P\cos\omega t+Q\sin\omega t \quad \text{(Particular solution)}$$

$$\frac{dU_n}{dt}=-\omega P\sin\omega t+\omega Q\cos\omega t$$

$$\frac{d^2U_n}{dt^2}=-\omega^2P\cos\omega t-\omega^2Q\sin\omega t$$

Equation (2.158) becomes:

$$\left(-\omega^2P\cos\omega t-\omega^2Q\sin\omega t\right)-2\omega\tau P\sin\omega t+2\omega\tau Q\cos\omega t+\xi^2P\cos\omega t+\xi^2Q\sin\omega t$$

$$=\frac{4AF_0}{\left(n^2-4\right)\pi}\left(\cos n\pi-1\right)\sin\omega t\left[\left(\xi^2-\omega^2\right)P+2\omega\tau Q\right]\cos\omega t$$

$$+\left[\left(\xi^2-\omega^2\right)Q-2\omega\tau P\right]\sin\omega t\frac{4AF_0}{\left(n^2-4\right)\pi}\left(\cos n\pi-1\right)\sin\omega t$$

$$(\xi^2-\omega^2)P+2\omega\tau Q=0$$

$$P=-\frac{2\omega\tau Q}{\left(\xi^2-\omega^2\right)}$$

$$\left(\xi^2-\omega^2\right)P+2\omega\tau P=\frac{4AF_0}{\left(n^2-4\right)\pi}\left(\cos n\pi-1\right)$$

$$\left(\xi^2-\omega^2\right)Q+\frac{4\omega^2\tau^2Q}{\left(\xi^2-\omega^2\right)}=\frac{4AF_0}{\left(n^2-4\right)\pi}\left(\cos n\pi-1\right)$$

$$\frac{\left(\xi^2-\omega^2\right)Q+4\omega^2\tau^2Q}{\left(\xi^2-\omega^2\right)}=\frac{4AF_0}{\left(n^2-4\right)\pi}\left(\cos n\pi-1\right)$$

$$Q=\frac{4AF_0\left(\cos n\pi-1\right)}{\left(n^2-4\right)\pi}\frac{\left(\xi^2-\omega^2\right)}{\left(\xi^2-\omega^2\right)^2+4\omega^2\tau^2}$$

$$P=\frac{-2\omega\tau}{\left(\xi^2-\omega^2\right)}\frac{4AF_o\left(\cos n\pi-1\right)}{\left(n^2-4\right)\pi}\frac{\left(\xi^2-\omega^2\right)}{\left(\xi^2-\omega^2\right)^2+4\omega^2\tau^2}$$

$$=-\frac{4AF_o\left(\cos n\pi-1\right)}{\left(n^2-4\right)\pi}\frac{2\omega\tau}{\left(\xi^2-\omega^2\right)^2+4\omega^2\tau^2}$$

Therefore,

$$U_n(t)=-\frac{4AF_0\left(\cos n\pi-1\right)}{\left(n^2-4\right)\pi}\left\{\frac{2\omega\tau}{\left(\xi^2-\omega^2\right)^2+4\omega^2\tau^2}\right\}\cos\omega t + \frac{4AF_0\left(\cos n\pi-1\right)}{\left(n^2-4\right)\pi}\left\{\frac{\left(\xi^2-\omega^2\right)}{\left(\xi^2-\omega^2\right)^2+4\omega^2\tau^2}\right\}\sin\omega t \tag{2.159}$$

Hence the general solution for $U_n(t)$ is:

$$U_n(t) = \left[a\cosh\Delta_n t + b\sinh\Delta_n t\right]e^{-\tau t} - \frac{4AF_0(\cos n\pi - 1)}{(n^2-4)\pi} \left\{\frac{2\omega\tau}{\left(\xi^2-\omega^2\right)^2 + 4\omega^2\tau^2}\right\}\cos\omega t + \frac{4AF_0(\cos n\pi - 1)}{(n^2-4)\pi} \left\{\frac{\left(\xi^2-\omega^2\right)}{\left(\xi^2-\omega^2\right)^2 + 4\omega^2\tau^2}\right\}\sin\omega t \tag{2.160}$$

Using the initial condition, $M_y(x,0) = 0$, it follows that:

$$M_y(x,0) = \sum_{n=1}^{\infty} U_n(0)\sin\frac{n\pi x}{\lambda} + \sum_{n=1}^{\infty} U_n(0)\cos\frac{n\pi x}{\lambda} = 0$$

where $U_n(0) = 0$. That is,

$$\left[a\cosh 0 + b\sinh 0\right]e^0 - \frac{4AF_0(\cos n\pi - 1)}{(n^2-4)\pi}\left\{\frac{2\omega\tau}{\left(\xi^2-\omega^2\right)^2 + 4\omega^2\tau^2}\right\}\cos 0 + \frac{4AF_0(\cos n\pi - 1)}{(n^2-4)\pi}\left\{\frac{\left(\xi^2-\omega^2\right)}{\left(\xi^2-\omega^2\right)^2 + 4\omega^2\tau^2}\right\}\sin 0 = 0 \; a = 0, \quad \frac{4AF_0(\cos n\pi - 1)}{(n^2-4)\pi}\left\{\frac{2\omega\tau}{\left(\xi^2-\omega^2\right)^2 + 4\omega^2\tau^2}\right\} = 0 \tag{2.161}$$

then,

$$U_n(t) = be^{-\tau t}\sinh\Delta_n t + \frac{4AF_0(\cos n\pi - 1)}{(n^2-4)\pi}\frac{\left(\xi^2-\omega^2\right)}{\left(\xi^2-\omega^2\right)^2 + 4\omega^2\tau^2}\sin\omega t$$

Therefore,

$$M_y(x,t) = \sum_{n=1}^{\infty} be^{-\tau t} \sinh \Delta_n t \sin \frac{n\pi x}{\lambda}$$
$$+4AF_0 \sum_{n=1}^{\infty} \frac{(\cos n\pi - 1)}{(n^2-4)\pi} \frac{(\xi^2 - \omega^2)}{(\xi^2 - \omega^2) + 4\omega^2\tau^2} \sin \omega t \sin \frac{n\pi x}{\lambda}$$
$$+\sum_{n=1}^{\infty} be^{-\tau t} \sinh \Delta_n t \cos \frac{n\pi x}{\lambda}$$
$$+4AF_0 \sum_{n=1}^{\infty} \frac{(\cos n\pi - 1)}{(n^2-4)\pi} \frac{(\xi^2 - \omega^2)}{(\xi^2 - \omega^2) + 4\omega^2\tau^2} \sin \omega t \cos \frac{n\pi x}{\lambda} \quad (2.162)$$

$$M_y(x,t) = \sum_{n=1}^{\infty} be^{-\tau t} \sinh \Delta_n t \sin \frac{n\pi x}{\lambda} + \sum_{n=1}^{\infty} be^{-\tau t} \sinh \Delta_n t \cos \frac{n\pi x}{\lambda}$$
$$+4AF_o \sum_{n=1}^{\infty} \frac{(\cos n\pi - 1)}{(n^2-4)\pi} \frac{(\xi^2 - \omega^2)}{(\xi^2 - \omega^2) + 4\omega^2\tau^2} \sin \omega t \sin \frac{n\pi x}{\lambda}$$
$$+4AF_0 \sum_{n=1}^{\infty} \frac{(\cos n\pi - 1)}{(n^2-4)\pi} \frac{(\xi^2 - \omega^2)}{(\xi^2 - \omega^2) + 4\omega^2\tau^2} \sin \omega t \cos \frac{n\pi x}{\lambda}$$

Case (ii)

$$\gamma B_1(x,t) = A \sin\left(\frac{2\pi x}{\lambda} - \omega t\right),$$

Equation (2.153) becomes:

$$\frac{d^2U_n}{dt^2} + 2\tau \frac{dU_n}{dt} + \xi^2 U_n = \frac{2AF_o}{\lambda} \int_0^{\lambda} \sin\left(\frac{2\pi x}{\lambda} - \omega t\right) \cos \frac{n\pi x}{\lambda} dx \quad (2.163)$$

and

$$\frac{2AF_o}{\lambda} \int_0^{\lambda} \sin\left(\frac{2\pi x}{\lambda} - \omega t\right) \cos \frac{n\pi x}{\lambda} dx \quad (2.164)$$

let

$$I_2 = \int_0^{\lambda} \sin\left(\frac{2\pi x}{\lambda} - \omega t\right) \cos\frac{n\pi x}{\lambda}\, dx$$

$$I_2 = \left[\sin\left(\frac{2\pi x}{\lambda} - \omega t\right)\frac{\lambda}{n\pi}\sin\frac{n\pi x}{\lambda}\right]_0^{\lambda} - \int_0^{\lambda}\frac{2\pi}{\lambda}\cos\left(\frac{2\pi x}{\lambda} - \omega t\right)\frac{\lambda}{n\pi}\sin\frac{n\pi x}{\lambda}\, dx$$

$$= -\frac{2}{n}\int \cos\left(\frac{2\pi x}{\lambda} - \omega t\right)\sin\frac{n\pi x}{\lambda}\, dx$$

$$I_2 = -\frac{2}{n}\left\{\left[\cos\left(\frac{2\pi x}{\lambda} - \omega t\right).-\frac{\lambda}{n\pi}\cos\frac{n\pi x}{\lambda}\right]_0^{\lambda} - \int_0^{\lambda}\frac{2\pi}{\lambda}\sin\left(\frac{2\pi x}{\lambda} - \omega t\right)\frac{\lambda}{n\pi}\cos\frac{n\pi x}{\lambda}\, dx\right\}$$

$$= \frac{2}{n}\left\{\left[\frac{\lambda}{n\pi}\cos\left(\frac{2\pi x}{\lambda} - \omega t\right)\cos\frac{n\pi x}{\lambda}\right]_0^{\lambda} + \frac{2}{n}\int_0^{\lambda}\sin\left(\frac{2\pi x}{\lambda} - \omega t\right)\cos\frac{n\pi x}{\lambda}\, dx\right\}$$

$$= \frac{2}{n}\left\{\left[\frac{\lambda}{n\pi}\cos\left(\frac{2\pi x}{\lambda} - \omega t\right)\cos\frac{n\pi x}{\lambda}\right]_0^{\lambda} + \frac{2}{n}I_2\right\}$$

$$= \frac{2}{n}\left\{\frac{\lambda}{n\pi}\cos(2\pi - \omega t)\cos n\pi - \frac{\lambda}{n\pi}\cos(-\omega t) + \frac{2}{n}I_2\right\}$$

but $\cos(-\omega t) = \cos\omega t$ and $\cos(2\pi - \omega t) = \cos\omega t$, it follows that:

$$I_2 = \frac{2\lambda}{n^2\pi}\cos\omega t\cos n\pi - \frac{2\lambda}{n^2\pi}\cos\omega t + \frac{4}{n^2}I_2$$

Re – arranging the above equation gives:

$$I_2 = \frac{2\lambda}{\left(n^2 - 4\right)\pi}\left(\cos n\pi - 1\right)\cos\omega t$$

Equation (2.164) thus becomes:

$$\frac{4AF_o}{\left(n^2 - 4\right)\pi}\left(\cos n\pi - 1\right)\cos\omega t$$

Then equation (2.153) can be written as:

$$\frac{d^2U_n}{dt^2} + 2\tau\frac{dU_n}{dt} + \xi^2 U_n = \frac{4AF_o}{\left(n^2 - 4\right)\pi}\left(\cos n\pi - 1\right)\cos\omega t \qquad (2.165)$$

If we assume a solution of the form:

$$U_n(t) = p\cos\omega t + q\sin\omega t$$

$$\frac{dU_n(t)}{dt} = -\omega p\sin\omega t + \omega q\cos\omega t$$

$$\frac{d^2U_n(t)}{dt^2} = -\omega^2 p\cos\omega t - \omega^2 q\sin\omega t$$

Equation (2.165) becomes:

$$\begin{aligned}
&-\omega^2 p\cos\omega t - \omega^2 q\sin\omega t - 2\tau\omega p\sin\omega t + 2\tau\omega q\cos\omega t \\
&+\xi^2 p\cos\omega t + \xi^2 q\sin\omega t \\
&= \frac{4F_0}{\left(n^2-4\right)\pi}\left(\cos n\pi - 1\right)\cos\omega t\left[\left(\xi^2-\omega^2\right)P + 2\tau\omega q\right]\cos\omega t \\
&+\left[\xi^2 - \omega^2 q 2\tau\omega p\right]\sin\omega t \\
&= \frac{4F_0}{\left(n^2-4\right)\pi}\left(\cos n\pi - 1\right)\cos\omega t\left(\xi^2-\omega^2\right)P + 2\tau\omega q \\
&= 0
\end{aligned}$$

$$q = \frac{2\tau\omega}{\left(\xi^2-\omega^2\right)}p$$

$$\left(\xi^2-\omega^2\right)p + 2\tau\omega q = \frac{4AF_o\left(\cos n\pi - 1\right)}{\left(n^2-4\right)\pi}$$

$$\frac{(\xi^2-\omega^2)p + 4\tau^2\omega^2 p}{\left(\xi^2-\omega^2\right)} = \frac{4AF_0\left(\cos n\pi - 1\right)}{\left(n^2-4\right)\pi}$$

$$p = \frac{4AF_0\left(\cos n\pi - 1\right)}{\left(n^2-4\right)\pi}\frac{\left(\xi^2-\omega^2\right)}{(\xi^2-\omega^2)^2 + 4\tau^2\omega^2}$$

$$q = \frac{4AF_0\left(\cos n\pi - 1\right)}{\left(n^2-4\right)\pi}\frac{2\omega\tau}{(\xi^2-\omega^2)^2 + 4\tau^2\omega^2}$$

$$U_n(t) = \frac{4AF_0(\cos n\pi - 1)}{(n^2-4)\pi} \frac{(\xi^2 - \omega^2)}{(\xi^2-\omega^2)^2 + 4\omega^2\tau^2} \cos\omega t + \frac{4AF_0(\cos n\pi - 1)}{(n^2-4)\pi} \frac{2\omega\tau}{(\xi^2-\omega^2)^2 + 4\omega^2\tau^2} \sin\omega t \tag{2.166}$$

Equation (2.166) is the particular solution. The general solution for $U_n(t)$ is given as:

$$U_n(t) = [a\cosh\Delta_n t + b\sinh\Delta_n t]e^{-\tau t} + \frac{4AF_0(\cos n\pi - 1)}{(n^2-4)\pi} \frac{(\xi^2 - \omega^2)}{(\xi^2-\omega^2)^2 + 4\omega^2\tau^2} \cos\omega t + \frac{4AF_0(\cos n\pi - 1)}{(n^2-4)\pi} \frac{2\omega\tau}{(\xi^2-\omega^2)^2 + 4\omega^2\tau^2} \sin\omega t \tag{2.167}$$

Again, the initial condition, $M_y(x,0) = 0$ requires that:

$$U_n(0) = 0$$

$$[a\cosh 0 + b\sinh 0]e^0 + \frac{4AF_0(\cos n\pi - 1)}{(n^2-4)\pi} \frac{(\xi^2 - \omega^2)}{(\xi^2-\omega^2)^2 + 4\omega^2\tau^2} \cos 0 + \frac{4AF_0(\cos n\pi - 1)}{(n^2-4)\pi} \frac{2\omega\tau}{(\xi^2-\omega^2)^2 + 4\omega^2\tau^2} \sin 0 = 0$$

This implies:

$$a = 0, \quad \frac{4AF_0(\cos n\pi - 1)}{(n^2-4)\pi} \frac{(\xi^2 - \omega^2)}{(\xi^2-\omega^2)^2 + 4\tau^2\omega^2} = 0 \tag{2.168}$$

$$U_n(t) = be^{-\tau t}\sinh\Delta_n t + \frac{4AF_0(\cos n\pi - 1)}{(n^2-4)\pi} \frac{2\omega\tau}{(\xi^2-\omega^2)^2 + 4\omega^2\tau^2} \sin\omega t \tag{2.169}$$

then,

$$M_y(x,t)=\sum_{n=1}^{\infty} be^{-\tau t}\sinh\Delta_n t\sin\frac{n\pi x}{\lambda}+4AF_0\sum_{n=1}^{\infty}\frac{(\cos n\pi-1)}{(n^2-4)\pi}$$
$$\frac{2\omega\tau}{(\xi^2-\omega^2)^2+4\omega^2\tau^2}\sin\omega t\sin\frac{n\pi x}{\lambda}\sum_{n=1}^{\infty} be^{-\tau t}\sinh\Delta_n t\cos\frac{n\pi x}{\lambda}$$
$$+4AF_0\sum_{n=1}^{\infty}\frac{(\cos n\pi-1)}{(n^2-4)\pi}\frac{2\omega\tau}{(\xi^2-\omega^2)^2+4\omega^2\tau^2}\sin\omega t\cos\frac{n\pi x}{\lambda} \quad (2.170)$$
$$M_y(x,t)=\sum_{n=1}^{\infty} be^{-\tau t}\sinh\Delta_n t\sin\frac{n\pi x}{\lambda}+\sum_{n=1}^{\infty} be^{-\tau t}\ \mathrm{Sinh}\Delta_n t\cos\frac{n\pi x}{\lambda}$$
$$+4AF_0\sum_{n=1}^{\infty}\frac{(\cos n\pi-1)}{(n^2-4)\pi}\frac{2\omega\tau}{(\xi^2-\omega^2)^2+4\omega^2\tau^2}\sin\omega t\sin\frac{n\pi x}{\lambda}$$
$$+4AF_0\sum_{n=1}^{\infty}\frac{(\cos n\pi-1)}{(n^2-4)\pi}\frac{2\omega\tau}{(\xi^2-\omega^2)^2+4\omega^2\tau^2}\sin\omega t\cos\frac{n\pi x}{\lambda}$$

In equation (2.170) the following parameters are defined:

(i)
$$2\tau=T_0+\frac{2v n\pi}{\lambda}=\frac{T_0}{2}+\frac{v n\pi}{\lambda}$$
$$\tau^2=\frac{T_0}{4}+T_0\frac{v n\pi}{\lambda}+v^2\left(\frac{n\pi}{\lambda}\right)^2$$

(ii)
$$\xi^2=T_g+\frac{T_0 v n\pi}{\lambda}-v^2\left(\frac{n\pi}{\lambda}\right)^2$$

$$\Delta^2=\tau^2-\xi^2=\frac{T_0{}^2}{4}+v^2\left(\frac{n\pi}{\pi}\right)^2-T_g+v^2\left(\frac{n\pi}{\lambda}\right)^2$$

(iii)
$$=\frac{T_0{}^2}{4}-T_g+2v^2\left(\frac{n\pi}{\lambda}\right)^2$$
$$\Delta=\sqrt{\frac{T_o^2}{4}-T_g+2v^2\left(\frac{n\pi}{\lambda}\right)^2}$$

(iv) $$2\omega\tau = 2\omega\left(\frac{T_o}{2} + \frac{vn\pi}{\lambda}\right) = \omega T_o + \frac{2\omega vn\pi}{\lambda}$$

$$4\omega^2\tau^2 = \left(\omega T_o + \frac{2\omega vn\pi}{\lambda}\right)^2 = \omega^2 T_o^2 + 4\omega^2 T_o \frac{vn\pi}{\lambda} + 4\omega^2 v^2 \left(\frac{n\pi}{\lambda}\right)^2$$

2.16 Solutions to the NMR Travellling Wave Equation

Based on equation (2.35), the NMR wave equation can be written in the form:

$$v^2 \frac{\partial^2 M_y}{\partial x^2} + \frac{\partial^2 M_y}{\partial t^2} = F_O \gamma B_1(t) \tag{2.171}$$

or

$$v^2 \frac{\partial^2 M_y}{\partial x^2} = -\frac{\partial^2 M_y}{\partial t^2} + F_O \gamma B_1(t)$$

$$v^2 \frac{\partial^2 M_y}{\partial x^2} = F_O \gamma B_1(t) - \frac{\partial^2 M_y}{\partial t^2} \tag{2.172}$$

In generalizing equation (2.172), we write:

$$v^2 \nabla^2 M_y = F_O \gamma B_1(t) - \frac{\partial^2 M_y}{\partial t^2} \tag{2.173}$$

In the polar coordinate, equation (2.173) becomes:

$$v^2 \left(\frac{\partial^2 M_y}{\partial r^2} + \frac{1}{r}\frac{\partial M_y}{\partial r} + \frac{1}{r^2}\frac{\partial^2 M_y}{\partial \phi^2}\right) = F_O \gamma B_1(t) - \frac{\partial^2 M_y}{\partial t^2} \tag{2.174}$$

Case (1)

For a steady state condition, $\frac{\partial^2 M_y}{\partial t^2} = 0$, and equation (2.174) becomes:

$$v^2 \left(\frac{\partial^2 M_y}{\partial r^2} + \frac{1}{r}\frac{\partial M_y}{\partial r} + \frac{1}{r^2}\frac{\partial^2 M_y}{\partial \phi^2}\right) = F_O \gamma B_1(t)$$

(a) The homogeneous equation gives:

$$v^2 \left(\frac{\partial^2 M_y}{\partial r^2} + \frac{1}{r}\frac{\partial M_y}{\partial r} + \frac{1}{r^2}\frac{\partial^2 M_y}{\partial \phi^2}\right) = 0 \quad [M_0=0 \text{ or } \gamma B_1(t) = 0\ ]$$

And the solution follows exactly as in the case of the diffusion equation, that is:

$$M_y(\mathrm{r}, \phi) = \frac{A_0}{2} + \sum_{M=1}^{\infty} r^m \left(A_m \,\mathrm{Cosm}\phi + \mathrm{B_m} \sin \mathrm{m}\phi\right) \tag{2.175}$$

(b) The inhomogeneous equation is:

$$\mathrm{v}^2 \left(\frac{\partial^2 M_y}{\partial r^2} + \frac{1}{r} \frac{\partial M_y}{\partial r} + \frac{1}{r^2} \frac{\partial^2 M_y}{\partial \phi^2} \right) = F_O \gamma B_1(\mathrm{t})$$

We need to give a definition to the function $\gamma B_1(\mathrm{t})$ before solving it.

Case (ii)

If $\frac{\partial M_y}{\partial t} \neq 0$ and m_0 =0 or $\gamma B_1(t) = 0$, (2.4) becomes:

$$\mathrm{v}^2 \left(\frac{\partial^2 M_y}{\partial r^2} + \frac{1}{r} \frac{\partial M_y}{\partial r} + \frac{1}{r^2} \frac{\partial^2 M_y}{\partial \phi^2} \right) = -\frac{\partial^2 M_y}{\partial t^2} \tag{2.176}$$

We can then write that:

$$\frac{\partial^2 M_y}{\partial r^2} + \frac{1}{r} \frac{\partial M_y}{\partial r} + \frac{1}{r^2} \frac{\partial^2 M_y}{\partial \phi^2} = -\frac{1}{V^2} \frac{\partial^2 M_y}{\partial t^2} \tag{2.177}$$

By the method of separation of variables we have:

$$M_y = \mathrm{R(r)}\, \Phi(\phi) T(t)$$

$$\frac{\partial M_y}{\partial r} = \Phi \mathrm{T} \frac{\partial \mathrm{R}}{\partial \mathrm{r}}, \quad \frac{\partial^2 M_y}{\partial r^2} = \Phi \mathrm{T} \frac{\partial^2 R}{\partial r^2}, \quad \frac{\partial M_y}{\partial \phi} = RT \frac{\partial \Phi}{\partial \phi}, \quad \frac{\partial^2 M_y}{\partial \phi^2} = RT \frac{\partial^2 \Phi}{\partial \phi^2}$$

$$\frac{\partial M_y}{\partial t} = R\Phi \frac{\partial T}{\partial t}, \quad \frac{\partial^2 M_y}{\partial t^2} = R\Phi \frac{\partial^2 T}{\partial t^2}$$

Equation (2.177) becomes:

$$\Phi T \frac{\partial^2 R}{\partial r^2} + \frac{\Phi \mathrm{T}}{\mathrm{r}} \frac{\partial R}{\partial r} + \frac{RT}{r^2} \frac{\partial^2 \Phi}{\partial \Phi^2} = -\frac{R\Phi}{V^2} \frac{\partial^2 T}{\partial t^2}$$

Multiplying all through by $\frac{1}{R\Phi \mathrm{T}}$,

$$\frac{1}{R}\frac{\partial^2 R}{\partial r^2} + \frac{1}{rR}\frac{\partial R}{\partial r} + \frac{1}{r^2\Phi}\frac{\partial^2 \Phi}{\partial \phi^2} = -\frac{1}{V^2}\cdot\frac{1}{T}\frac{\partial^2 T}{\partial t^2}$$

Both the RHS and LHS must be equal to a constant: $-\alpha^2$

$$\frac{1}{R}\frac{\partial^2 R}{\partial r^2} + \frac{1}{rR}\frac{\partial R}{\partial r} + \frac{1}{r^2\Phi}\frac{\partial^2 \Phi}{\partial \phi^2} = -\frac{1}{V^2}\cdot\frac{1}{T}\frac{\partial^2 T}{\partial t^2} = -\alpha^2$$

$$\frac{1}{R}\frac{\partial^2 R}{\partial r^2} + \frac{1}{rR}\frac{\partial R}{\partial r} + \frac{1}{r^2\Phi}\frac{\partial^2 \Phi}{\partial \phi^2} = -\alpha^2$$

$$\frac{r^2}{R}\frac{\partial^2 R}{\partial r^2} + \frac{r}{R}\frac{\partial \mathrm{R}}{\partial \mathrm{r}} + \frac{1}{\Phi}\frac{\partial^2 \Phi}{\partial \phi^2} = -\alpha^2 r^2 \tag{2.178}$$

$$\frac{\partial^2 T}{\partial t^2} = \alpha^2 v^2 T \tag{2.179}$$

If we assume that:

$$\mathrm{T} = Ce^{mt}$$

Then equation (2.179) becomes:

$$m^2 = \alpha^2 v^2$$

$$m = \pm \alpha v$$

$$\mathrm{T(t)} = C_1 e^{\alpha v t} + C_2 e^{-\alpha v t} \tag{2.180}$$

Equation (2.178) can be written as:

$$\frac{r^2}{R}\frac{\partial^2 R}{\partial r^2} + \frac{r}{R}\frac{\partial \mathrm{R}}{\partial \mathrm{r}} + \alpha^2 r^2 = -\frac{1}{\Phi}\frac{\partial^2 \Phi}{\partial \phi^2}$$

This equation must also be equal to a constant β^2,

$$\frac{r^2}{R}\frac{\partial^2 R}{\partial r^2} + \frac{r}{R}\frac{\partial \mathrm{R}}{\partial \mathrm{r}} + \alpha^2 r^2 = -\frac{1}{\Phi}\frac{\partial^2 \Phi}{\partial \phi^2} = \beta^2$$

Where

$$\frac{r^2}{R}\frac{\partial^2 R}{\partial r^2} + \frac{r}{R}\frac{\partial \mathrm{R}}{\partial \mathrm{r}} + \alpha^2 r^2 = \beta^2 \tag{2.181}$$

and

$$-\frac{1}{\Phi}\frac{\partial^2 \Phi}{\partial \phi^2} = \beta^2 \tag{2.182}$$

From (2.181), we obtain:

$$r^2\frac{\partial^2 R}{\partial r^2} + r\frac{\partial R}{\partial r} + (\alpha^2 r^2 - \beta^2)\,\mathrm{R} = 0$$

A solution of which is given as:

$$\mathrm{R(r)} = A_1 J_\beta(\alpha r) + B_1 Y_\beta(\alpha r) \tag{2.183}$$

From (2.182), we write that:

$$\frac{\partial^2 \Phi}{\partial \phi^2} = -\beta^2 \Phi \tag{2.184}$$

If we assume that:

$$\Phi = p\mathrm{e}^{\mathrm{n}\phi},$$

it follows from (2.184) that:

$$\mathrm{n}^2 = -\beta^2$$

$$\mathrm{n} = \pm \mathrm{i}\beta$$

Therefore, $\Phi(\phi) = \mathrm{P}_1\mathrm{e}^{\mathrm{i}\beta\phi} + \mathrm{P}_2\mathrm{e}^{-\mathrm{i}\beta\phi}$.

From which we have that:

$$\Phi(\phi) = P\cos\beta\phi + \mathrm{Q}\sin\beta\phi \tag{2.185}$$

$$\mathrm{P} = \mathrm{P}_1 + \mathrm{P}_2,\ \mathrm{Q} = \mathrm{i}(\mathrm{P}_1 - \mathrm{P}_2)$$

Therefore,

$$\mathrm{M_y} = \{\mathrm{C}_1\mathrm{e}^{\alpha \mathrm{vt}} + \mathrm{C}_2\mathrm{e}^{-\alpha \mathrm{vt}}\}\{\mathrm{A}_1\mathrm{J}_\beta(\alpha \mathrm{r}) + \mathrm{B}_1\mathrm{Y}_\beta(\alpha \mathrm{r})\}\{\mathrm{P}\cos\beta\phi + \mathrm{Q}\sin\beta\phi \tag{2.186}$$

We can then make use of the appropriate boundary condition as required.

Case (iii)

If $\frac{\partial M_y}{\partial t} \neq 0$ and, $M_o \neq 0$ and $\gamma B_1(t) \neq 0$,

$$v^2\left(\frac{\partial^2 M_y}{\partial r^2} + \frac{1}{r}\frac{\partial M_y}{\partial r} + \frac{1}{r^2}\frac{\partial^2 M_y}{\partial \phi^2}\right) = -\partial^2 \frac{M_y}{\partial t^2} + F_O \gamma B_1(t) \qquad (2.187)$$

If we write that:

$$M_y(r, \varphi, t) = X(r, \varphi, t) + Y(t)$$

$$\frac{\partial M_y}{\partial r} = \frac{\partial X}{\partial r}, \frac{\partial^2 M_y}{\partial r^2} = \frac{\partial^2 X}{\partial r^2}, \quad \frac{\partial M_y}{\partial \phi} = \frac{\partial X}{\partial \phi}, \frac{\partial^2 M_y}{\partial \phi^2} = \frac{\partial^2 X}{\partial \phi^2}, \frac{\partial M_y}{\partial t} = \frac{\partial X}{\partial t} + Y'(t),$$
$$\frac{\partial^2 M_y}{\partial t^2} = \frac{\partial^2 X}{\partial t^2} + Y''(t)$$

Hence equation (2.187) becomes:

$$v^2\left(\frac{\partial^2 X}{\partial r^2} + \frac{1}{r}\frac{\partial X}{\partial r} + \frac{1}{r^2}\frac{\partial^2 X}{\partial \phi^2}\right) = \frac{-\partial^2 X}{\partial t^2} + Y''(t) \qquad (2.188)$$

If we simplify the problem by assuming:

$$Y''(t) = 0,$$

Then equation (2.188) becomes:

$$v^2\left(\frac{\partial^2 X}{\partial r^2} + \frac{1}{r}\frac{\partial X}{\partial r} + \frac{1}{r^2}\frac{\partial^2 X}{\partial \phi^2}\right) = \frac{-\partial^2 X}{\partial t^2} \qquad (2.189)$$

$$\frac{\partial^2 X}{\partial r^2} + \frac{1}{r}\frac{\partial X}{\partial r} + \frac{1}{r^2}\frac{\partial^2 X}{\partial \phi^2} = -\frac{1}{v}\frac{\partial^2 X}{\partial t^2} \qquad (2.190)$$

The solution to this equation is:

$$X(r,\phi,t) = \{C_1 e^{\alpha v t} + C_2 e^{-\alpha v t}\}\{A_1 J_\beta(\alpha r) + B_1 Y_\beta(\alpha r)\}\{P\cos\beta\phi + Q\sin\beta\phi\}$$

Therefore, the general solution in this case is:

$$M_y(rC\phi,t) = \{C_1 e^{\alpha vt} + C_2 e^{-\alpha vt}\}$$
$$\{A_1 J_\beta(\alpha r) + B_1 Y_\beta(\alpha r)\}\{P\cos\beta\phi + Q\sin\beta\phi\} + \gamma(t) \quad (2.191)$$

Case (iv)

If M_y is radially symmetric, it does not depend on ϕ and if $F_0\gamma B_1(t) = 0$, we have:

$$v^2\left(\frac{\partial^2 M_y}{\partial r^2} + \frac{1}{r}\frac{\partial M_y}{\partial r}\right) = -\frac{\partial^2 M_y}{\partial t^2}$$
$$\frac{\partial M_y}{\partial r} + \frac{1}{r}\frac{\partial M_y}{\partial r} = -\frac{1}{V^2}\frac{\partial^2 M_y}{\partial t^2} \quad (2.192)$$

By the method of separation by variables, we have:

$$M_y = R(r)\,T(t)$$
$$\frac{\partial^2 M_y}{\partial r^2} = T\frac{\partial^2 R}{\partial r^2},\ \frac{\partial M_y}{\partial r} = T\frac{\partial R}{\partial r},\ \frac{\partial^2 M_y}{\partial t^2} = R\frac{\partial^2 T}{\partial t^2}$$

Equation (2.192) becomes:

$$T\frac{\partial^2 R}{\partial r^2} + \frac{T}{r}\frac{\partial R}{\partial r} = -\frac{R}{v^2}\frac{\partial^2 T}{\partial t^2}$$

Multiplying all through by $\frac{1}{RT}$,

$$\frac{1}{R}\frac{\partial^2 R}{\partial r^2} + \frac{1}{rR}\frac{\partial R}{\partial r} = -\frac{1}{v^2}\cdot\frac{1}{T}\frac{\partial^2 T}{\partial t^2} \quad (2.193)$$

It follows that:

$$\frac{1}{R}\frac{\partial^2 R}{\partial r^2} + \frac{1}{rR}\frac{\partial R}{\partial r} = -\frac{1}{v^2}\cdot\frac{1}{T}\frac{\partial^2 T}{\partial t^2} = -\lambda^2$$

Where we have:

$$\frac{1}{R}\frac{\partial^2 R}{\partial r^2} + \frac{1}{rR}\frac{\partial R}{\partial r} = -\lambda^2$$

$$\frac{\partial^2 R}{\partial r^2} + \frac{1}{\mathrm{r}}\frac{\partial \mathrm{R}}{\partial \mathrm{r}} + \lambda^2 R = 0 \tag{2.194}$$

and

$$-\frac{1}{\mathrm{v}^2}\cdot\frac{1}{\mathrm{T}}\frac{\partial^2 T}{\partial t^2} = -\lambda^2$$

$$\frac{\partial^2 \mathrm{T}}{\partial \mathrm{t}^2} = \lambda^2 \mathrm{v}^2 \mathrm{T} \tag{2.195}$$

The solution of equation (2.194) is given as:

$$\mathrm{R(r)} = P_2 J_0(\lambda r) + Q_2 y_0(\lambda r)$$

To solve equation (2.195), we write:

$$\mathrm{T(t)} = De^{nt}$$

Then equation (2.195) becomes:

$$n^2 = \lambda^2 \mathrm{v}^2$$

$$n = \pm \lambda v$$

Hence,

$$\mathrm{T(t)} = D_1 e^{\lambda v t} + D_2 e^{-\lambda v t}$$

Therefore,

$$M_y(r,t) = \left\{ D_1 e^{\lambda v t} + D_2 e^{-\lambda v t} \right\} \{ P_2 J_0(\lambda r) + Q_2 y_0(\lambda r) \} \tag{2.196}$$

We can then apply the boundary conditions as appropriate.

2.17 MRI Bessel Equation

We study the flow properties of the modified time independent Bloch NMR flow equations which describes the dynamics of the hydrogen atom under the influence of rf magnetic field as follows:

$$v^2 \frac{d^2 M_y}{dx^2} + T_0 v \frac{dM_y}{dx} + S(x) M_y = \frac{M_0 \gamma B_1(x)}{T_1} \tag{2.197}$$

where

$$S(x) = \gamma^2 B_1^2(x) + T_g, \quad T_g = \frac{1}{T_1 T_2},$$

$$T_0 = \frac{1}{T_1} + \frac{1}{T_2}$$

However, if the fluid velocity is dependent on x as follows:

$$v = \frac{x}{\delta} \tag{2.198}$$

where δ is the time required for the spins to cover the distance x. Since v is no longer constant, we may write:

$$v^2 \frac{d^2 M_y}{dx^2} + \left(T_0 + \frac{dv}{dx} \right) v \frac{dM_y}{dx} + S(x) M_y = \frac{M_0 \gamma B_1(x)}{T_1} \tag{2.199}$$

$$v^2 \frac{d^2 M_y}{dx^2} + \left(T_0 + \frac{1}{\delta} \right) v \frac{dM_y}{dx} + S(x) M_y = \frac{M_0 \gamma B_1(x)}{T_1} \tag{2.200}$$

If we design the radiofrequency field such that:

$$\gamma B_1(x) = i \alpha x^r, \quad \alpha = \frac{\gamma G \tau}{\delta}, \quad r = 1 \tag{2.201}$$

where G is the gradient magnetic field, γ is the gyromagnetic ratio and τ is the length of time for which the gradient pulse is applied and the time δ is defined as:

$$\delta = \frac{T_1 T_2}{T_1 + T_2} \tag{2.202}$$

If the NMR signal is sampled when the applied radiofrequency energy successfully displaces most of the spin unto the transverse plane ($M_0 \approx 0$), equation (2.197) then becomes:

$$v^2 \frac{d^2 M_y}{dx^2} + 2T_0 v \frac{dM_y}{dx} + \left(-\left(\frac{\gamma G \tau}{\delta} \right)^2 x^2 + \frac{1}{T_1 T_2} \right) M_y = 0 \tag{2.203}$$

$$x^2 \frac{d^2 M_y}{dx^2} + 2x \left(\frac{T_1 + T_2}{T_1 T_2} \right) \left(\frac{T_1 T_2}{T_1 + T_2} \right) \frac{dM_y}{dx} + \left(-(\gamma G \tau)^2 x^2 + \frac{1}{T_1 T_2} \left(\frac{T_1 T_2}{T_1 + T_2} \right)^2 \right) M_y = 0 \tag{2.204}$$

If we also set,

$$k = \gamma G \tau$$

and

$$\beta^2 = \frac{T_1 T_2}{(T_1 + T_2)^2} = \frac{T_g}{(T_0)^2} \tag{2.205}$$

we may therefore write:

$$x^2 \frac{d^2 M_y}{dx^2} + 2x \frac{dM_y}{dx} - \left(k^2 x^2 - \beta^2 \right) M_y = 0 \tag{2.206}$$

Equation (2.206) is an equation transformable to Bessel function [60]. Since we require that the transverse magnetization be finite as x tends to infinity, the solution is given as:

$$M_y(x) = C_1 \sqrt{x} J_n(kx) \tag{2.207}$$

where:

$$n = \frac{\sqrt{1-\beta^2}}{2} \tag{2.208}$$

Phase of the Spin

In equation (2.205), if we set:

$$\alpha = kx \tag{2.209}$$

$$\frac{dM_y}{dx} = \frac{dM_y}{d\alpha}\frac{d\alpha}{dx} = k\frac{dM_y}{d\alpha}$$

$$\frac{d^2M_y}{dx^2} = \frac{d^2M_y}{d\alpha^2}\left(\frac{d\alpha}{dx}\right)^2 + \frac{dM_y}{d\alpha}\frac{d^2\alpha}{dx^2} = k^2\frac{d^2M_y}{d\alpha^2}$$

Equation (2.206) becomes:

$$k^2x^2\frac{d^2M_y}{d\alpha^2} + 2kx\frac{dM_y}{d\alpha} + \left(k^2x^2+\beta^2\right)M_y = 0$$

$$\alpha^2\frac{d^2M_y}{d\alpha^2} + 2\alpha\frac{dM_y}{d\alpha} + \left(\alpha^2+\beta^2\right)M_y = 0 \tag{2.210}$$

We shall make another transformation as follows:

$$M_y = \frac{U}{\alpha} \tag{2.211}$$

$$\frac{dM_y}{d\alpha} = \frac{1}{\alpha}\frac{dU}{d\alpha} - \frac{U}{\alpha^2}$$

$$\frac{d^2M_y}{d\alpha^2} = \frac{1}{\alpha}\frac{d^2U}{d\alpha^2} - \frac{2}{\alpha^2}\frac{dU}{d\alpha} + \frac{2U}{\alpha^3} \tag{2.212}$$

Hence, equation (2.211) becomes:

$$\alpha^2\left(\frac{1}{\alpha}\frac{d^2U}{d\alpha^2} - \frac{2}{\alpha^2}\frac{dU}{d\alpha} + \frac{2U}{\alpha^3}\right) + 2\alpha\left(\frac{1}{\alpha}\frac{dU}{d\alpha} - \frac{U}{\alpha^2}\right) + \left(\alpha^2+\beta^2\right)\frac{U}{\alpha} = 0$$

$$\left(\alpha\frac{d^2U}{d\alpha^2}-2\frac{dU}{d\alpha}+\frac{2U}{\alpha}\right)+\left(2\frac{dU}{d\alpha}-\frac{2U}{\alpha}\right)+\left(\alpha^2+\beta^2\right)\frac{U}{\alpha}=0$$

$$\alpha\frac{d^2U}{d\alpha^2}+\left(\alpha^2+\beta^2\right)\frac{U}{\alpha}=0 \tag{2.213}$$

$$\frac{d^2U}{d\alpha^2}+\left(1+\frac{\beta^2}{\alpha^2}\right)U=0 \tag{2.214}$$

Based on the Short Gradient Pulse (SGP) approximation [66], the parameter α represents the phase of the spin such that the effect of a gradient pulse of duration τ on a spin at position x is given by, neglecting the effect of the static field,

$$\alpha(x)=\gamma G\tau x=\phi(x) \tag{2.215}$$

Hence, if we consider the phase change of a spin which was at position χ_0 during the first gradient pulse and at position χ_1 during the second, then the change in phase in moving from χ_0 to χ_1 is given by

$$\Delta\alpha(x_1-x_0)=\gamma G\tau(x_1-x_0) \tag{2.216}$$

Therefore, we see that:

$$\frac{\beta^2}{\alpha^2}=\frac{T_g}{(\phi(x)T_0)^2} \tag{2.217}$$

2.18 Equation of Motion for Pulsed NMR

In a typical MRI procedure where G is the pulsed gradient applied for the length of time τ, equation (2.40) becomes:

$$x^2\frac{d^2M_y}{dx^2}+x\sigma\frac{dM_y}{dx}+\left(\left(\gamma\frac{\sigma}{T_o}G\right)^2x^2+\frac{\sigma^2}{T_1T_2}\right)M_y=\frac{M_o\gamma B_1(x)}{T_1} \tag{2.218}$$

where

$$\gamma B_1(x)=\gamma Gx$$

and

$$v=xT_o=\frac{x}{\tau}$$

For 90^o pulse M_o is minimum (say $M_o = 0$), we can write equation (2.218) as:

$$x^2\frac{d^2M_y}{dx^2}+x\sigma\frac{dM_y}{dx}+\left((\gamma G\tau)^2x^2+\frac{\tau^2}{T_1T_2}\right)M_y=0 \tag{2.219a}$$

$$x^2\frac{d^2M_y}{dx^2}+x\sigma\frac{dM_y}{dx}+\left((\theta)^2x^2+\frac{\tau^2}{T_1T_2}\right)M_y=0 \tag{2.219b}$$

where

$$\frac{1}{T_o}=\tau \tag{2.220}$$

Equation (2.219) is a general form of an equation transformable into Bessel equation of order β with parameter k. In equation (2.219), the flip angel is defined as:

$$\theta(rad)=\gamma(rad\ \ \sec^{-1}\ G^{-1})(G)\tau(\sec) \tag{2.221}$$

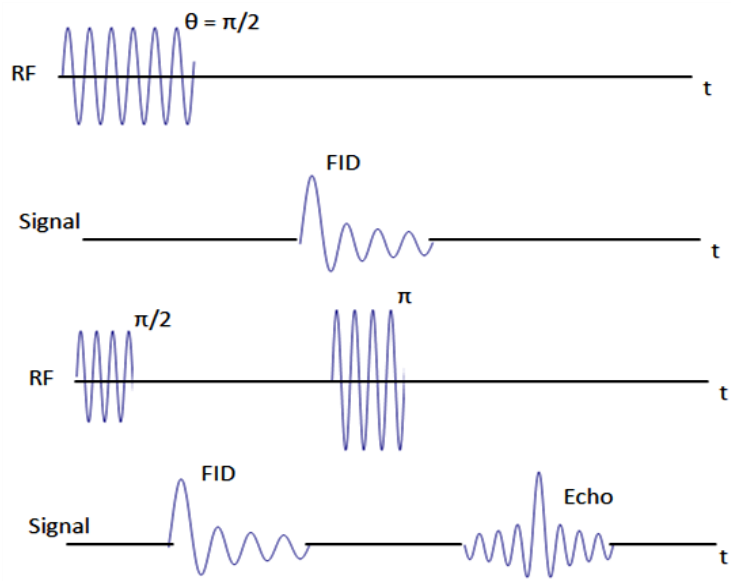

Fig. 2.1 *The NMR Pulse sequence.*

Equation (2.219) presents new ways of generating the NMR signal using the Bessel functions. As shown in figure 1, the experiment is started with a $\frac{\pi}{2}$ pulse, following which the magnetic vector M_y precesses in the plane perpendicular to the direction of static magnetic field B_o and free induction decay (FID) occurs. The maximum amplitude of the FID is measured to obtain a voltage-amplitude. After a delay which is typically of the order of 10ms, a π rf pulse is introduced. Following another interval τ, the magnetic spins recluster and a spin echo voltage signal is observed. The voltage amplitude of the spin echo is taken as proportional to $M_{y,}$ equation (2.219) is then solved. To solve equation (2.219b), the value of G must be known, as well as the gyromagnetic ratio γ of the specific nuclei under study. The voltage amplitude of the spin echo M_y is easily computed by solving the Bessel equation of order β and parameter θ as shown in equation (2.219b) where:

$$\beta = \tau\sqrt{T_g} \tag{2.222a}$$

and

$$\theta = \gamma G\tau \tag{2.222b}$$

2.19 Application to Molecular Imaging

In this section, new magnetic resonance methodology to solve the Bloch NMR flow equation based on Hermite, Bessel and simple quantum mechanical functions for detailed studies of processes taking place at the molecular level in living tissues have been developed. We show how these quantum mechanical functions may be very crucial in the assessment of Cancer cells, Multiple sclerosis (MS) and Brain edema using magnetic resonance imaging.

We apply a fundamental transformation procedure on equation (2.40) given by:

$$\mathrm{M_y(x) = \psi(x)e^{\lambda x}} \tag{2.223a}$$

provided that:

$$\lambda = -\frac{1}{2\nu T_0}, \tag{2.223b}$$

Equation (2.40) becomes:

$$\frac{d^2\psi(x)}{dx^2} + \frac{1}{\nu^2}\left(T_g - T_R - \gamma^2 G^2 x^2\right)\psi(x) = 0; \tag{2.224a}$$

where

$$T_g = \frac{1}{T_1 T_2};\ T_R = \frac{1}{4T_0^2} \tag{2.224b}$$

and G is the strength of the gradient field. With further assumptions:

$$\gamma B_1(x) = i\gamma G x;\ \alpha = i\sqrt{\frac{\gamma G}{v}}x; \tag{2.225}$$

we obtain:

$$\frac{d^2\psi}{d\alpha^2} + \left(\frac{T_g - T_R}{\gamma G v} - \alpha^2\right)\psi = 0. \tag{2.226}$$

If we make another transformation as follows:

$$\psi(\alpha) = M_y(\alpha)e^{-\frac{\lambda}{i}\sqrt{\frac{v}{\gamma G}}\alpha} \text{ and } \frac{\lambda}{i}\sqrt{\frac{v}{\gamma G}} = \frac{\zeta\alpha}{2}, \tag{2.227}$$

we have:

$$\frac{d^2M_y}{d\alpha^2} - 2\alpha\frac{dM_y}{d\alpha} + 2nM_y = 0 \tag{2.228}$$

and given that:

$$\left.\begin{aligned} T_g - T_R &= (2n+1)\gamma G v \\ \zeta &\approx 1 \end{aligned}\right\}, \tag{2.229}$$

the final solution becomes:

$$M_y(x) = H_n\left(i\sqrt{\frac{\gamma G}{v}}x\right) = (-1)^n \exp\left(-\frac{\gamma G}{v}x^2\right)\frac{d^n}{dx^n}\exp\left(-\frac{\gamma G}{v}x^2\right) \tag{2.230a}$$

where

$$n = \frac{T_R - T_g}{2\gamma G v} - \frac{1}{2} \tag{2.230b}$$

From equations (2.222, 2.230), the term $\frac{1}{\zeta}$ represents the phase change of the spin at the position x, provided that the relaxation times T_1 and T_2 are properly chosen to represent the gradient pulse duration in the pulsed-field gradient (PFG) NMR as shown in figures 2.2-2.3.

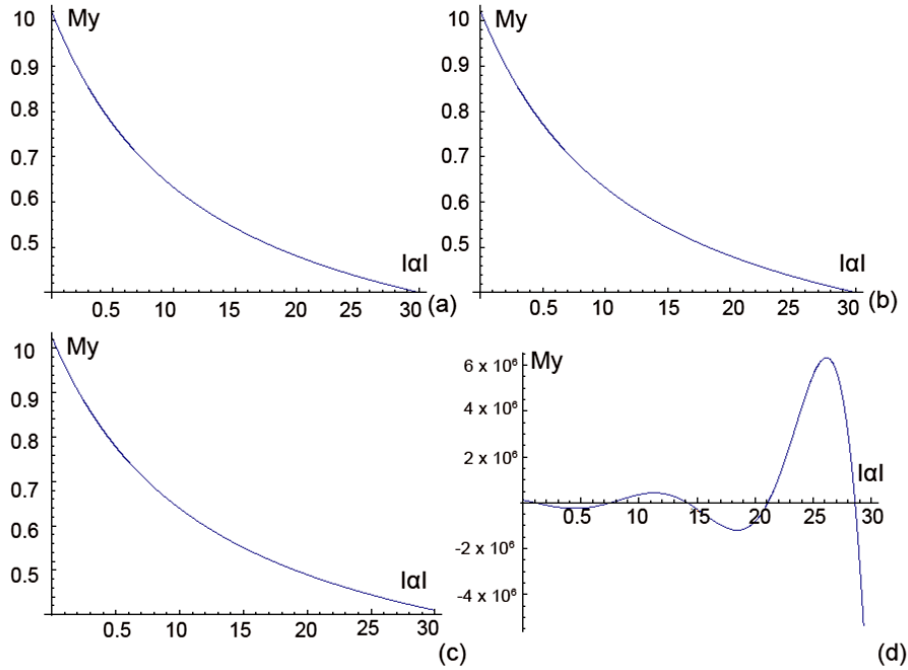

Fig. 2.2 *Plots of the transverse magnetization M_y against the absolute (positive) values of α using the relaxations time – values of kidney at 1.5T [3], G = 10mT/m, γ = 42.5781 x 10^6/T/s for (a) v = 3.0m/s (b) v = 0.3m/s (c) v = 0.003m/s (d) v = 0.000003m/s.*

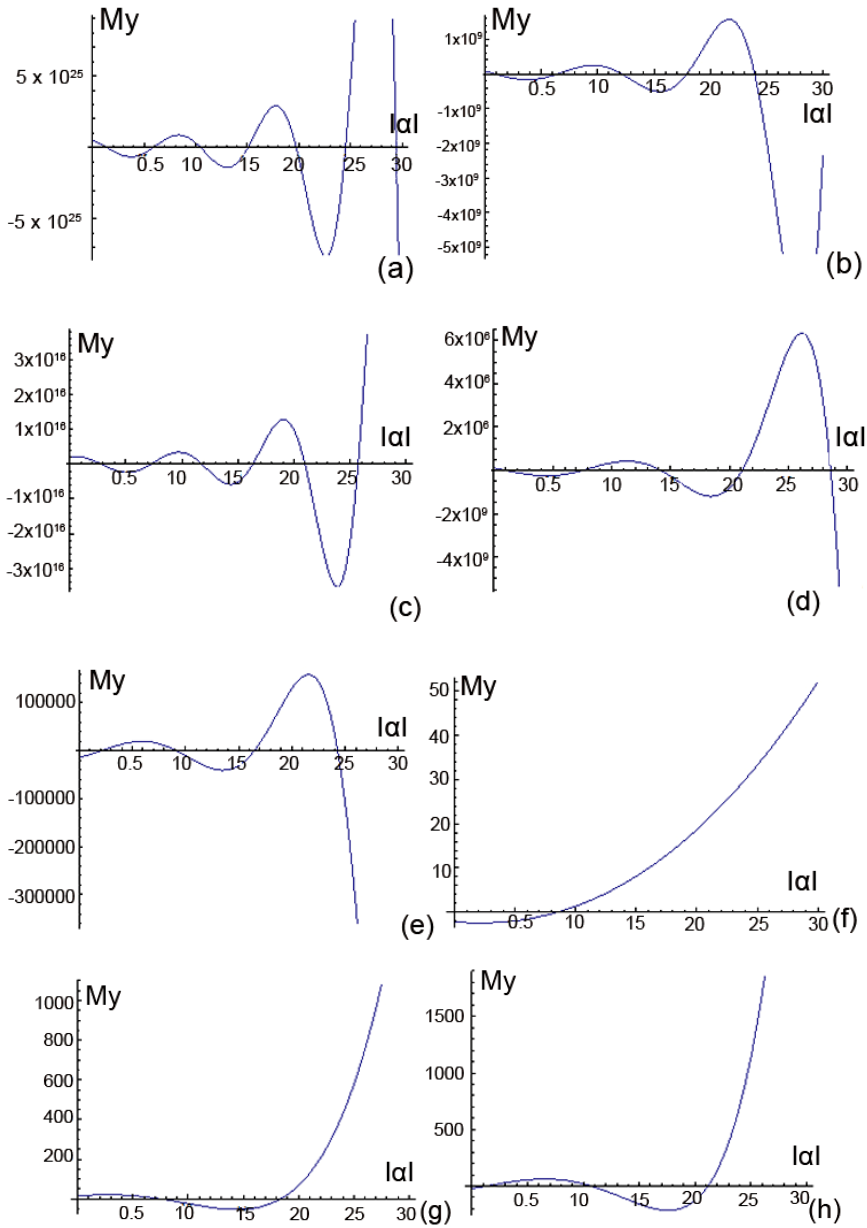

Fig. 2.3 *Plots of the transverse magnetization M_y against the absolute (positive) values of α; G = 10mT/m, γ = 42.5781 x 10^6/T/s, v = 0.000003m/s using the relaxations time – values, at 1.5T [3], of (a) skeletal muscle (b) heart muscle (c)liver (d) kidney (e) spleen (f) fatty tissue (g) gray brain matter (h) white brain matter.*

It is observed from figures (2.1) and (2.2) that as the fluid velocity reduces as often encountered in cellular processes, the imaging equation as given in equation (2.224) shows contrast in terms of MR signals. Figure (2.2) shows that the behaviour of the MR signals is completely different for different tissues. It is quite interesting to note that the magnitude of the signals becomes so large at the molecular level. This can make it possible to follow processes at molecular level in real time with brighter images.

2.20 The Hermite Polynomials

Based on equations (2.224-2.225), equation (2.40) becomes:

$$\frac{d^2\psi(x)}{dx^2} + \left(\alpha - \beta^2 x^2\right)\psi(x) = 0 \tag{2.231}$$

$$\alpha = \frac{T_g - T_R}{v^2} : \beta = \frac{\gamma G}{v}; \; T_g = \frac{1}{T_1 T_2} \text{ and } T_R = \frac{1}{4T_0^2}.$$

where G is the strength of the gradient field, The solutions of equation (2.40) are shown in table 1;

Table 1. *Solution of the Bloch NMR flow equation in terms of Hermite Polynomials.*

n	$\left\|\frac{(T_G - T_R)}{v\gamma G}\right\|$	M_{yn}
0	1	$\left(\frac{\gamma G}{\pi v}\right)^{\frac{1}{4}} e^{-\left(\frac{x}{2vT_o}+\frac{\gamma G x^2}{2v}\right)}$
1	3	$\frac{1}{\sqrt{2}}\left(\frac{\gamma G}{\pi v}\right)^{\frac{1}{4}}\left(2\sqrt{\frac{\gamma G}{v}}x\right)e^{-\left(\frac{x}{2vT_o}+\frac{\gamma G x^2}{2v}\right)}$
2	5	$\frac{1}{\sqrt{8}}\left(\frac{\gamma G}{\pi v}\right)^{\frac{1}{4}}\left(\frac{4\gamma G x^2}{v}-2\right)e^{-\left(\frac{x}{2vT_o}+\frac{\gamma G x^2}{2v}\right)}$
3	7	$\frac{1}{\sqrt{48}}\left(\frac{\gamma G}{\pi v}\right)^{\frac{1}{4}}\left(8\left(\frac{\gamma G}{v}\right)^{\frac{3}{2}}x^3-12\sqrt{\frac{\gamma G}{v}}x\right)e^{-\left(\frac{x}{2vT_o}+\frac{\gamma G x^2}{2v}\right)}$

where: $\frac{\alpha}{\beta} = (2n+1)$

$$\text{or } \left|\frac{(T_G - T_R)}{(2n+1)\gamma G}\right| = v \text{ and n = 0, 1, 2, 3, 4, 5,.....} \quad (2.232)$$

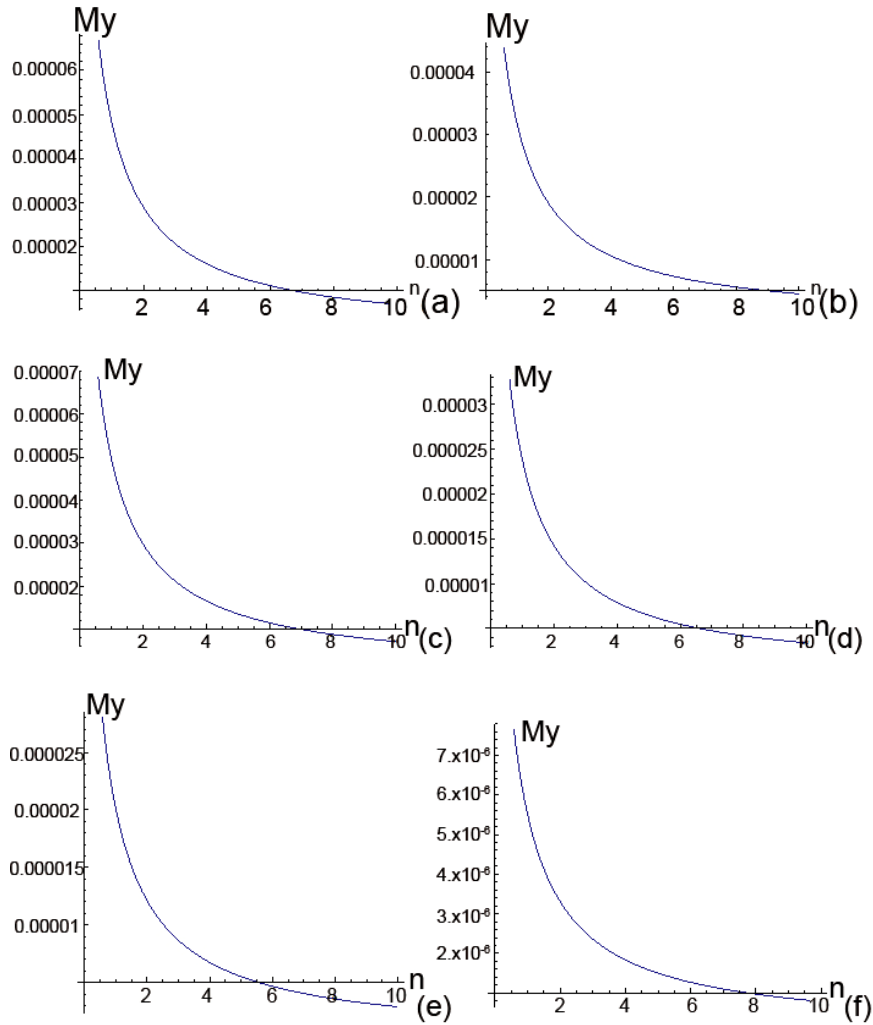

Fig. 2.4 *Plots of fluid velocity against parameter n when $G = 10mTm^{-1}$, $\gamma = 42.5781 \times 10^{6}T^{-1}s^{-1}$ using the relaxations time – values, at 1.5T [3], of (a) skeletal muscle (b) heart muscle (c)liver (d) kidney (e) spleen (f) fatty tissue (g) gray brain matter (h) white brain matter.*

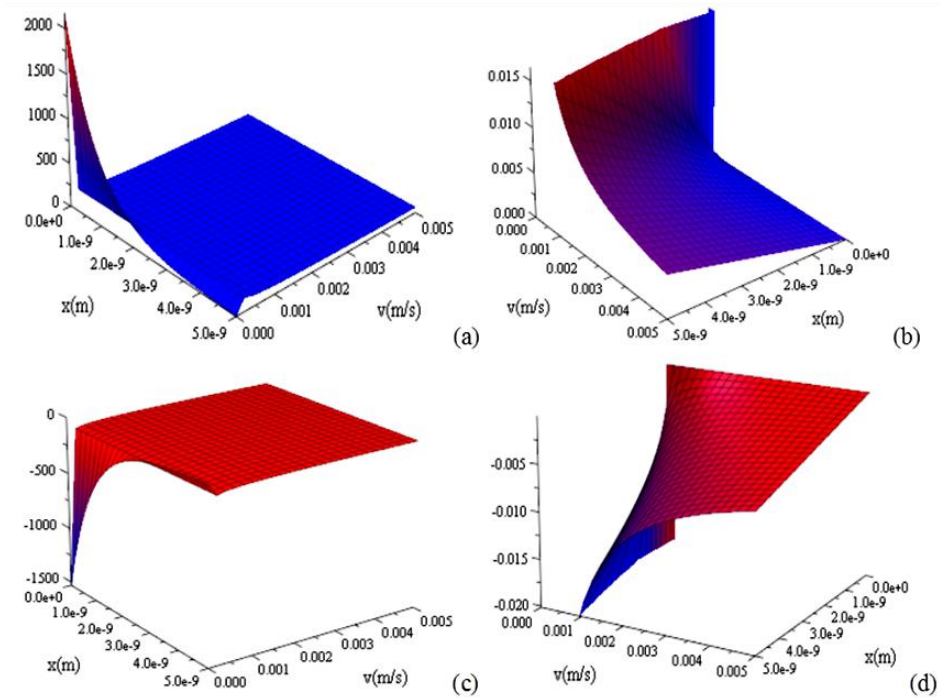

Fig. 2.5 *Plots of transverse magnetization against v and x; G = 10mTm^{-1}, γ = 42.5781 x 10^{6}T^{-1}s^{-1} using the relaxations time – values of kidney at 1.5T [2] for (a) n = 0 (b) n = 1(c) n = 2 (d) n = 3.*

Based on equation (2.232) and figure (2.3), the highest velocity is recorded when n = 0 and the velocity decreases when n increases. For each value of n, the NMR signal at the molecular level is obtained as Based on equation (2.232) and figure (2.4), the highest velocity is recorded when n = 0 and the velocity decreases when n increases. For each value of n, the NMR signal at the molecular level is obtained as shown in table 1 and equation (2.218). If Ax^2 is defined as the cross sectional area of blood vessels, the method can be very useful in estimating blood flow in capillaries or veins at the molecular level, especially in the assessment of angiogenesis and cancer proliferation. It is worthy of note that as the values of n increases (moderate decrease in the fluid velocity), the signal behaves like that of electron spin resonance (Figs 2.5c and

2.5d). This may be very important in the imaging of the complex molecular changes often observed in cancer cells.

2.21 Application to Multiple Sclerosis

Multiple sclerosis (MS) is an inflammatory disease in which the fatty myelin sheaths around the axons of the brain and spinal cord are damaged, leading to demyelination and scarring as well as a broad spectrum of signs and symptoms. MS affects the ability of nerve cells in the brain and spinal cord to communicate with each other effectively. Nerve cells communicate by sending electrical signals called action potentials down long fibers called axons, which are contained within an insulating substance called myelin. In MS, the body's own immune system attacks and damages the myelin. When myelin is lost, the axons can no longer effectively conduct signals [67]. Although much is known about the mechanisms involved in the disease process, the cause remains unknown.

MRI has been considered to be the most informative noninvasive method to diagnose and monitor disease progression in patients with multiple sclerosis (MS) [68]. However, conventional T_2-weighted MR images do not sufficiently correlate with histo-pathological substrates and clinical disability [68]. Conventional T_2-weighted images are unable to distinguish underlying histo-pathological substrates, such as inflammation, edema, demyelination, gliosis, and axonal loss, because all of these lesions have identical high signal on T_2-weighted images. We study equation (2.206) when the transverse magnetization is finite as x tends to infinity. The solution is given as:

$$M_y(x) = C_1\sqrt{x}J_n(kx) \tag{2.233a}$$

where:

$$n = \frac{\sqrt{1-\beta^2}}{2} \tag{2.233b}$$

Since the abnormalities observed in MS mostly involve the white matter (T_1 = 0.78s, T_2 = 0.09s), gray matter (T_1 = 0.92s, T_2 = 0.10s) and CSF (T_1 = 4.50s, T_2 = 2.30s), we shall make use of their relaxation properties at 1.5T to compare their transverse magnetization for different ranges of x as shown in figure 2.5.

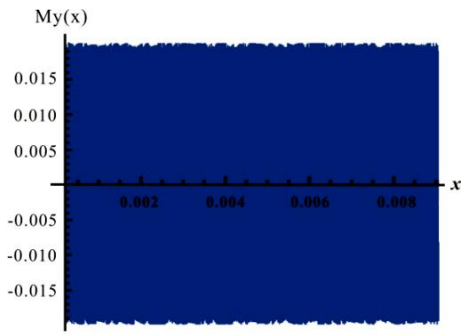

(a1)

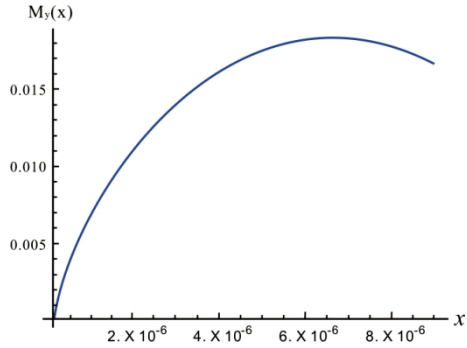

(a2)

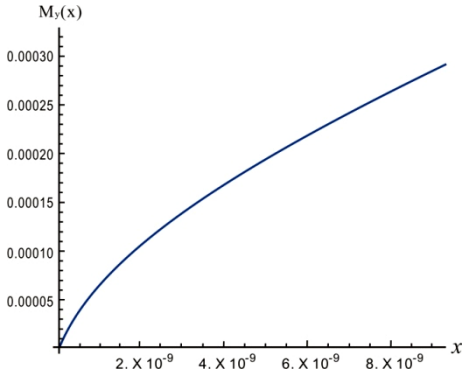

(a3)

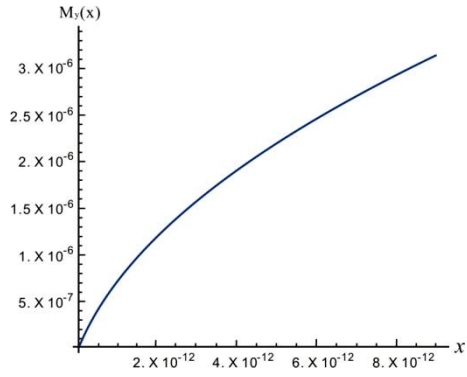

(a4)

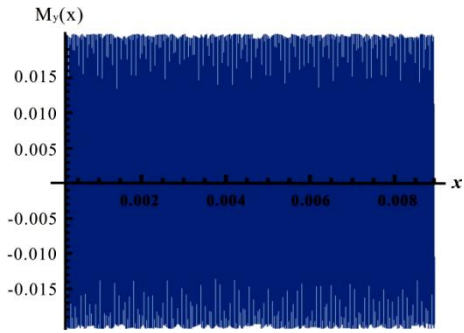

(b1)

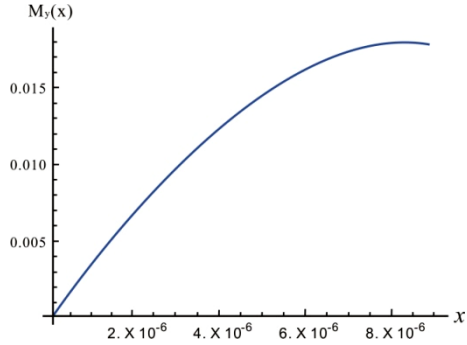

(b2)

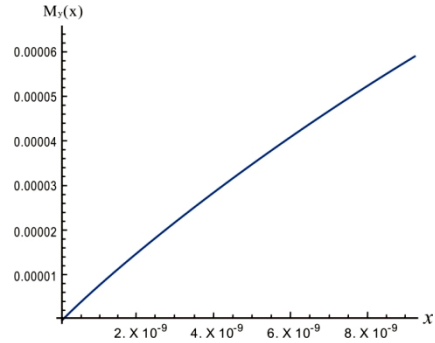

(b3)

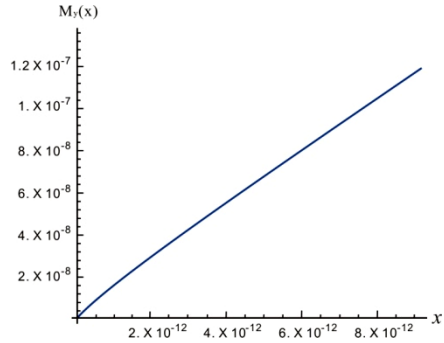

(b4)

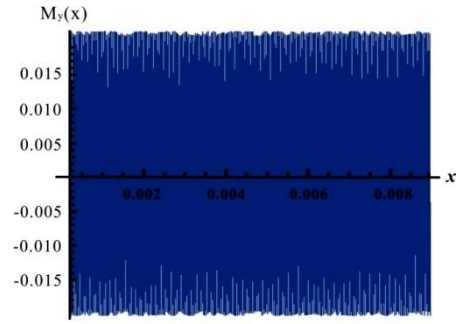

(c1)

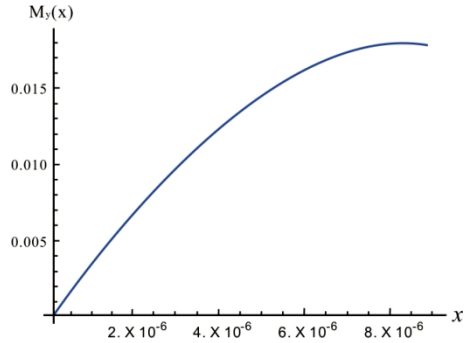

(c2)

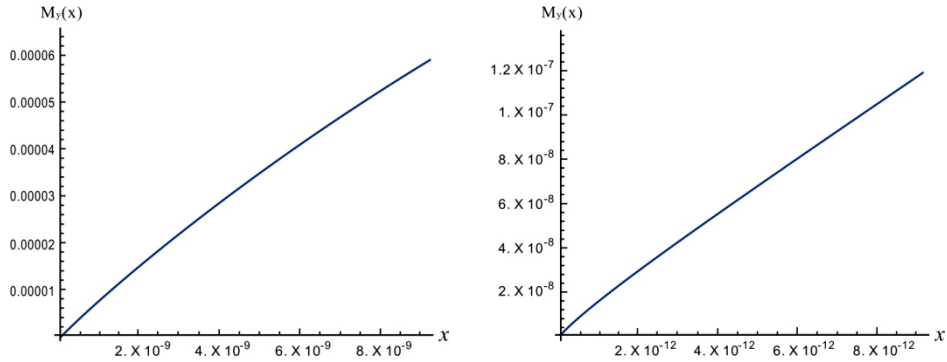

(c3) (c4)

Fig. 2.6 *Plots of transverse magnetization against x for C_1 = 10, G = 0.033T/m and τ = 0.02s; using the relaxation times of (ai) CSF in milli range (a2) CSF in micro range (a3) CSF in nano range (a4) CSF in pico range (bi) Gray matter in milli range (b2) Gray matter in micro range (b3) Gray matter in nano range (b4) Gray matter in pico range (ci) White matter in milli range (c2) White matter in micro range (c3) White matter in nano range (c4) Whiet matter in pico range.*

The results obtained in Fig. 2.6 confirm what has been observed in T_2 – weighted MR experiments. Changes in relaxation times that are direct indication of histo-pathological substrates do not contribute significantly to the magnitude of the MR signal. That is, dynamics of these important substrates cannot easily be seen on MR scans. However, from figure 2.6, we have observed that the transverse magnetization is actually responding very slowly to small changes in T_0. The magnitude of M_y is changing very slowly from one tissue to another. Secondly, we see that whenever x is in the microscopic range, the behavior of M_y changes uniquely and since most tissue processes are found in this geometrical range, inflammation, edema formation, demyelination, gliosis and axonal may easily be imaged. However, to realize this, the MR algorithm must be designed such that C_1 takes on very high values in order to improve signal magnitudes. Finally, we suggest that higher static field strength may be required for good MR assessment of multiple sclerosis, although the

influence of such high fields and the associated gradient fields on normal tissue functions must first be taken into consideration.

2.22 Bloch - Torrey Equation for NMR Studies of Molecular Diffusion

Since the diffusion coefficient varies very slowly with the radial distance r, it is interesting to note that $B_1(x,t)$ in equation (2.33) can be defined appropriately based on the problems to be solved. For example if we define $B_1(x,t)$ as:

$$\gamma B_1(r,t) = f(r) M_y(r,t) \tag{2.234}$$

Parameter f(r) in equations (2.234) can be appropriately defined to solve specific biological and medical problems. Generally, equation (2.33) becomes:

$$\frac{\partial M_y}{\partial t} = \frac{D}{r^2}\frac{\partial}{\partial r}\left(r^2 \frac{\partial M_y}{\partial r}\right) + F_0 f(r) M_y \tag{2.235}$$

The Bloch –Torey equation for the magnetization density $M_y(r,t)$ arising from spins diffusing with diffusion coefficient D and an arbitrary time-dependent linear gradient field is obtained from equation (2.33) if we define $B_1(x,t)$ as:

$$\gamma B_1(r,t) = -igf(t) M_y(r,t) \tag{2.236}$$

where g denotes the product of F_o and the gradient strength, the gradient field has the temporal shape function f(t) in the direction x, where r is is the position vector of the spin. For one dimensional motion, equations (2.33) becomes:

$$\frac{\partial M_y}{\partial t} = D\frac{\partial^2 M_y}{\partial x^2} - igf(t) M_y(x,t) \tag{2.237}$$

Equation (2.237) is the Bloch-Torrey equation which has been solved for the NMR study of molecular diffusion [69, 70].

2.23 Adiabatic Model of Bloch NMR Flow Equation

In this section, we consider equation (2.25) under adiabatic condition when the rf B_1 field is a constant. The adiabatic condition is defined as:

$$\gamma^2 B_1^2(x) >> \left(\frac{1}{T_1 T_2}\right) \tag{2.238}$$

Based on equation (2.238), equation (2.25) can be written as:

$$v^2 T_1^2 \frac{d^2 M_y}{dx^2} + v T_1^2 \left(\frac{1}{T_1} + \frac{1}{T_2}\right) \frac{dM_y}{dx} + \varsigma^2 M_y = \varsigma M_o \tag{2.239}$$

where

$$vT_1 = \sqrt{1 - x^2} \qquad 0 < x < 1 \quad \text{for real value of v} \tag{2.240}$$

$$v = \frac{-4xT_1T_2}{T_1^2(T_1 + T_2)} \quad \text{when n odd n} = 1, 3, 5, 7, 9, \ldots\ldots \tag{2.241}$$

$$\varsigma = T_1 \gamma B_1 \tag{2.242}$$

For human blood flow of T_1 = 1.0s, the parameter ς is a real constant which completely defines constant values of rf B_1 field for the NMR system [71, 72].

$$\varsigma = \gamma B_1 \tag{2.243}$$

The application of equation (2.239-2.242) has been demonstrated [71].

2.24 Application of Time Dependent Bloch NMR Equation and Pennes Bioheat Equation to Theranostics

Theranostics is the combination of therapeutics and diagnostics. It has been regarded as a key part of personalized medicine and requires considerable

advances in predictive medicine; novel theranostic agents are developed and carefully designed for in vivo quantitative assessment of the amount of drug reaching a pathological region and the visualization of molecular changes due to the therapeutic effects of the delivered drug. This study intends to mathematically model a closely knitted theranostic method in which a specially selected radiofrequency field is used to heat up a tissue and at the same time cause the spins of the tissue to emit MR signals.

The key to this application is the specific absorption rate (SAR) which drives both rf power heating within a tissue and is related directly to the B_1 field which is needed to cause spin resonance. If we consider bioheat flow in one direction [73, 42] with uniform tissue properties, we have:

$$\rho c \frac{\partial T}{\partial t} = k \frac{\partial^2 T}{\partial x^2} + SAR - w_b c_b (T - T_b) \tag{2.244}$$

where ρ is tissue density, c is the specific heat of tissue, T is the tissue temperature, t is the time, w_b is the blood perfusion rate, c_b is the specific heat of blood, T_b is the supplying arterial blood temperature, k is the thermal conductivity of tissue, and x is the distance from the skin surface. SAR is the applied rf power per unit volume. If the tissue temperature changes very slowly with x, we have:

$$\rho c \frac{\partial T}{\partial t} = SAR - w_b c_b (T - T_b) \tag{2.245}$$

The solution to equation (245) is given as follows:

$$T(t) = T_b + \frac{SAR}{w_b c_b} + A \exp\left(- \frac{w_b c_b}{\rho c} t \right) \tag{2.246}$$

If the tissue temperature before the application of the rf field does not defer significantly from the arterial temperature, the initial the condition for this problem is given as:

$$T(t=0) = T_b \tag{2.247}$$

We finally have:

$$T(t) = T_b + \frac{SAR}{w_b c_b}\left\{1 - \exp\left(-\frac{w_b c_b}{\rho c} t\right)\right\} \tag{2.248}$$

SAR and Oscillating Magnetic Field: The rf power for the voxel volume V_{vox} is P_{rf} = *(SAR)* V_{vox} . The energy of the oscillating radio wave is given as E_{rf} = $\hbar\gamma B_1$, whose rate of change is:

$$P_{rf} = \frac{dE_{rf}}{dt} \text{ and } E_{rf} = \int_{t_0}^{t} (SAR) V_{vox} dt \tag{2.249}$$

$$\gamma B_1(t) = \frac{V_{vox}}{\hbar}(SAR)(t - t_0) \tag{2.250}$$

SAR and Time dependent NMR Equation: We can relate time dependent MRI signal to SAR using the time independent NMR equation [42] given by equation (2.251) and (2.252):

$$\frac{d^2 M_y}{dt^2} + T_o \frac{dM_y}{dt} + \left(T_g + \gamma^2 B_1{}^2(t)\right) M_y = \frac{M_o}{T_1} \gamma B_1(t) \tag{2.251}$$

$$\text{where } T_g = \frac{1}{T_1 T_2} \text{ and } T_0 = \frac{1}{T_1} + \frac{1}{T_2} \tag{2.252}$$

If we sample the signal when the transverse component of the magnetization has the largest amplitude, we write $M_0 \approx 0$. Provided that the condition $T_g \ll \gamma^2 B_1^2(t)$ holds, equation (2.251) becomes [42]:

$$\frac{d^2M_y}{dt^2} + T_o\frac{dM_y}{dt} + \gamma^2 B_1^{\,2}(t)M_y = 0 \tag{2.257}$$

From equations (2.251) and (2.252), we obtain:

$$\frac{d^2M_y}{dt^2} + T_o\frac{dM_y}{dt} + \left(\frac{V_{vox}}{\hbar}\right)^2 (SAR)^2(t-t_0)^2 M_y = 0 \tag{2.258}$$

If the rf B_1 field is applied at time $t_0 = 0$, we have:

$$M_y(t) = (\beta)^n(t)^n\left[C_1 J_n\left(\frac{V_{vox}}{2\hbar}t^2\right) + C_2 Y_n\left(\frac{V_{vox}}{2\hbar}t^2\right)\right];\ n = \frac{1-T_0 t}{2} \tag{2.259}$$

This solution is valid for $T_0(t-t_0) \le 1$. It is always required that the transverse magnetization be finite as time tends to infinity, hence, we write:

$$M_y(t) = C_1(\beta)^{\frac{1-T_0t}{2}}(t)^{\frac{1-T_0t}{2}} J_{\frac{1-T_0t}{2}}\left(\frac{V_{vox}}{2\hbar}t^2\right) \tag{2.260}$$

The results obtained in equations (2.248, 2.260) have been simulated with relaxation parameters of human liver at 1.5T [74] and the corresponding thermal properties [72, 73]: $T_1 = 0.610$s, $T_2 = 0.057$s, $w_b = 2.86$kg/m^{3}s, $c_b = 3960$J/kg.K, $\rho = 1060$kg/m^3, $c = 3600$J/kg.K. Plots (a) and (b) (SAR = 4W/m^3) give the distribution of the tissue temperature and transverse magnetization on a log scale while plot (c) (SAR = 40000W/m^3) gives the density plot of the transverse magnetization as a function of time and tissue temperature.

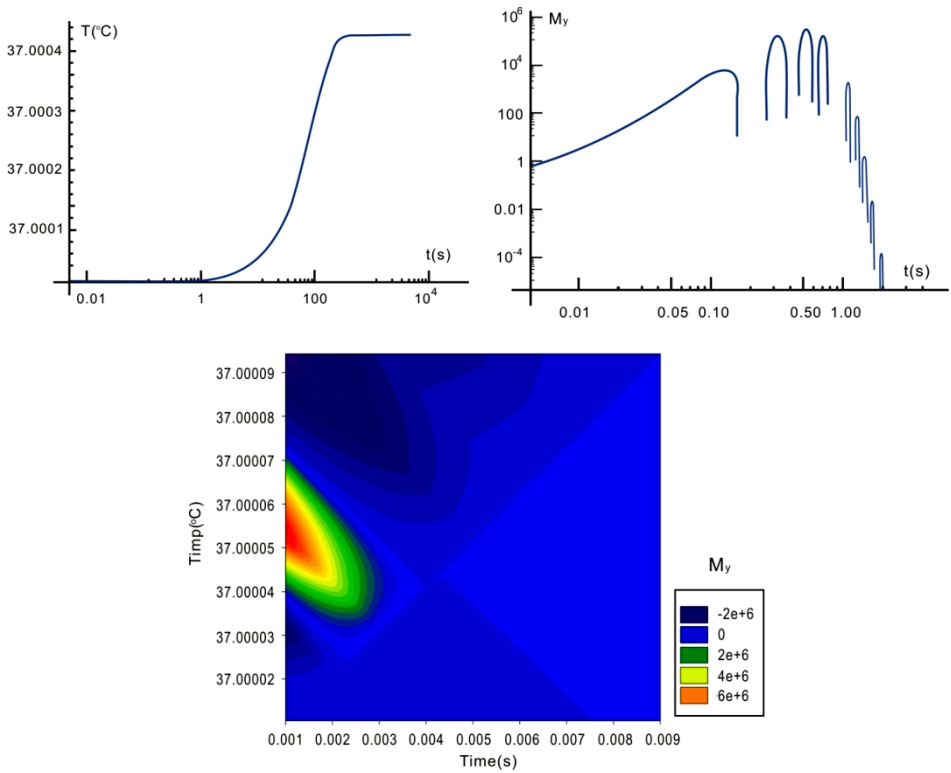

Fig. 2.7 *show (a) Temperature profile (b) Transverse magnetization profile (c) density image. This shows that provided the conditions which led to equation (2.248) are met, real time theranostic imaging can easily be done with equations (2.248, 2.260).*

The temperature distribution and the rf power needed to generate rf $B_1(t)$ field within the medically acceptable SAR limit during MRI scanning procedure have been investigated by solving the Pennes Bioheat equation in terms of MRI parameters. The relationship between temperature, SAR and rf $B_1(t)$ at any given time (under the assumed conditions) is clearly shown in equations (2.248, 2.260) and Fig.2.7. a, b, c. With this, accurate estimate of the amount of rf field needed for a particular power deposition for safe imaging of different tissues can be done. What is most interesting about the results in this study is that time, SAR and voxel volume can easily be used to manipulate the range of

temperature needed for therapy without unnecessarily increasing the tissue temperature. These changes directly influence the NMR signal as clearly illustrated in Fig, 2.7c and shows that we can do tissue imaging and temperature mapping at the same time.

2.25 Summary

The major contributions of this book can be seen at a glance by the development of the following differential equations derived from the Bloch NMR flow equations. These differential equations can be referred to as the Awojoyogbe-Bloch NMR flow equations.

$$v^2\frac{\partial M_y}{\partial x^2}+2v\frac{\partial^2 M_y}{\partial x\partial t}+v\left(\frac{1}{T_1}+\frac{1}{T_2}\right)\frac{\partial M_y}{\partial x}+\left(\frac{1}{T_1}+\frac{1}{T_2}\right)\frac{\partial M_y}{\partial t}+\frac{\partial^2 M_y}{\partial t^2}+\left(\frac{1}{T_1T_2}+\gamma^2 {B_1}^2(x,t)\right)M_y=\frac{\gamma B_1(x,t)M_o}{T_1} \tag{S1}$$

$$\frac{d^2M_y}{dx^2}+\frac{1}{v}\left(\frac{1}{T_1}+\frac{1}{T_2}\right)\frac{dM_y}{dx}+\frac{1}{v^2}\left(\gamma^2B_1^2(x)+\frac{1}{T_1T_2}\right)M_y=\frac{M_o\gamma B_1(x)}{v^2T_1} \tag{S2}$$

$$\frac{d^2\psi}{dx^2}+\frac{1}{v^2}\left(\gamma^2B_1^2+\frac{1}{T_1T_2}\right)\psi=0 \tag{S3}$$

$$\frac{d^2M_y}{dt^2}+\left(\frac{1}{T_1}+\frac{1}{T_2}\right)\frac{dM_y}{dt}+\left(\gamma^2B_1^2(t)+\frac{1}{T_1T^2}\right)M_y=\frac{M_0}{T_1}\gamma B_1(t) \tag{S4}$$

$$v^2 \frac{\partial^2 M_y}{\partial x^2} + \left(\frac{1}{T_1} + \frac{1}{T_2}\right)\frac{\partial M_y}{\partial t} = 0 \tag{S5}$$

$$D\frac{\partial^2 M_y}{\partial x^2} + \frac{\partial M_y}{\partial t} = 0$$

where

$$D = \frac{v^2}{T_o} \tag{S6}$$

$$v^2 \frac{\partial^2 M_y}{\partial x^2} + 2v\frac{\partial^2 M_y}{\partial x \partial t} + \frac{\partial^2 M_y}{\partial t^2} = 0 \tag{S7}$$

$$\frac{d^2 M_y}{dt^2} + T_o \frac{dM_y}{dt} + \left(T_g + \gamma^2 B_1{}^2(t)\right)M_y = \frac{M_o}{T_1}\gamma B_1(t) \tag{S8}$$

$$i\hbar\frac{\partial M_y}{\partial t} = -\frac{\hbar^2}{2m}\frac{\partial^2 M_y}{\partial x^2} + \frac{i\hbar F_o}{T_o}\gamma B_1(x,t) \tag{S9}$$

$$\left(1-\varsigma^2\right)\frac{d^2 M_y}{d\varsigma^2} - 2\varsigma\frac{dM_y}{d\varsigma} + n(n+1)M_y = 0 \tag{S10}$$

$$\frac{d^2 M_y}{d\alpha^2} - 2\alpha\frac{dM_y}{d\alpha} + 2nM_y = 0 \tag{S11}$$

$$\frac{d^2\psi(x)}{dx^2} + \left(\alpha - \beta^2 x^2\right)\psi(x) = 0 \tag{S12}$$

$$x^2\frac{d^2 M_y}{dx^2} + x\sigma\frac{dM_y}{dx} + \left(\left(\gamma\frac{\sigma}{T_o}G\right)^2 x^2 + \frac{1}{T_1 T_2}\left(\frac{\sigma}{T_o}\right)^2\right)M_y = 0 \tag{S13}$$

$$x^2\frac{d^2 M_y}{dx^2} + x\sigma\frac{dM_y}{dx} + \left((\gamma G\tau)^2 x^2 + \frac{\tau^2}{T_1 T_2}\right)M_y = 0 \tag{S14}$$

$$x^2\frac{d^2 M_y}{dx^2} + x\sigma\frac{dM_y}{dx} + \left((\gamma GnTR)^2 x^2 + \frac{(nTR)^2}{T_1 T_2}\right)M_y = 0 \tag{S15}$$

$$x^2 \frac{d^2 M_y}{dx^2} + x\sigma \frac{dM_y}{dx} + \left((\theta)^2 x^2 + \frac{\tau^2}{T_1 T_2} \right) M_y = 0 \tag{S16}$$

$$v^2 T_1^2 \frac{d^2 M_y}{dx^2} + v T_1^2 \left(\frac{1}{T_1} + \frac{1}{T_2} \right) \frac{dM_y}{dx} + \varsigma^2 M_y = \varsigma M_o \tag{S17}$$

$$v^2 \frac{\partial^2 M_y}{\partial x^2} + \frac{\partial^2 M_y}{\partial t^2} = F_o \gamma B_1(x,t) \tag{S18}$$

$$\frac{\partial M_y}{\partial t} = D \frac{\partial^2 M_y}{\partial x^2} - igf(t) M_y(x,t) \tag{S19}$$

The ideal approach to exhaust most of the quantitative and qualitative information for studying biological systems at the macroscopic and microscopic levels by magnetic resonance imaging technique with particular reference to the theory, dynamics and applications of MRI would be to find generalized (time dependent and time independent) analytical solutions to these equations. The advantages of such solutions are related to the fact that the magnetizations and signals obtainable from them are synthesis of many parameters that are of clinical importance for most magnetic resonance imaging analyses.

Solutions to these equations will result to new developments in MRI physics. Quantitative and computational analyses, mathematical modeling and analytical solutions of these equations can lead to breath taking innovations and novel applications of MRI for improved health care. High quality and novel contributions related to biological, biomedical, clinical, geophysical and any other exciting applications are welcomed in the next volume of this book. All proposals can be addressed to the editor at abamidele@futminna.edu.ng or awojoyogbe@yahoo.com.

2.26 Conclusion

In this chapter, we have modeled the Bloch NMR flow equations into Bessel equation, Diffusion equation, Wave equation, Schrödinger's equation, Legendre's equation, Euler's equation and Boubaker polynomials. While the detailed analytical solutions of the time dependent NMR flow equation and the NMR wave equation are presented, solutions to other several equations that may be derived from equation (2.18) are available in standard textbooks on physics, mathematics and engineering mathematics. With appropriate initial and boundary conditions, solutions to these equations can be applied to solve most problems that may enhance the theory, dynamics and applications of MRI. This may open a large window of opportunities for researchers in all research fields to contribute to this high intellectually adventurous field thereby improving the image quality with better treatment of deceases at the most affordable cost. It is hoped that due to the ability of magnetic resonance imaging to probe right to the fundamental level, scientists may be able to image human cellular functions and such imaging modalities would definitely help in the understanding of the human diseased conditions. Information gathered from the images can then be added to the present medical database to make it more comprehensive and thus permit the physician to make a more specific diagnosis, prognosis and possibly the appropriate therapy. The basic challenge in this direction is finding the right mathematical frameworks which appropriately describe the processes involved.

References

[1] J.T. Ngo, P.G. Morris, General Solution to the NMR excitation problem for noninteracting spins. Magn. Reson. Med. 5 (1987) pp. 217-237.

[2] D. E. Rourke, P. G. Morris. The inverse scattering transform and its use in the exact inversion of the Bloch equation for non-interacting spins. J Magn Reson 99 (1992) pp. 118-138.

[3] M.G. Abele, H. Rusinek, F. Bertora, and A. Trequattrini. Compensation of field distortion with ferromagnetic material and permanent magnets. Journal of Applied Physics, 75(10):6990–699, 1994.

[4] A. Alexander, J. Tsuruda, and D. Parker. Elimination of Eddy current artifacts in diff usion weighted Echo Planar Images: the use of bipolar gradients. Journal of Magnetic Resonance in Medicine, 38:1016–1021, 1997.

[5] J.F. Schenck. The role of magnetic susceptibility in magnetic resonance imaging. Med. Phys., 23(6):815– 850, 1996.

[6] S. Balac and G. Caloz. Mathematical modeling and numerical simulation of magnetic susceptibility artifacts in Magnetic Resonance Imaging. Computer Methods in Biomechanics and Biomedical Engineering, 3:335–349, 2001.

[7] S. Balac, H. Benoit-Cattin, T. Lamotte, and C. Odet. Analytic solution to boundary integral computation of susceptibility induced magnetic field inhomogeneities. Mathematical and Computer Modelling, 39:437– 455, 2004.

[8] C.R. Camacho, D.B. Pleves, and R.M. Henkelman. Non-susceptibility artifacts due to metallic objects in MR imaging. JMRI, 5:75–88, 1995.

[9] J.A. Malko, J.C. Hoff man, and P.J. Jarret. Eddy-current induced artifacts caused by a MR compatible halo device. Radiology, 173:563–564, 1989.

[10] L.H. Bennett, P.S. Wang, and M.J. Donahue. Artifacts in magnetic resonance imaging from metals. J. appl. phys., 79(8):4712–4714, 1996.

[11] J.G. Sled and G.B. Pike. Standing-wave a rf penetration artifacts caused by elliptic geometry: an electrodynamic analysis of MRI. IEEE Trans. Med. Imag., 17(4):653–662, 1998.

[12] G. Sebastiani and P. Barone. Mathematical principles of basic magnetic resonance imaging in medicine. Signal Processing, 25:227–250, 1991. 16. P.F.

Hsieh and Y. Sibuya. Basic theory of ordinary diff erential equations. Springer, 1999.

[13] W. Walter. Ordinary diff erential equations. Springer, 1998.

[14] T.O. Levante, M. Baldus, B.H. Meier, and R.R. Ernst. Formalized quantum mechanical Floquet theory and its application to sample spinning in nuclear magnetic resonance. Molecular Physics, 86(5):1195 – 1212, 1995.

[15] A.D. Bain and R.S. Dumont. Introduction to Floquet theory: The calculation of spinning sideband intensities in magic-angle spinning NMR. Concepts in Magnetic Resonance, 13(3):159–170, 2001.

[16] F. Casas, J.A. Oteo, and J. Ros. Floquet theory: Exponential perturbative treatment. J. Phys. A, Math. Gen., 34(16):3379–3388, 2001.

[17] W. L. Hart. The Cauchy-Lipschitz method for infinite systems of diff erential equations. American Journal of Mathematics, 43(4):226–231, 1921.

[18] S. Balac and M. Sadkane. On the computation of eigenvectors of a symmetric tridiagonal matrix: comparison of accuracy improvements of Givens and inverse iteration methods. Technical report, Laboratoire de Math ématiques Appliqu ées de Lyon, France, 2003. http://hal.archives-ouvertes.fr/hal- 00137149.

[19] G. W. Stewart and J.-G. Sun. Matrix perturbation theory. Academic Press, New York, 1990.

[20] J.D. Jackson. Classical electrodynamics. John Wiley and Sons, 1999.

[21] H. Benoit-Cattin, G. Collewet, B. Belaroussi, H. Saint-Jalmes, and C. Odet. The SIMRI project: a versatile and interactive mri simulator. J. Magn. Reson. Imaging, 173:97–115, 2005.

[22] R. A. Horn and C. R. Johnson. Matrix Analysis. Cambridge University Press, 1985.

[23] J. A. Nyenhuis and O. P. Yee. Simulation of nuclear magnetic resonance spin echoes using the Bloch equation: Influence of magnetic field inhomogeneities. Journal of Applied Physics, 76(10):6909–6911, 1994.

[24] D. E. Rourke. Solutions and linearization of the nonlinear dynamics of radiation damping. Concepts in Magnetic Resonance, 14(2):112–129, 2002.

[25] D. Zill. A first course in diff erential equations. ITP, 1997.

[26] O.C. Zienkiewicz and R.L. Taylor. The finite element method. Mac Graw Hill, 1989.

[27] S. Balac, G. Caloz, G. Cathelineau, B. Chauvel, and J.D. De Certaines. An integral representation method for numerical simulation of MRI artifacts induced by metallic implants. Journal of Magnetic Resonance in Medicine, 45:724–727, 2001.

[28] Rourke DE, Morris PG Half solitons as solutions to the Zakharov-Shabat eigenvalue problem for rational reflection coefficient with application in the design of selective pulses in nuclear magnetic resonance. Phys. Rev. A 46 (1992) pp. 3631-3636.

[29] Cowan, B. P. (1997). Nuclear Magnetic Resonance and Relaxation, First Edition (Cambridge: Cambridge University Press).

[30] V. A. Antonov, E. I. Timoshkova, and K. V. Kholoshevnikov, *An Introduction to Theory of Newton's Potential* [in Russian], Nauka, Moscow, 1988.

[31] P. K. Suetin, *Classical Orthogonal Polynomials* [in Russian], Nauka, Moscow, 1979.

[32] I. S. Gradshtein and I. M. Ryzhik, *Tables of Integrals*, *Series*, *and Products* [in Russian], Nauka, Moscow, 1971; English transl.: Academic Press, New York–London, 1994.

[33] H. Bateman and A. Erd élyi, *Higher Transcendental Functions*, vol. 3: *Elliptic and Modular Functions*. *Lame and Mathieu Functions*, McGraw–Hill, New York–Toronto–London, 1955; Russian transl.: Nauka, Moscow, 1967.

[34] B. E. Chapman and P. W. Kuchel, Fluoride transmembrane exchange in human erythrocytes measured with ^{19}F NMR magnetization transfer, European Biophysics Journal, 19 (1990) pp. 41-45.

[35] P. Donnat and J. Rauch, Global Solvability of the Maxwell-Bloch Equations from Nonlinear Optics, Archive for Rational Mechanics and Analysis, 136 (1996) pp. 291 – 303.

[36] F. Bloch. Nuclear induction. Physical Review, 70(7):460–474, 1946.

[37] C.P. Slichter, editor. Principles of Magnetic Resonance. Springer-Verlag, New-York, 1990. 2. P.T. Callaghan. Principles of Nuclear Magnetic Resonance Microscopy. Oxford University Press, 1994.

[38] O.B. Awojoyogbe, Analytical Solution of the Time Dependent Bloch NMR Equations: A Translational Mechanical Approach. Physica A, 339, (2004) pp 437-460.

[39] Awojoyogbe, O. B. A Mathematical Model of Bloch NMR Equations for Quantitative Analysis of Blood Flow in Blood Vessels with Changing Cross-section II. Physica A, 323c, pp 534-550, (2003).

[40] Awojoyogbe, O. B. A quantum mechanical model of the Bloch NMR flow equations for electron dynamics in fluids at the molecular level. Phys, Scr.75, 788-794. (2007).

[41] Awojoyogbe, O. B. A Mathematical Model of Bloch NMR Equations for Quantitative Analysis of Blood Flow in Blood Vessels with Changing Cross-section I. Physica A, 303, pp 163-175, (2002).

[42] Awojoyogbe O.B., Dada O.M., Faromika O.P., Dada O.E. Mathematical Concept of the Bloch Flow Equations for General Magnetic Resonance Imaging: A Review; Concepts in Magnetic Resonance Part A, Vol. 38A (3) 85–101 (2011).

[43] O. B. Awojoyogbe and K. Boubaker, A solution to Bloch NMR flow equations for the analysis of hemodynamic functions of blood flow system using m – Boubaker polynomials, Current Applied Physics, Elsevier, DOI: 10.1016/j.cap.2008.01.0193. Vol. 9 (1), (2009). pp. 278-283.

[44] Awojoyogbe OB, Karem B, Aweda MA, Dada M. (2010). BPES-Related Mathematical Development For The Phase Shift Due to rf Magnetic Field In Heart Inferior Coronary Artery NMR Imaging. J.Clinic. Experiment Cardiol. 1: 111, doi. 10.4172/2155-9880, 111.

[45] M. Dada, M. A. Aweda, O. B. Awojoyogbe and K. Boubaker. Boubaker Polynomials Expression to the Magnetic Phase-Shift Induced In Leon Vigmond 3d-Model of the Human Heart. Journal of Mechanics in Medicine and Biology Vol. 12, No. 1 (2012) 1250016 (7 pages) World Scientific Publishing Company DOI: 10.1142/S021951941100454X.

[46] Bamidele O Awojoyogbe, Exploring new dimensions in cardiovascular flow and motion: application of Bloch NMR flow equations, Bessel and spherical harmonic functions J Cardiovasc Magn Reson. (2012); 14(Suppl 1): W28. Published online 2012 February 1. Doi: 10.1186/1532-429X-14-S1-W28.

[47] O. B Awojoyogbe, O.P. Faromika, M. Dada, O.S. Ojambati, K. Boubaker. Mathematical Models of real Geometrical Factors in Restricted Blood vessels for the Analysis of CAD (Coronary Artery Diseases) Using Legendre, Boubaker and

Bessel polynomials. Journal of Medical Systems. DOI 10.1007/s10916-009-9428-9 (2010).

[48] Awojoyogbe, O.B, Dada, M. Basis for the Applications of Analytical models of the Bloch NMR Flow Equations for Functional Magnetic Resonance Imaging (fMRI): A Review. Recent Patents on medical imaging, 2010, 2.22-56.

[49] M. Dada, O.P. Faromika, O.B. Awojoyogbe, M.A. Aweda and I.A Fuwape. Mathematical Formulation of NMR Experimental Parameters for Diffusion Magnetic Resonance Imaging: Part I (Cylindrical Geometry). International Journal of Mathematics, Game Theory and Algebra. Volume 20 Issue 1.pp, 1-21, (2010).

[50] O.B. Awojoyogbe, M. Dada, O.P. Faromika, M.A. Aweda and I.A. Fuwape Mathematical Formulation of NMR Experimental Parameters for Diffusion Magnetic Resonance Imaging: Part II (Spherical Geometry). International Journal of Mathematics, Game Theory and Algebra. Volume 20 Issue 1, pp.21-40, (2010).

[51] M. Dada, O. B. Awojoyogbe, Olufemi Folorunsho Moses, O.S. Ojambati, D.K. De and K. Boubaker, A mathematical analysis of Stenosis Geometry, NMR magnetizations and signals based on the Bloch NMR flow equations, Bessel and Boubaker polynomial expansions. Journal of Biological Physics and chemistry 9 (2009) 24DA09A.

[52] O.B. Awojoyogbe, O.P. Faromika, Olufemi Folorunsho Moses, M. Dada, I.A. Fuwape, K. Boubaker Mathematical model of the Bloch NMR flow equations for the analysis of fluid flow in restricted geometries using Boubaker expansion scheme. Current Applied Physics Ms. Ref. No.: CAP-D-09-00222 June 2009 (Available Online from www.sciencedirect.com).

[53] M. Dada, O.P. Faromika, O. B. Awojoyogbe, O.E. Dada, M.A. Aweda. The Impact of Geometry Factors on NMR Diffusion Measurements by the Stejskal and Tanner Pulsed Gradients Method. Int. J of Theoretical Physics, Group Theory and Nuclear Optics. Volume 15, Number 1/2, 2011.

[54] O.M. Dada, O.B. Awojoyogbe O. A. Adesola and K. Boubaker: Magnetic Resonance Imaging Derived Flow Parameters for the Analysis of Cardiovascular Diseases and Drug Development, Magnetic Resonance Insights: 2013:6 83–93, doi: 10.4137/MRI.S12195. This article is available from http://www.la-press.com.

[55] M. Dada, O. B. Awojoyogbe, Olufemi Folorunsho Moses, O.S. Ojambati, D.K. De and K. boubaker. A mathematical analysis of Stenosis Geometry, NMR magnetizations and signals based on the Bloch NMR flow equations, Bessel and

Boubaker polynomial expansions. Journal of Biological Physics and Chemistry. Volume 9, Number 3, p.p. 101–106 (2009).

[56] H. Labiadh and K. Boubaker, A Sturm-Liouville shaped characteristic differential equation as a guide to establish a quasi-polynomial expression to the Boubaker polynomials, *Journal of Differential Equations and C.P*. vol.(2),2007, pp. 117-133.

[57] M. Dada, O.B. Awojoyogbe O.S. Ojambati, K. Boubaker: *BPES Analysis of a new diffusion-Advection equation* for fluid flow in Blood vessels under Different Bio-Physico-Geometrical Conditions. Journal of Biophysics and structural Biology.Vol 2(3). Pp 28-34, April, (2010).

[58] K. Boubaker. On modified Boubaker polynomials: Some differential and analytical properties of the new polynomials issued from an attempt for solving bi-varied heat equation. *Trends in Applied Science Research, by Academic Journals, 'aj' N.Y;* Vol. 2(6) 2007, 540-544.

[59] O.B. Awojoyogbe M. Dada, K. Boubaker and O.A. Adesola, Flow Dynamics in Restricted Geometries: A Mathematical Concept Based on Bloch NMR Flow Equation and Boubaker Polynomial Expansion Scheme *Journal of Applied Mathematics and Physics*, 2013, Published Online November 2013 (http://www.scirp.org/journal/jamp).

[60] O.B. Awojoyogbe, M. Dada: Mathematical Design of A Magnetic Resonance Imaging Sequence Based on Bloch NMR Flow Equations and Bessel Functions. Chin J Magn Reson Imaging, 2013, Vol 4, No5 379-386.

[61] H. Labiadh and K. Boubaker, A Sturm-Liouville shaped characteristic differential equation as a guide to establish a quasi-polynomial expression to the Boubaker polynomials, *Journal of Differential Equations and C.P*. vol.(2), 2007, pp. 117-133.

[62] M. Dada, O.B. Awojoyogbe O.S. Ojambati, K. Boubaker: *BPES Analysis of a new diffusion-Advection equation* for fluid flow in Blood vessels under Different Bio-Physico-Geometrical Conditions. Journal of Biophysics and structural Biology.Vol 2(3). Pp 28-34, April, (2010).

[63] K. Boubaker. On modified Boubaker polynomials: Some differential and analytical properties of the new polynomials issued from an attempt for solving bi-varied heat equation. *Trends in Applied Science Research, by Academic Journals, 'aj' N.Y;* Vol. 2(6) 2007, 540-544.

[64] O.B. Awojoyogbe M. Dada, K. Boubaker and O.A. Adesola, Flow Dynamics in Restricted Geometries: A Mathematical Concept Based on Bloch NMR Flow Equation and Boubaker Polynomial Expansion Scheme *Journal of Applied*

Mathematics and Physics, 2013, Published Online November 2013 (http://www.scirp.org/journal/jamp).

[65] O.B. Awojoyogbe, M. Dada: Mathematical Design of A Magnetic Resonance Imaging Sequence Based on Bloch NMR Flow Equations and Bessel Functions. Chin J Magn Reson Imaging, 2013, Vol 4, No5 379-386.

[66] Price WS. Pulsed Field Gradient Nuclear Magnetic Resonance as a Tool for Studying Translational Diffusion: Part I. Basic Theory. Concepts Magn. Reson. 1997; 9: 299-336].

[67] Compston A, Coles A (April 2002). Multiple sclerosis. *Lancet* 359 (9313): 1221–31. doi:10.1016/S0140-6736(02)08220-X.

[68] Miller S, Vigneron D, Henry R, et al. Serial quantitative diffusion tensor MRI of the premature brain: development in newborns with and without injury. J Magn Reson. Imaging 2002; 16: 621–632.

[69] V.M. Kenkre, EiichiFakuchima, and D. Sheltraw. Simple solutions of the Bloch-Torrey equation for the NMR study of molecular diffusion. Journal of magnetic resonance: 128, 62-69 (1997).

[70] Samuel Odey, Dada O, Michael and O.B. Awojoyogbe. Physics and Mathematics of Magnetic Resonance Imaging for Nanomedicine: An Overview. World Journal of Translational Medicine. 2014, April 12: 3(1):17-30.

[71] Awojoyogbe O. B., M. Dada, Olufemi Folorunsho Moses. Mathematical analysis of adiabatic model of Bloch NMR flow equations for functional magnetic resonance imaging. African Journal of physics, Special Edition, proceedings of the first international seminar on the theoretical physics and national development.(paired reviewed) pp.177-201, (2008).

[72] Tzu-Ching Shih, Ping Yuan, Win-Li Lin, Hong-Sen Kou. Analytical analysis of the Pennes bioheat transfer equation with sinusoidal heat flux condition on skin surface, Medical Engineering & Physics 29 (2007) 946–953.

[73] Michael O. Dada, Simona Baroni, Bamidele Awojoyogbe, Computational Model of the Bloch NMR Flow Equation for in-vivo assessment of Contrast agents Journal of Cardiovascular Magnetic Resonance, 2014 16 (Suppl 1) 093.

[74] Bottomley PA, Foster TH, Argersinger RE, Pfeifer LM (1984) A review of normal tissue NMR relaxation times and relaxation mechanisms from 1 to 100 MHz: dependence on tissue type, NMR frequency, temperature, species, excision, and age. Med Phys 11: 425–448.

The Physics and Mathematics of Magnetic Resonance Imaging (MRI) based on the fundamental Bloch NMR flow equation as presented in this volume can lead to breath taking innovations and novel applications of MRI for improved health care. High quality and novel contributions related to biological, biomedical, clinical, geophysical and further exciting applications are welcomed. All contributions (computational, analytical, experimental and further theory) towards the next volumes of this book can be addressed to the editor at abamidele@futminna.edu.ng OR awojoyogbe@yahoo.com

To order additional copies of this book, please contact:
Science Publishing Group
service@sciencepublishinggroup.com
www.sciencepublishinggroup.com